Cambridge Texts in Applied Mathematics

MANAGING EDITOR
D.G. Crighton, University of Cambridge

EDITORIAL BOARD
M. Ablowitz, University of Colorado; J.-L. Lions, Collège de France;
A. Majda, New York University; J. Ockendon, University of Oxford;
E.B. Saff, University of South Florida

Maximum and Minimum Principles
M.J. Sewell

Solitons
P.G. Drazin and R.S. Johnson

The Kinematics of Mixing
J.M. Ottino

Introduction to Numerical Linear Algebra and Optimisation
Philippe G. Ciarlet

Integral Equations
David Porter and David S.G. Stirling

Perturbation Methods
E.J. Hinch

The Thermomechanics of Plasticity and Fracture
Gerard A. Maugin

Boundary Integral and Singularity Methods for Linearized Viscous Flow
C. Pozrikidis

Nonlinear Wave Processes in Acoustics
K. Naugolnykh and S. Ostrovsky

Nonlinear Systems
P.G. Drazin

Stability, Instability and Chaos
Paul Glendinning

Viscous Flow
H. Ockendon and J.R. Ockendon

Applied Analysis of the Navier-Stokes Equations
Charles R. Doering and J.D. Gibbon

Scaling, self-similarity, and intermediate asymptotics

Grigory Isaakovich Barenblatt
Emeritus G. I. Taylor Professor of Fluid Mechanics, University of Cambridge;
Fellow of Gonville and Caius College, Cambridge

CAMBRIDGE
UNIVERSITY PRESS

Contents

	Preface	xi
	Foreword	xvii
0	**Introduction**	**1**
0.1	Dimensional analysis and physical similarity	1
0.2	Assumptions underlying dimensional analysis	9
0.3	Self-similar phenomena	14
0.4	Self-similar solutions as intermediate asymptotics. The solutions of the first and second kind. Renormalization group	18
0.5	Self-similarities and travelling waves	26
1	**Dimensions, dimensional analysis and similarity**	**28**
1.1	Dimensions	28
1.2	Dimensional Analysis	39
1.3	Similarity	52
2	**The construction of intermediate-asymptotic solutions using dimensional analysis. Self-similar solutions**	**64**
2.1	Heat propagation from a concentrated instantaneous source	64
2.2	Phenomena at the initial stage of a nuclear explosion	76
2.3	Self-similarity. Intermediate asymptotics	86
3	**Self-similarities of the second kind: first examples**	**95**
3.1	Flow of an ideal fluid past a wedge	95
3.2	Filtration in an elasto-plastic porous medium: the modified instantaneous heat source problem	104

10

Scaling in turbulence

10.1 Homogeneous and isotropic turbulence

10.1.1 The problem of turbulence

This chapter differs from the previous ones in that scaling laws and self-similar solutions of the first and second kind will be established by making essential use of experimental data and without turning to a mathematical formulation of the problem, which, for turbulence, is lacking at the present time.

The problem of turbulence, to which this chapter is devoted, is considered with good reason to be the number-one problem of contemporary classical physics. Discovered by Leonardo and baptized by Lord Kelvin†, it has attracted the greatest minds of the century, including such giants as W. Heisenberg, A.N. Kolmogorov, G.I. Taylor, L. Prandtl, and Th. von Kármán. Nevertheless, it remains an open problem: none of the results available has been obtained from first principles. They are based essentially on strong additional assumptions, which may or may not be correct.

The phenomenon of turbulence, as is well known, consists in the following. As we have seen in chapter 1, the basic similarity parameter that governs the global properties of the flow of an incompressible viscous fluid is the Reynolds number $\rho U l/\mu$ (ρ being the density and μ the viscosity of the fluid, U a characteristic speed, and l a characteristic

† Professor U. Frisch showed me the place in the diaries of Leonardo where the word 'turbulent' was used in exactly the same sense as we use it now. An instructive case of congeniality!

length scale of the flow). When the Reynolds number reaches a certain critical value $\mathrm{Re}_{\mathrm{cr}}$, different for different flows (for example, for flow in a smooth cylindrical pipe of circular cross section, $\mathrm{Re}_{\mathrm{cr}} \sim 10^3$, for flow in a boundary layer, $\mathrm{Re}_{\mathrm{cr}} \sim 10^5$), the character of the flow changes suddenly and sharply. A stream that at subcritical values of the Reynolds number was regular and ordered – *laminar* – becomes essentially irregular both in time and in space. The flow properties for supercritical values of the Reynolds number undergo sharp and disorderly variations in space and time, and the fields of flow properties, – pressure, velocity, etc. – can to a good approximation be considered random. Such a regime of flow is called *turbulent*.

At the present time there exist only more or less plausible conjectures regarding the origin of turbulence, sometimes very interesting, but not having conclusive strength. Also, there exists no complete mathematical description of developed turbulent flows. Under these circumstances, in all attempts to create theoretical models valid for certain classes of turbulent flows though not pretending to be universal, similarity, scaling, and renormalization group considerations occupy a primary place.

Together with the majority of investigators, we shall start from the assumption that, for velocities small compared with the speed of sound, turbulent motion can actually be described by the equations of motion for a viscous incompressible fluid, i.e., by the Navier–Stokes equations for momentum balance and the continuity equation, which in rectangular Cartesian coordinates can be written in the form (Kochin, Kibel' and Roze, 1964; Batchelor, 1967; Germain, 1986a; Landau and Lifshitz, 1987)

$$\begin{gathered} \partial_t u_i + u_\alpha \partial_\alpha u_i = -\frac{1}{\rho}\partial_i p + \nu \Delta u_i \,, \\ \partial_\alpha u_\alpha = 0 \,. \end{gathered} \tag{10.1}$$

Here the u_i are the components of the velocity vector, $\nu = \mu/\rho$ is the kinematic viscosity, p is the pressure, and one sums over repeated Greek indices from one to three.

To construct, for instance numerically, a solution of these equations corresponding to some special realization of a developed turbulent flow is impossible in view of their extreme instability†. Hence, and also in view of the possibility noted above of considering the properties of a turbulent flow field as random, the description of turbulent flows is always given in

† All attempts at the direct numerical simulation of turbulent flows are related to values of the Reynolds number for which the flow cannot be considered as a developed one.

statistical terms. As is known (for details see, e.g., Monin and Yaglom, 1971, 1975), a sufficiently complete description of a developed turbulent flow is given by a set of mean quantities

$$\langle u_i(\mathbf{x},t)\rangle, \quad \langle p(\mathbf{x},t)\rangle \tag{10.2}$$

and moment tensors

$$\begin{aligned} B_{ijk} \quad \ldots = \quad & \langle u_i(\mathbf{x},t)u_j(\mathbf{x}_1,t)u_k(\mathbf{x}_2,t)\ldots \quad \rangle\,, \\ B_{pij} \quad \ldots = \quad & \langle p(\mathbf{x},t)u_i(\mathbf{x}_1,t)u_j(\mathbf{x}_2,t)\ldots \quad \rangle\,, \\ \vdots \qquad\qquad & \qquad\qquad \vdots \end{aligned} \tag{10.3}$$

for all possible point systems: $\mathbf{x}$, $\mathbf{x}_1$; $\mathbf{x}$, $\mathbf{x}_1$, $\mathbf{x}_2$; $\mathbf{x}$, $\mathbf{x}_1$, $\mathbf{x}_2$, $\mathbf{x}_3$, ...

Here the sign $\langle\ldots\rangle$ denotes the probability mean value. Taking probability mean values is used in theoretical work on turbulence as a natural method of averaging. In experimental practice, one uses volume or time means, the identification of these types of averaging with the taking of probability means being made on the basis of the so-called ergodic hypothesis.

A system of equations for the moments can be obtained by multiplying (10.1) by the velocity components at different points of the flow and subsequently averaging. This was done by Keller and Friedmann (1924). As a special case one obtains a non-closed set of equations for the mean quantities, first given in the fundamental paper of Reynolds (1895).

10.1.2 Homogeneous isotropic turbulence

Essential progress in the development of a statistical theory of turbulence occurred when Taylor (1935) introduced the idea of considering homogeneous isotropic turbulence. This idea gained additional fundamental significance after Kolmogorov (1941) and Obukhov (1941) predicted that at small scales all developed turbulent flows (i.e., flows at large Reynolds numbers) are *statistically identical* and therefore have the properties of homogeneity and isotropy. A flow is called *homogeneous* and *isotropic* if all its moment tensors remain unchanged upon translation, rotation, or mirror reflection with respect to some plane, of the system of points $\mathbf{x}$, $\mathbf{x}_1$, $\mathbf{x}_2$, ... (To be unchanged means that in a coordinate system arranged relative to the transformed system of points in the same way as the original coordinate system was arranged relative to the original system of points, the values of the components of the tensor remain the same.) For a homogeneous isotropic flow the mean velocity vanishes, and the number of independent components of moment tensors is substantially reduced, as well as the number of quantities on which they

depend. Thus in an arbitrary Cartesian coordinate system the components of the second-order moment tensor for the velocity field of a homogeneous isotropic flow are expressed in the following way:

$$B_{ij} = \langle u_i(\mathbf{x},t)u_j(\mathbf{x}+\mathbf{r},t)\rangle = (B_{LL}-B_{NN})\xi_i\xi_j/r^2 + B_{NN}\delta_{ij}\,. \tag{10.4}$$

Here $r = |\mathbf{r}|$ is the distance between points, the ξ_i are the components of the radius vector $\mathbf{r}$ joining the two points $\mathbf{x}$ and $\mathbf{x}_1 = \mathbf{x}+\mathbf{r}$, t is the time, and

$$\begin{aligned} B_{LL}(r,t) &= \langle u_L(\mathbf{x},t)u_L(\mathbf{x}+\mathbf{r},t)\rangle\,, \\ B_{NN}(r,t) &= \langle u_N(\mathbf{x},t)u_N(\mathbf{x}+\mathbf{r},t)\rangle\,, \end{aligned} \tag{10.5}$$

where u_L is the projection of the velocity vector in the direction of the radius vector $\mathbf{r}$ and u_N is its projection in the direction normal to the $\mathbf{r}$. Because of the incompressibility of the flow, the quantities B_{LL} and B_{NN} are connected by the relation

$$B_{NN} = B_{LL} + (r/2)\partial_r B_{LL}\,. \tag{10.6}$$

Thus, the second-order moment tensor for the velocity field is determined by a single scalar function of two scalar arguments, $B_{LL}(r,t)$. The situation is analogous for the two-point third-order moment tensor

$$B_{ij,k} = \langle u_i(\mathbf{x},t)u_j(\mathbf{x},t)u_k(\mathbf{x}+\mathbf{r},t)\rangle\,,$$

which, because of homogeneity, isotropy and incompressibility, can be expressed in terms of one component, a scalar function of the scalar arguments r and t; for example,

$$B_{LL,L}(r,t) = \langle u_L^2(\mathbf{x},t)u_L(\mathbf{x}+\mathbf{r},t)\rangle\,. \tag{10.7}$$

A similar reduction in the number of independent variables and independent components of moment tensors, due to homogeneity, isotropy and incompressibility, holds also for moments of higher order.

We turn now to the Navier–Stokes equations, multiply them by velocity components at successively increasing numbers of points, take the average, and use the symmetry relation following from the homogeneity and isotropy of the flow. Thus we obtain an infinite system of equations, which is, however, not closed at any finite stage because of the presence of quadratic-nonlinearity in the Navier–Stokes equations.

The first equation of this system, connecting the two-point second and third moments can be reduced to the form

$$\partial_t B_{LL}(r,t) = 2\nu\frac{1}{r^4}\partial_r r^4 \partial_r B_{LL} + \frac{1}{r^4}\partial_r r^4 B_{LL,L}(r,t)\,. \tag{10.8}$$

This relation, connecting two unknown functions, is called the Kármán–Howarth equation. It should be noted that in the fundamental paper of von Kármán and Howarth (1938) this equation was presented in a

different, less convenient form. It was first expressed in the form (10.8) by Loitsiansky (1939) and Millionshchikov (1939).

The problem in its complete form consists of solving the infinite system of equations for given initial conditions on the moments; this is the so-called problem of the decay of homogeneous isotropic turbulence. As a matter of fact, we have at best only very general information concerning the initial conditions, and so are unable to give the complete initial distribution of the moments. Therefore the asymptotics of the solution for large t, which 'remembers' only some basic properties of the initial conditions, is of particular interest. Under broad assumptions the asymptotics can be considered self-similar.

10.1.3 The decay of homogeneous isotropic turbulence

1. If at some stage of the motion the contribution of the third moments in the Kármán-Howarth relation (10.8) is small, then this relation becomes a closed equation for the second moment $B_{LL}(r,t)$,

$$\partial_t B_{LL} = 2\nu \frac{1}{r^4} \partial_r r^4 \partial_r B_{LL}\,, \tag{10.9}$$

which coincides in form with the equation of heat conduction in five-dimensional space for the case of central symmetry. Self-similar solutions of this equation were obtained in the paper of von Kármán and Howarth (1938) (see also Sedov, 1944, 1959)); they have the form

$$B_{LL} = \frac{A}{(t-t_0)^n} f(\xi, n), \quad \xi = \frac{r}{\sqrt{\nu(t-t_0)}}\,, \tag{10.10}$$

where A, n and t_0 are constants, and the function $f(\xi, n)$ satisfies the equation

$$\frac{d^2 f}{d\xi^2} + \left(\frac{4}{\xi} + \frac{\xi}{2}\right)\frac{df}{d\xi} + nf = 0 \tag{10.11}$$

under the conditions

$$f(0,n) = 1, \quad f(\infty, n) = 0\,, \tag{10.12}$$

the first of which is a normalization condition and the second of which is obtained from a natural assumption concerning the statistical independence of the velocities at infinitely distant points: $B_{LL}(\infty, t) = 0$. The function $f(\xi, n)$ so defined can be expressed, as is easily found (see Abramowitz and Stegun, 1970), in terms of a well-known special function, the confluent hypergeometric function $M(\alpha, \beta, z)$:

$$f = M(n, 5/2, -\xi^2/8)\,. \tag{10.13}$$

The spectrum of the eigenvalues n that determine the rate of decay of the second-order moments turns out, upon direct construction of the self-similar solution (10.10), to be continuous: a solution of (10.11) under the conditions (10.12) exists for any $n > 0$. The value of n that is actually realized must be determined by the initial conditions of the problem, for which (10.10) is a self-similar intermediate asymptotics.

If the initial distribution $B_{LL}(r,0)$ is such that the quantity

$$\Lambda_0 = \int_0^\infty r^4 B_{LL}(r,0)\,dr \tag{10.14}$$

is finite and different from zero, i.e., $0 < \Lambda_0 < \infty$, then $n = 5/2$ and the asymptotics of the solution as $t \to \infty$ corresponding to such an initial distribution can be written in the form

$$B_{LL}(r,t) = \frac{\Lambda_0}{48\sqrt{2\pi\nu^5(t-t_0)^5}} \exp\left[-\frac{r^2}{8\nu(t-t_0)}\right]. \tag{10.15}$$

Here the quantity

$$\Lambda = \int_0^\infty r^4 B_{LL}(r,t)\,dr \tag{10.16}$$

is an integral of the motion, analogous to the total amount of heat in the theory of heat conduction; that is, it is independent of time, $\Lambda \equiv \Lambda_0$. Loitsiansky (1939) has shown that under certain assumptions this quantity remains independent of time even when third moments are taken into account.

One can prove, using properties of the confluent hypergeometric functions, that the solutions (10.10) with $n > 5/2$ have Λ equal to zero. These solutions are in a certain sense structurally unstable with respect to the initial conditions. In fact, if perturbations of such solutions have, say, small but finite Λ_0, then for sufficiently large t only the contribution of the perturbation will govern the decay law, since it corresponds to the smallest n:$n = 5/2$. For this reason self-similar solutions with $n > 5/2$ are of rather lesser interest. On the other hand there is considerable interest in solutions with $n < 5/2$, for which $\Lambda = \infty$. These solutions can be represented in the form

$$B_{LL}(r,t) = \frac{\Lambda_0}{\sqrt{\nu^5(t-t_0)^5}} \left(\frac{\sqrt{\nu(t-t_0)}}{l}\right)^{5-2n} f\left(\frac{r}{\sqrt{\nu(t-t_0)}}, n\right), \tag{10.17}$$

where Λ_0 and l are constants having dimensions L^7T^{-2} and L, respectively; they are chosen so that $A = \Lambda_0 l^{-(5-2n)}\nu^{5/2-n}$.

It is evident that all these solutions with $n \neq 5/2$ are self-similarities of the second kind, 'remembering' the characteristic length scale l of the initial distribution. (See chapter 3, where, for another problem, a

completely analogous situation was analyzed). The situation is that the asymptotics of the dimensionless function

$$\Phi(\xi,\eta,\ldots), \quad \xi = \frac{r}{\sqrt{\nu(t-t_0)}}, \quad \eta = \frac{l}{\sqrt{\nu(t-t_0)}},$$

which appears upon applying dimensional analysis to the solution of the original non-self-similar problem, has, for small η, the form

$$\Phi(\xi,\eta,\ldots) \cong \eta^{2n-5}\Phi_1(\xi,\ldots).$$

Therefore the characteristic length scale l of the initial distribution appears in the constant A governing the solution, but only in combination with Λ_0; therefore it does not spoil the self-similarity.

We note that the stage of development of homogeneous isotropic turbulence at which the third-order moments are negligibly small is sometimes called the final stage of decay. It is sometimes argued that at this final stage the velocity is small and hence so are the third-order moments, which are of the order of the velocity cubed and therefore small compared with the second-order moments, which are of the order of the velocity squared. Such an argument is insufficient. Actually, a stage at which the third-order moments are negligibly small can occur only at the start of the motion with a special choice of initial conditions.

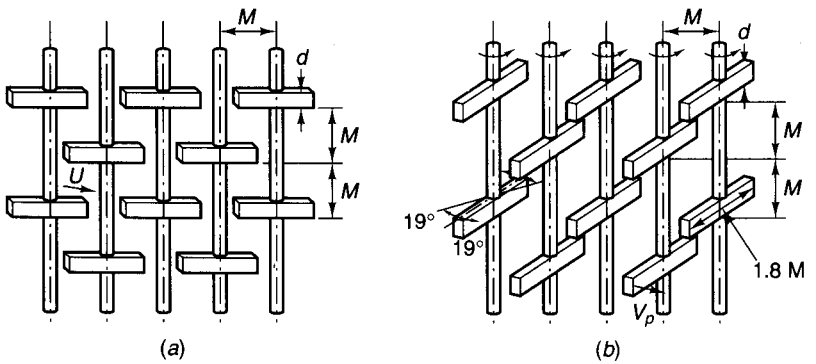

Figure 10.1. Turbulizing grids, used by S.C. Ling and co-workers: (*a*) passive; (*b*) active.

2. From the very first appearance in the papers of Taylor (1935) of the concept of homogeneous isotropic turbulent flow, attempts have been made to model this by the decay of turbulence in wind and water tunnels. There is a detailed summary of this work in the paper of Gad-el-Hak and Corrsin (1974). One should note especially the careful experiments performed by Ling and his associates (Ling and Huang, 1970; Ling and Wan, 1972) using a water tunnel – a long channel of square section into which water was introduced through a passive or active grid

of rods. Figure 10.1 shows the arrangements of grids used in these experiments: passive (Figure 10.1(*a*)) and active (Figure 10.1(*b*)). In the active grid the rods are equipped with agitating bars that perform oscillating motions at speeds and frequencies that can be varied. In the work of Gad-el-Hak and Corrsin (1974) a different type of active grid (a 'jet grid') was used; the rods of the grid were hollow and were provided with upwind or downwind controllable nozzles evenly distributed along each rod. Through the hollow rods and nozzles air was injected at varying rates into the flow. (In this work the experiments were performed in wind tunnels.) Thus in all these experiments turbulent fluctuations, introduced into the flow by a grid, then decayed as the fluid moved downstream. Here the fluctuations of velocity become close to isotropic even at small distances from the grid. Figure 10.2 shows the ratios of the mean square fluctuations of the measured longitudinal and transverse components of velocity (Ling and Huang, 1970); it is evident that they are close to unity. We see that if one takes as the time the quantity $t = x/U$ (U being the mean velocity of the flow and x the coordinate measured along the channel downstream from the grid), then the pattern of decay of turbulence along the channel corresponds sufficiently well to the scheme of decay of homogeneous isotropic turbulence in time. (The homogeneity was also specially checked by moving gauges, by means of which velocities were measured in the cross-flow planes x = constant.) This idea for the implementation of homogeneous isotropic turbulent flow was proposed and realized for the first time by Taylor (1935).

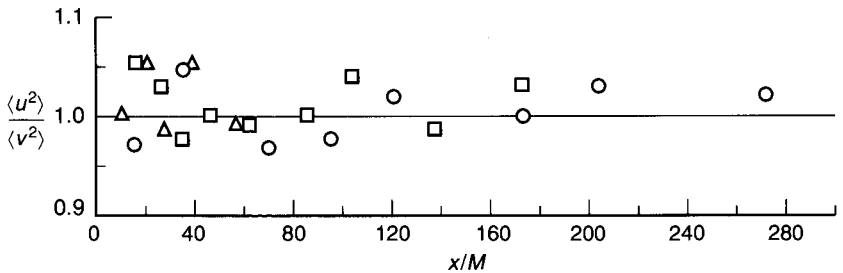

Figure 10.2. Velocity fluctuations in the turbulent flow behind a grid are nearly isotropic: ○, Re_M = 470, M = 1.78 cm, M/d = 2.8, U = 2.9 cm/s; □, Re_M = 940, M = 3.56 cm, M/d = 2.8, U = 2.9 cm/s; △, Re_M = 840, M = 3.18 cm, M/d = 5.0, U = 2.9 cm/s. From Ling and Huang (1970).

The statistical properties – the moment tensors of the turbulent motion under consideration – are thus governed by the mean velocity U of the flow, the characteristic length scale M of the grid, the thickness d of the rods, the viscosity coefficient ν, and the quantities r and $t-t_0$, where t_0 is the effective origin of time, about whose determination something will be said below. Furthermore, for active grids of the type used by Ling and Wan (1972) the moments are governed also by the speed V_p and frequency of oscillation ω of the tips of the agitating bars; for the active grids used by Gad-el-Hak and Corrsin (1974) an additional governing parameter for the moment tensors is the injection ratio $J = Q_1/Q$ (Q_1 being the flux rate of gas supplied through the hollow rods of the grid and Q the flux rate of gas supplied to the grid).

Dimensional analysis gives for the two-point moments of second and third order,

$$B_{LL} = \frac{\nu}{t-t_0}\Phi_{LL}\left(\xi, \eta, \frac{M}{d}, \frac{MU}{\nu}, \ldots\right), \tag{10.18}$$

$$B_{LL,L} = \left(\frac{\nu}{t-t_0}\right)^{3/2}\Phi_{LL,L}\left(\xi, \eta, \frac{M}{d}, \frac{MU}{\nu}, \ldots\right), \tag{10.19}$$

where the Φ's are dimensionless functions of their dimensionless arguments

$$\xi = \frac{r}{\sqrt{\nu(t-t_0)}}, \quad \eta = \frac{M}{(x-x_0)} = \frac{M}{U(t-t_0)},$$

of the grid parameter M/d and the Reynolds number MU/ν of the grid, and also of the parameters characterizing the activity of the grid.

It is of interest to consider the motion at sufficiently large distances from the grid such that $M/U(t-t_0) \ll 1$ and one can assume that random details of the initial conditions at the grid no longer influence the flow. The simplest assumption is that for $\eta \ll 1$ there is complete similarity in the parameter η. Such an assumption was introduced by von Kármán (von Kármán and Howarth, 1938), supposing that it is satisfied for large Reynolds numbers. Under the assumption of complete similarity in η for $\eta \ll 1$, one must have at sufficiently large distances from the grid the relations

$$\frac{B_{LL}(r,t)}{B_{LL}(0,t)} = f\left(\xi, \frac{M}{d}, \frac{MU}{\nu}, \ldots\right), \quad B_{LL}(0,t) = \frac{A}{(t-t_0)}, \tag{10.20}$$

$$\frac{B_{LL,L}(r,t)}{B_{LL}^{3/2}(0,t)} = g\left(\xi, \frac{M}{d}, \frac{MU}{\nu}, \ldots\right). \tag{10.21}$$

Here A is a constant depending on the initial conditions at the grid. Equations (10.20) and (10.21) were proposed by Dryden (1943) and Sedov (1944).

Next in degree of complexity is the assumption of incomplete similarity in the variable η for $\eta \ll 1$. In this case one must have at large distances from the grid the relations

$$B_{LL}(r,t) = \frac{\nu M^\alpha}{U^\alpha(t-t_0)^{1+\alpha}} \quad F\left(\xi, \frac{M}{d}, \frac{MU}{\nu}, \ldots\right), \tag{10.22}$$

$$\frac{B_{LL}(r,t)}{B_{LL}(0,t)} = f\left(\xi, \frac{M}{d}, \frac{MU}{\nu}, \ldots\right), \tag{10.23}$$

$$B_{LL}(0,t) = \frac{A}{(t-t_0)^{1+\alpha}}, \tag{10.24}$$

$$B_{LL,L}(r,t) = \frac{\nu^{3/2}M^\alpha}{U^\alpha(t-t_0)^{3/2+\alpha}}g\left(\xi, \frac{M}{d}, \frac{MU}{\nu}, \ldots\right), \tag{10.25}$$

$$\frac{B_{LL,L}(r,t)}{B_{LL}^{3/2}(0,t)} = B(t-t_0)^{\alpha/2}g\left(\xi, \frac{M}{d}, \frac{MU}{\nu}, \ldots\right). \tag{10.26}$$

Here A, B and α are again constant quantities. The equality of the powers to which $\eta = M/U(t-t_0)$ appears in the expressions for $B_{LL}(r,t)$ and $B_{LL,L}(r,t)$ follows from the Kármán-Howarth equation (10.8), which relates these quantities.

We turn to the results of experiments. In Figures 10.3 and 10.4 are shown the results of measuring the correlation function

$$f = \frac{B_{LL}(r,t)}{B_{LL}(0,t)}$$

in the cases of a passive grid (Ling and Huang, 1970) and an active grid (Ling and Wan, 1972) as a function of $\xi = r/[\nu(t-t_0)]^{1/2}$ (the effective origin t_0 being appropriately defined, see below). It is evident that in each case the experimental points lie close to a single curve, different for each different case. This confirms the self-similarity of the correlation function f, but does not determine the character of the self-similarity of the moment tensors; it is evident from (10.20) and (10.23) that a corresponding result must hold in both cases, for complete as well as for incomplete similarity.

In Figure 10.5 and Figure 10.6 are shown the results of measuring the quantity $B_{LL}(0,t)$ for, respectively, passive grids of different types (Ling and Huang, 1970) and active grids (Ling and Wan, 1972). It is evident that in all cases the decay, even at small distances, follows the law

$$B_{LL}(0,t) = \frac{A}{(t-t_0)^n}, \quad n = 1+\alpha. \tag{10.27}$$

The method for determining the effective origin of time t_0 is shown in Figure 10.7. The scaling law of decay $B_{LL}(0,t) = \langle u^2\rangle \sim (t-t_0)^{-n}$ leads to the fact that for large t the quantity $[U^2/\langle u^2\rangle]^{1/n}$ must be a

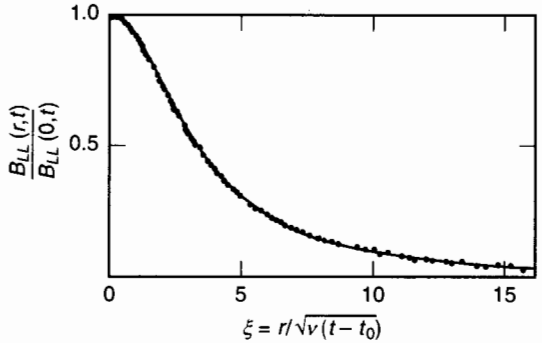

Figure 10.3. The correlation function f for flow behind a passive grid is self-similar: all experimental points lie on a single curve $f(\xi)$. From Ling and Huang (1970).

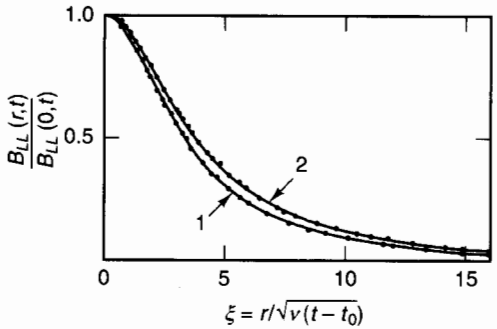

Figure 10.4. The velocity correlation functions for flow behind an active grid are self-similar: all experimental points lie on a single curve $f(\xi)$. Curve 1, $V_P/U = 3$; curve 2, $V_P/U = 17$. From Ling and Wan (1972).

linear function of time. Hence the intersections with the time axis of the straight lines drawn through the experimental points give the values of t_0.

We see that in all cases the exponent α turns out to be different from zero: it is equal to unity for passive grids, 0.73 for an active grid with $V_p/U = 3$, and 0.35 for an active grid with $V_p/U = 17$. This exponent thus depends on the initial conditions, i.e., the conditions at the grid.

The paper by Gad-el-Hak and Corrsin (1974) contains results of the data processing of other experiments of various researchers. In treating the variation of the quantity $B_{LL}(0,t)$ with t, this dependence was assumed to be a scaling law in accordance with (10.27). In some cases the turbulence was found to be weakly anisotropic, so the decay exponents are presented, in this paper, for all three components of velocity fluctuation. The experiments were performed on passive grids, as a rule, but the results of some experiments performed on active grids are also

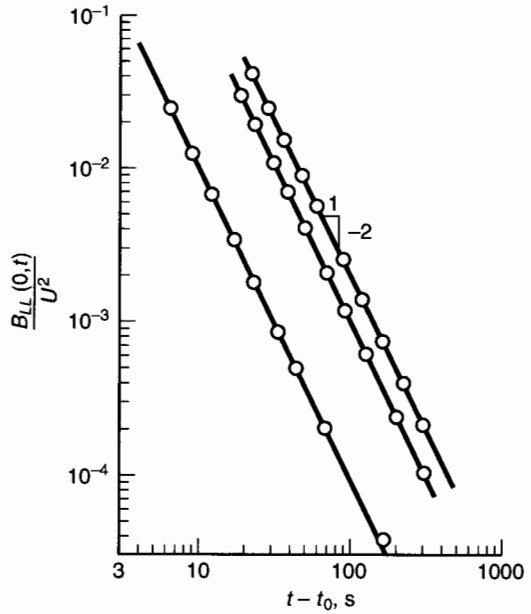

Figure 10.5. The moment $B_{LL}(0,t)$ behind a passive grid decays according to a scaling law, but the exponent is different from unity. Different curves correspond to different combinations of passive grids. From Ling and Huang (1970).

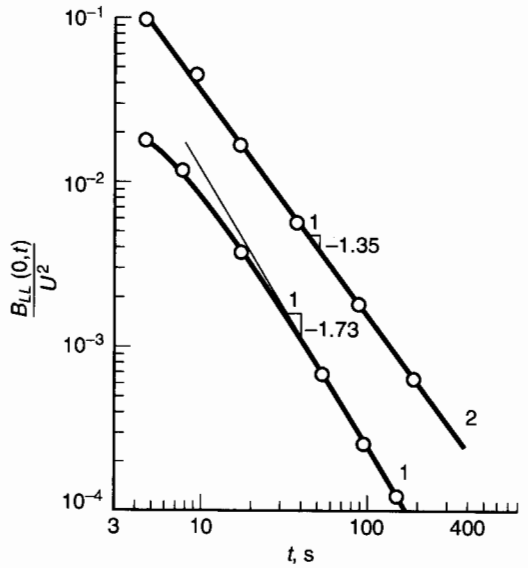

Figure 10.6. The moment $B_{LL}(0,t)$ behind an active grid decays according to a scaling law, but the exponent is different from unity. Curve 1, $V_P/U = 3$; curve 2, $V_P/U = 17$. From Ling and Wan, (1972).

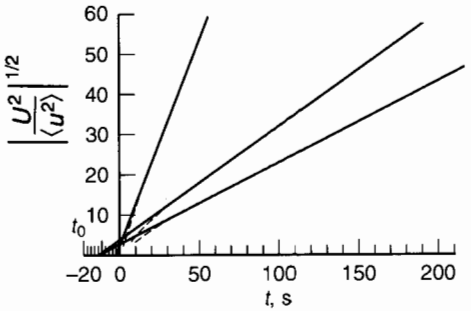

Figure 10.7. Determination of the effective origin of time, t_0, according to Ling and Huang (1970), for the case of a passive grid.

presented. In these experiments on active grids, as already mentioned, a grid of hollow rods was used with nozzles through which air was injected into the flow. The dependence of the exponent on the injection ratio J is shown in Figure 10.8.

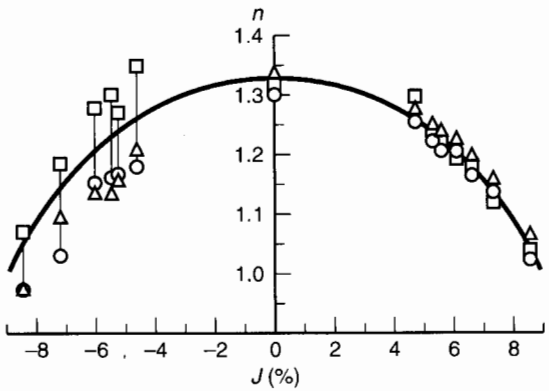

Figure 10.8. Dependence on injection rate J of the exponent n in the decay law for $B_{LL}(0,t)$, for an active grid. $J > 0$ corresponds to coflow injection and $J < 0$ to counterflow injection. For $J > 0$ the decay is isotropic and the exponent is different from unity. ○, lengthwise component of velocity; △,□, transverse components of velocity. From Gad-el-Hak and Corrsin (1974).

It is evident that the exponent in the decay law depends on conditions at the grid (the Reynolds number of the grid, and the characteristics of its activity, J, V_p/U, ω, etc.). The exponent α turns out to be equal to zero, i.e., the self-similarity of the decay turns out to be complete, only in the case of enormously large Reynolds numbers of the grid, reached by Kistler and Vrebalovich (1966).

Unfortunately, third-order moments have been measured by almost no one: one of the few papers up to now in which measurements of third moments are given is that of Stewart (1951). In this paper the self-similarity of the correlation function is emphasized, and attention is especially given to the absence of a unique dependence of the quantity $B_{LL,L}(r,t)/B_{LL}^{3/2}(0,t)$ on the self-similar variable for different instants of time (Figure 10.9). This conforms to incomplete similarity of the decay (cf. (10.26)) and would not hold for complete similarity.

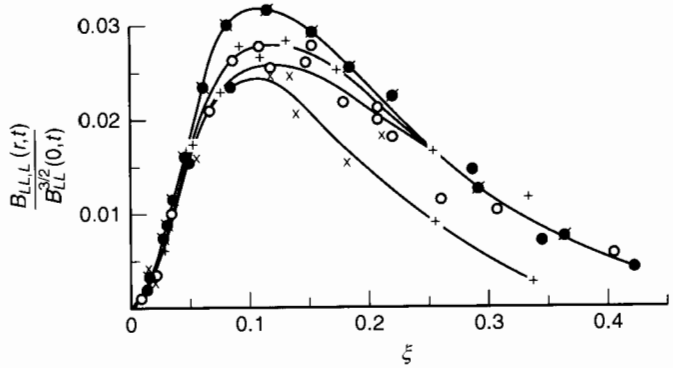

Figure 10.9. Unique dependence of the quantity $B_{LL,L}(r,t)/B_{LL}^{3/2}(0,t)$ on the self-similar variable is lacking – the curves for different moments of time do not coincide. ×, $t = 0.041$ s.; •, $t = 0.0615$ s.; ○, $t = 0.123$ s.; +, $t = 0.184$ s.; ↘ and ↙, $t = 0.246$ s. From Stewart (1951).

Thus we have arrived at the conclusion that in experiments the decay of turbulenceis self-similar even at small distances from the grid, but this self-similarity is of the second kind, so that the influence of the initial scale – the length scale of the grid – never vanishes, but, because of the peculiarities of homogeneous isotropic turbulence, appears only in combination with various parameters. The exponent in the law of decay cannot be determined from considerations of dimensional analysis, but is selected from the continuous spectrum of possible values by the initial conditions (the conditions at the grid), the situation in principle being analogous to what we met above when considering the self-similar analogue of the Korteweg-de Vries equation.

The analysis of the self-similar decay of homogeneous isotropic turbulence presented above was given by Barenblatt and Gavrilov (1974).

10.1.4 Locally homogeneous and isotropic turbulence

The investigation of the local structure of turbulent flows of an incompressible viscous fluid at large Reynolds numbers in the papers of Kolmogorov (1941, 1962) and Obukhov (1941, 1962) also furnishes very

instructive examples of self-similar intermediate asymptotics of various types. The outstanding work of their predecessor, the great British physicist L.F. Richardson (1922), who proposed a qualitative scheme of vortex cascade in turbulent flow, should also be acknowledged.

According to the basic hypothesis of Kolmogorov and Obukhov, at large Reynolds numbers hydrodynamic fields have the properties of local isotropy, homogeneity and stationarity. Local isotropy and homogeneity mean that the moment tensors, in which the relative velocities

$$\Delta_{\mathbf{r}}\mathbf{u} = \mathbf{u}(\mathbf{x}+\mathbf{r},t) - \mathbf{u}(\mathbf{x},t) \tag{10.28}$$

appear, are homogeneous and isotropic at sufficiently small $|\mathbf{r}|$. The condition of stationarity of the statistical properties of local fields results from the fact that the characteristic times of variation for the local fields are much smaller than those for the basic flow.

Thus, as in the case of an ordinary homogeneous and isotropic incompressible turbulent flow, the tensor of second-order moments of the quantities $\Delta_{\mathbf{r}}\mathbf{u}$ can be expressed in terms of one of its components, for example,

$$D_{LL} = \langle (u_L(\mathbf{x}+\mathbf{r},t) - u_L(\mathbf{x},t))^2 \rangle \tag{10.29}$$

(u_L being, as before, the component of the velocity vector $\mathbf{u}$ in the direction $\mathbf{r}$). The quantity D_{LL}, in principle, may depend on r, the modulus of the vector $\mathbf{r}$, and also on the kinematic viscosity of the fluid ν, the external scale Λ, and the energy transmitted per unit time from the large-scale motions to the fine-scale motions under consideration; this, by virtue of stationarity, is equal to the mean rate of turbulent energy dissipation per unit volume, $\langle\epsilon\rangle$. Introducing in place of the viscosity the linear scale λ of the motion in which viscous dissipation occurs,

$$\lambda = \nu^{3/4}\langle\epsilon\rangle^{-1/4}, \tag{10.30}$$

the *internal Kolmogorov scale*, we have

$$D_{LL} = f(r, \langle\epsilon\rangle, \lambda, \Lambda). \tag{10.31}$$

Dimensional analysis gives by the standard procedure

$$D_{LL} = \langle\epsilon\rangle^{2/3} r^{2/3} \Phi\left(\frac{r}{\lambda}, \frac{r}{\Lambda}\right). \tag{10.32}$$

The relationships valid in the so-called inertial range of scales, i.e. for $\lambda \ll r \ll \Lambda$, are intermediate asymptotics of (10.32) as $r/\lambda \to \infty$ but $r/\Lambda \to 0$. (For large Reynolds numbers, $\lambda \lll \Lambda$.) In the classical version of the Kolmogorov-Obukhov theory an assumption is implicitly made that is equivalent to the assumption that there is a finite non-zero limit of $\Phi(r/\lambda, r/\Lambda)$ as $r/\lambda \to \infty$ and $r/\Lambda \to 0$, i.e., that there is

complete self-similarity in both parameters r/λ and r/Λ. Therefore for $\lambda \ll r \ll \Lambda$ we obtain the famous 'two-thirds scaling law' of Kolmogorov,

$$D_{LL} = C\langle\epsilon\rangle^{2/3} r^{2/3}, \tag{10.33}$$

where C is a universal constant that must be equal to $\Phi(\infty, 0)$.

In fact, the existence of complete similarity in the parameter r/Λ for small r/Λ is in some doubt owing to the so-called intermittency effect. Intermittency consists in the non-uniform spatial distribution of the energy transfer rate towards smaller vortices. Indeed this energy transfer rate is also a random quantity and the contribution of its fluctuations in larger scales than the scale of the 'equilibrium range' $r \ll \Lambda$, which is the only scale possessing local isotropy and homogeneity, can turn out to be essential. This point was attributed by A.N. Kolmogorov to L.D. Landau, although the relevant note in the book of Landau and Lifchitz (1987), (the first edition was published in 1944) in fact concerns a different matter.

We therefore assume that there is complete similarity in the parameter r/λ for $r/\lambda \gg 1$, and incomplete similarity in the parameter r/Λ for $r/\Lambda \ll 1$, so that, as $r/\lambda \to \infty$ and $r/\Lambda \to 0$,

$$\Phi\left(\frac{r}{\lambda}, \frac{r}{\Lambda}\right) \simeq C_1 \left(\frac{r}{\Lambda}\right)^{\alpha} \tag{10.34}$$

where C_1 and α are universal constants. Then (10.32) gives

$$D_{LL} = C_1 \langle\epsilon\rangle^{2/3} r^{2/3+\alpha} \Lambda^{-\alpha}. \tag{10.35}$$

But we find just such a relation in the refined Kolmogorov–Obukhov theory, which takes account of the influence of fluctuations in the energy dissipation (Kolmogorov, 1962; Obukhov, 1962). The constant α, according to this theory, is related to a coefficient in the relation for the variance of the energy transfer rate averaged on a scale r (see Monin and Yaglom, 1975),

$$\langle [(\ln\epsilon)']^2 \rangle = A - \mu \ln r, \tag{10.36}$$

so that $\alpha = \mu/9$. According to experimental data, $\mu = 0.4$, so that $\alpha \simeq 0.04$ and the dependence (10.35) actually differs from the two-thirds law only slightly.

In the paper by Castaing, Gagne and Hopfinger (1990) an alternative relation for the variance of the energy transfer rate averaged on a scale r was proposed,

$$\langle [(\ln\epsilon)']^2 \rangle = (r/r_0)^{-\beta} \tag{10.37}$$

(r_0 is a constant length parameter), which exactly corresponds to the incomplete similarity assumption. The experiments presented in this paper confirm the incomplete similarity relation (10.37) rather than the logarithmic relation (10.36). The authors also presented a model

that leads to the relation $\beta = \beta_1/\ln \mathrm{Re}$, where β_1 is a constant, Re a global-flow Reynolds number based on the Taylor linear scale parameter. So, according to this work, the exponent α depends on the global-flow Reynolds number and therefore is not a universal constant.

Moreover, recently Barenblatt and Goldenfeld (1995) came, under certain additional assumptions, to the relation for D_{LL} in the inertial range

$$D_{LL} = \left[A_0 + \frac{A}{\ln \mathrm{Re}}\right] (\langle\epsilon\rangle r)^{2/3} \left(\frac{r}{\Lambda}\right)^{\alpha/\ln \mathrm{Re}} \tag{10.38}$$

where A_0, A and α are universal constants. In this formula the correction $\alpha/\ln \mathrm{Re}$ is not substantial in comparison with the exponent 2/3 to which r enters (10.33) and can hardly be observed at present. The essential point is that according to (10.38) the correction to the Kolmogorov constant appears to be inversely proportional to $\ln \mathrm{Re}$. This is consistent with the experimental data of Praskovsky and Oncley (1994).

10.2 Turbulent shear flows

10.2.1 Similarity laws for the velocity distribution in the wall region of a turbulent shear flow

A turbulent flow whose mean properties do not depend on the coordinate x in the direction of the mean velocity is called a *shear flow*. Thus, the mean velocity and all the other mean properties of a shear flow depend on only one coordinate, z, transverse to the mean flow and having its origin at the rigid wall that constrains the flow (Figure 10.10). This type of flow occurs in a channel or pipe far from the inlet, in the flow past a plate far from the leading edge, in the boundary layer of the atmosphere, etc.

In the vicinity of the wall bounding the flow, it can be assumed that the shear stress is constant, i.e., independent of the transverse coordinate z. The part of the shear flow in which this assumption is valid is called the *wall region*.

Thus, the properties of the motion at some point in the wall region of a turbulent shear flow are governed by the shear stress τ (which is, by assumption, constant), the properties of the fluid (its density ρ and kinematic viscosity ν), the distance z of the point under consideration from the wall, and some external flow scale Λ – the diameter of the pipe or depth of the channel, etc.

We shall adopt the gradient of the mean velocity u at a given point,

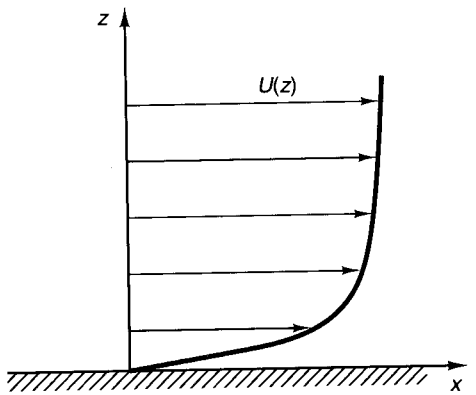

Figure 10.10. Shear flow.

$\partial_z u$, as the quantity being determined; it will become clear below why we do not choose the velocity itself. Thus, we have

$$\partial_z u = f(\tau, \rho, z, \nu, \Lambda)\,. \tag{10.39}$$

The LMT class of systems of units is appropriate here. In this class, the governing parameters have the following dimensions:

$$[\tau] = \frac{M}{LT^2}, \quad [\rho] = \frac{M}{L^3}, \quad [\nu] = \frac{L^2}{T}, \quad [z] = [\Lambda] = L\,. \tag{10.40}$$

The dimensions of the first three governing parameters τ, ρ and z are obviously independent. The dimension of the determined parameter $\partial_z u$ and those of the last two governing parameters can be expressed in terms of the dimensions of the first three parameters in the following way:

$$[\partial_z u] = [\tau]^{1/2}[\rho]^{-1}[z]^{-1}, \quad [\Lambda] = [z], \quad [\nu] = [\tau]^{1/2}[\rho]^{-1/2}[z]\,. \tag{10.41}$$

Thus, we obtain the following dimensionless form for the relation under study:

$$\begin{aligned} \Pi &= \frac{z\partial_z u}{(\tau/\rho)^{1/2}} = \Phi(\Pi_1, \Pi_2)\,, \\ \Pi_1 &= \frac{\nu}{(\tau/\rho)^{1/2} z}, \quad \Pi_2 = \frac{\Lambda}{z}\,. \end{aligned} \tag{10.42}$$

According to tradition, we shall now introduce the notation $u_* = (\tau\rho)^{-1/2}$; this quantity u_*, which has the dimension of velocity, is called the *dynamic*, or *friction, velocity*. It is both natural and convenient, for the analysis that follows, to transform from the parameter Π_1 to its reciprocal, $\Pi_1^{-1} = u_* z/\nu = \mathrm{Re}_l$, which serves as a local Reynolds number, and an analogous quantity $\Pi_2\Pi_1^{-1} = \mathrm{Re}_* = u_*\Lambda/\nu$, which serves as a global Reynolds number. (The local Reynolds number contains the

local coordinate z, while the global Reynolds number contains the external length scale Λ. The global Reynolds number Re_* differs from that normally used in the hydraulics of flow in pipes in that it contains the dynamical velocity u_* rather than the average flow velocity in the pipe.)

Thus, we obtain

$$\Pi = \frac{z\partial_z u}{u_*} = \Phi_1(\mathrm{Re}_l, \mathrm{Re}_*)\,. \tag{10.43}$$

We shall now estimate the values of the parameters Re_l and Re_*. For flowing water ($\nu = 10^{-2}\mathrm{cm}^2/\mathrm{s}$) with a relatively low dynamical velocity, $u_* = 10$ cm/s, the local Reynolds number at a distance of just one millimetre from the wall is equal to 100 and the global Reynolds number is 10 000 for a pipe 10 cm in diameter. Both these parameters are therefore large outside the immediate vicinity of the wall; it seems natural to investigate whether it is possible to use limiting similarity laws in this region. Note that it was precisely the desire to construct limiting similarity laws that led us to consider the gradient of the velocity rather than the velocity itself. The point is that the velocity at any distance from the wall, unlike the velocity gradient, obviously depends on the situation in the immediate vicinity of the wall, where the local Reynolds number cannot be assumed to be large.

Thus, under the assumption of complete similarity with respect to the local and global Reynolds numbers (this assumption dates back to von Kármán, 1930 and Prandtl, 1932b), we obtain the following result from (10.43):

$$\Pi = \frac{z\partial_z u}{u_*} = \Phi_1(\infty, \infty) = \mathrm{const}. \tag{10.44}$$

The constant in (10.44) is traditionally denoted by $1/\kappa$; the constant κ is called the von Kármán constant. Clearly, under the assumption of complete similarity in Re_l and Re_* made above, the von Kármán constant must be universal, i.e., independent of the Reynolds number.

Integration of (10.44) yields a universal logarithmic law for the velocity distribution across the flow,

$$u = \frac{u_*}{\kappa} \ln z + \mathrm{const}\,,$$

which is usually written in the form

$$\varphi = \frac{1}{\kappa} \ln \eta + C_1\,, \tag{10.45}$$

where

$$\varphi = \frac{u}{u_*}, \quad \eta = \frac{u_* z}{\nu}, \quad C_1 = \mathrm{const}\,.$$

At first glance, this universal logarithmic law seems to be fairly well confirmed by measured data on the mean velocity distributions in smooth

pipes, boundary layers and channels (Figure 10.11), and a numerical value of approximately 0.4 is obtained for the von Kármán constant κ. However, more detailed analysis of the experimental data reveals a systematic dependence of the von Kármán constant on the Reynolds number for the flow. Thus, small but systematic deviations from the universal logarithmic law are observed in the velocity distribution.

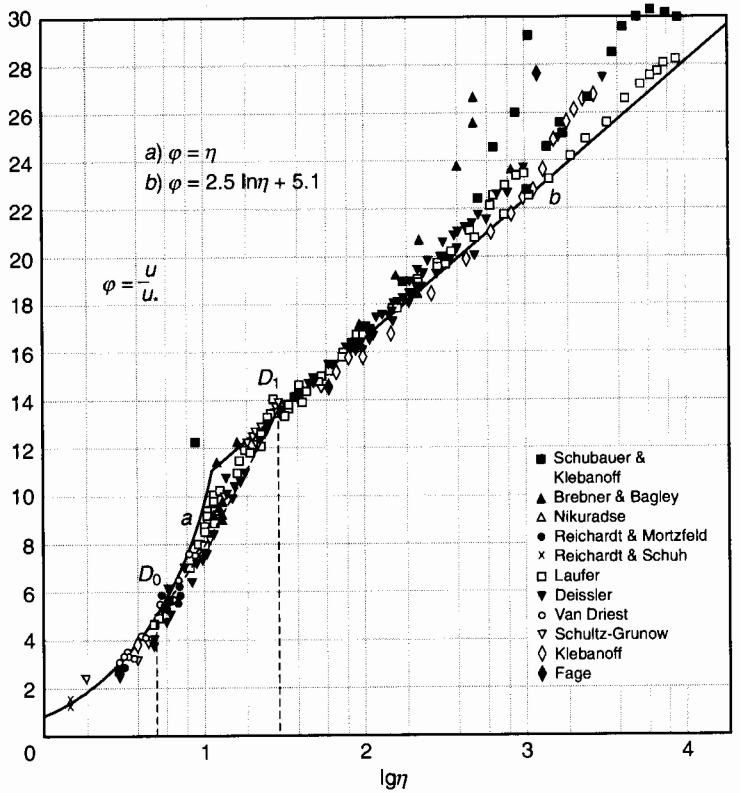

Figure 10.11. Universal dimensionless mean velocity profile $\varphi = u/u_*$ of turbulent flow close to a smooth wall according to the data of pipe-, channel-, and boundary-layer measurements (Kestin and Richardson, 1963). After Monin and Yaglom (1971, 1992): region a, $\varphi = \eta$; region b, $\varphi = 2.5 \ln \eta + 5.1$.

In accordance with the recipe outlined in chapter 5, we shall look (Barenblatt and Monin, 1979) at the possible assumption of incomplete similarity with respect to the local Reynolds number and lack of self-similarity with respect to the global Reynolds number. Under the assumption of incomplete similarity with respect to Re_l, (10.43) yields

$$\frac{z\partial_z u}{u_*} = \left(\frac{u_* z}{\nu}\right)^{\alpha} \Phi(\mathrm{Re}_*)\,, \tag{10.46}$$

where the exponent α is also assumed to depend on the global Reynolds number Re_*. Integrating (10.46) and assuming, in agreement with experiment, that the constant of integration is equal to zero, we obtain the scaling velocity distribution

$$\varphi = C\eta^{\alpha} \tag{10.47}$$

where we have defined $C = (1/\alpha)\Phi(\mathrm{Re}_*)$. The global Reynolds number $\mathrm{Re}_* = u_*\Lambda/\nu$ is a function of a commonly used Reynolds number for the flow, based on the mean flow velocity $\bar{u}$ rather than on the friction velocity:

$$\mathrm{Re}_* = f(\mathrm{Re}), \quad \mathrm{Re} = \frac{\bar{u}\Lambda}{\nu};$$

this follows directly from dimensional analysis. Therefore the constants C and α in (10.47) can be considered also as functions of the flow Reynolds number Re.

Scaling laws for the velocity distribution in various turbulent shear flows have been suggested as empirical relationships for a long time. One recognises (cf. Schlichting, 1968; Hinze, 1959) that scaling (power) laws for velocity distributions, with exponents depending on global Reynolds number, are confirmed by experiment at least as well as is the universal logarithmic law. Nevertheless the latter is generally considered to have, in contrast to the scaling law, a theoretical basis whereas the scaling law is considered as simply an empirical relation. As a matter of fact, however, we have seen that the scaling law can be derived from the assumption of incomplete similarity of the flow in the local Reynolds number not less rigorously than the universal logarithmic law can be derived from the assumption of complete similarity, i.e., complete independence on the molecular viscosity. Therefore neither the logarithmic law (10.45) nor the power law (10.47) should be considered only as a convenient representation of the experimental data; both have rigorous theoretical foundations based, however, on different assumptions. Moreover, the assumption of the lack of a characteristic length in the flow leads in general to the scaling law, and as a special case to the logarithmic law[†].

† Indeed, according to this assumption the ratio of velocity gradients $\partial_y u$ at heights z_1 and z_2 is a function of z_1/z_2 only. This leads to the well-known functional equation, which we have used more than once:

$$\varphi\left(\frac{y}{x}\right) = \frac{\varphi(y)}{\varphi(x)}$$

whose solution is $\varphi(x) = x^n$, where the constant n remains indeterminate. If $n = -1$, the logarithmic law is obtained; if $n \neq -1$, the scaling law.

Therefore an important qualitative question arises: which of these assumptions is correct?

The results presented below (Barenblatt, 1991, 1993a; Barenblatt and Prostokishin, 1993) give some evidence in favour of the power-type law (10.47) with exponent α inversely proportional to the logarithm of the flow Reynolds number and constant C a linear function of this logarithm:

$$\alpha = \frac{3}{2\ln \mathrm{Re}}, \tag{10.48}$$

$$C = \frac{1}{\sqrt{3}}\ln \mathrm{Re} + \frac{5}{2} = \frac{\sqrt{3} + 5\alpha}{2\alpha}. \tag{10.49}$$

As a matter of fact, the inverse proportionality of α to $\ln \mathrm{Re}$ was suggested by the idea that the local structure of developed turbulent flow should imprint the velocity distribution, and by the result of Castaing, Gagne and Hopfinger (1990) mentioned in subsection 10.1.4.

To check the dependence (10.48) all 16 sets of experimental data[‡], available in the paper by Nikuradze (1932) of average velocity measurements in smooth cylindrical tubes at various distances from the wall and at various Reynolds numbers[§] were subjected to a stringent procedure for the verification of (10.47), (10.48). Namely, the functions $\varphi^{(2\ln \mathrm{Re})/3}$ as functions of η were constructed and inspected. The question was whether the straight lines would be found for intermediate values of η. The processing of the experimental data clearly revealed (Figures 10.12(a)–(e)) such intermediate straight lines for all 16 sets. We note a good level of accuracy: the exponent $1/\alpha = (2\ln \mathrm{Re})/3$ is large, of the order of 10 or so, therefore even small deviations in exponent from those that are needed could destroy the straight lines. The revealing of straight lines in the intermediate intervals can be considered as experimental verification of (10.48).

One point should be explained. There exists an obvious arbitrariness in the definition of Re – for instance, the maximum velocity can be taken instead of the mean velocity, or the radius instead of the diameter. For (10.48) it is immaterial, because in fact this relation should be considered as the first term in an asymptotic expansion, valid when $\ln \mathrm{Re}$, not only Re itself, is large, so that a different definition of Re will influence only higher-order terms in the expressions for C and α.

Further processing allowed one to obtain with rather good accuracy

‡ It is essential that they are presented in tabular form, contrary to the data of other experimentalists.

§ Covering nearly three decimal orders of magnitude.

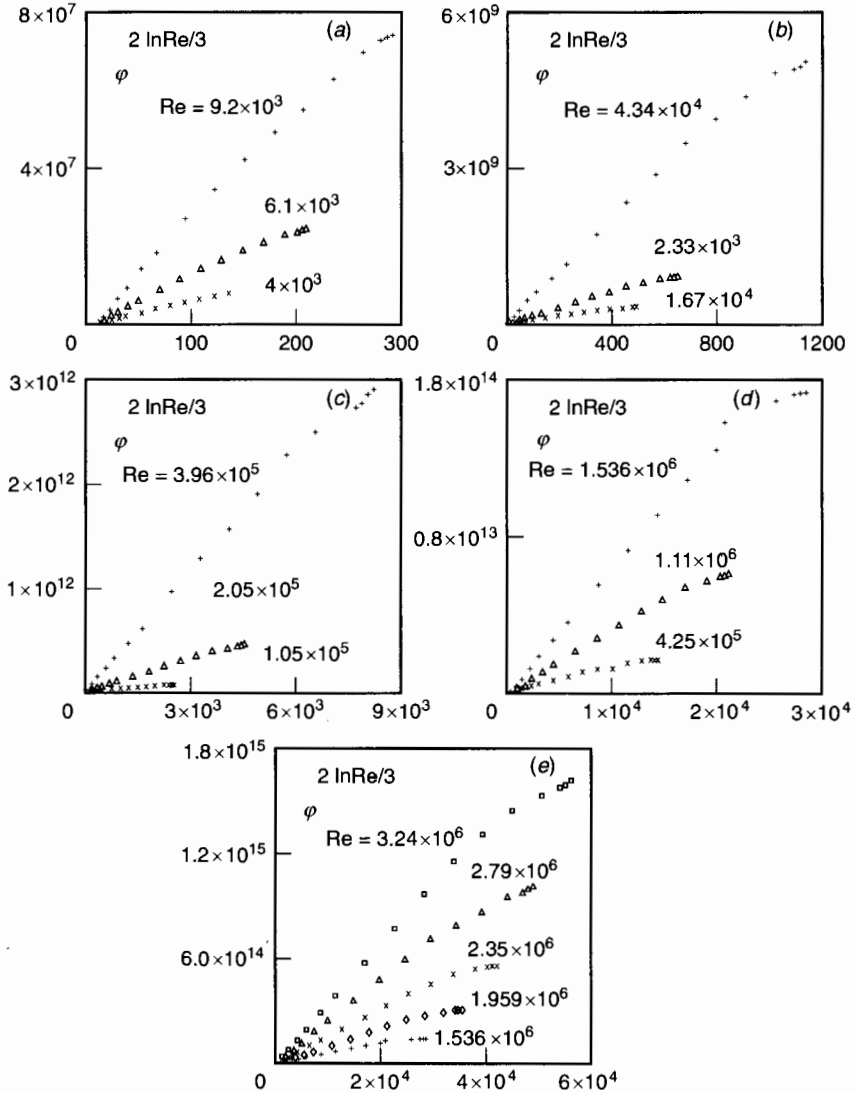

Figure 10.12(*a*)–(*e*). Each set of data for $\varphi^{(2\ln \mathrm{Re})/3}(\eta)$ reveals a straight line for an intermediate interval of values of η.

(Figure 10.13) the linear dependence (10.49) of the coefficient C in the power law (10.47) on $\ln \mathrm{Re}$. Therefore the power law (10.47) can be represented in the form

$$\varphi = \left(\frac{1}{\sqrt{3}} \ln \mathrm{Re} + \frac{5}{2}\right) \eta^{3/(2\ln \mathrm{Re})}. \tag{10.50}$$

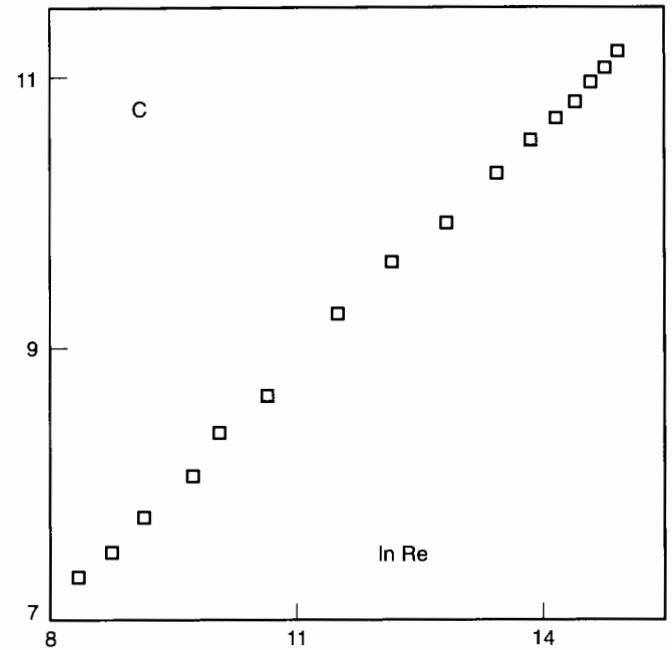

Figure 10.13. The function $C(\ln \mathrm{Re})$ obtained by the processing of experimental data.

Simple transformations allow to reduce the relation (10.50) to another form,

$$\Psi = \frac{1}{\alpha} \ln \frac{2\alpha\varphi}{\sqrt{3} + 5\alpha} = \ln \eta, \tag{10.51}$$

which is quasi-universal, i.e. independent of Reynolds number. It means that if the relations (10.50), (10.51) are correct, all experimental points for sufficiently large η and various Reynolds numbers (large enough to correspond to developed turbulence) should lie on a single curve in the Ψ, $\ln \eta$-plane, in fact, a straight line, the bisectrix of the first quadrant. Figure 10.14 shows that the overwhelming majority of the 256 experimental points available in the tables of the paper by Nikuradze (1932) occur, for large η, close to the bisectrix in accordance with (10.51). Certain points that occur rather far from the bisectrix correspond to measurements either in close proximity to the wall, where η is not sufficiently large for turbulence to have developed, or at comparatively low Reynolds numbers for which the turbulence is not fully developed. (Some errors

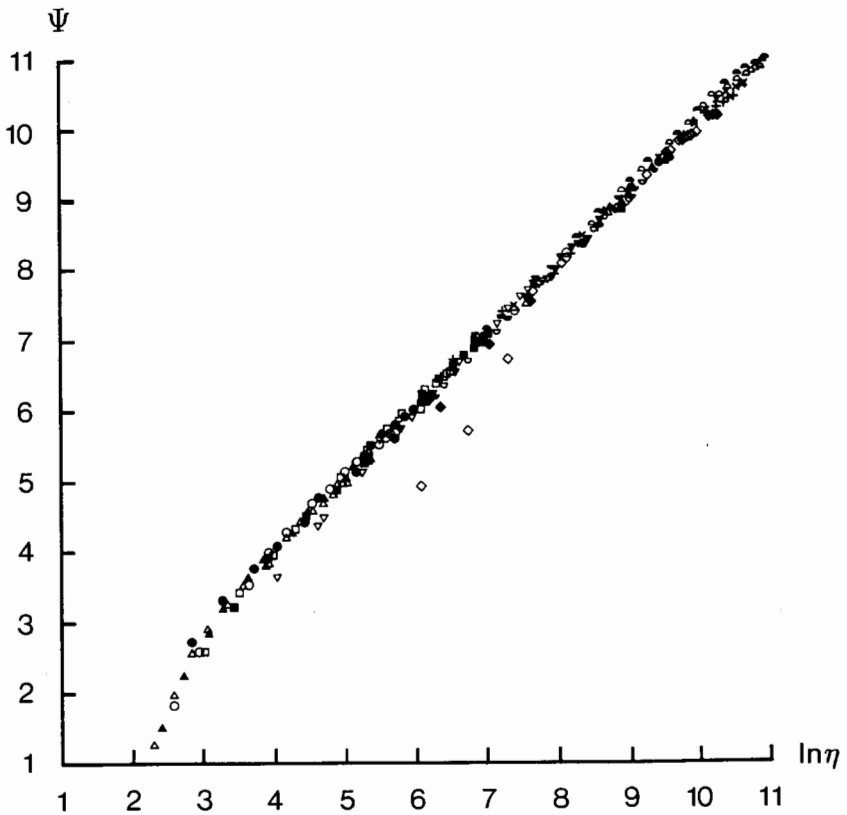

Figure 10.14. The experimental points in the coordinates Ψ, $\ln\eta$ settle down for large η close to the bisectrix of the first quadrant, confirming the quasi-universal form of the scaling law. The values of Re are as follows: △, 4×10^3; ▲, 6.1×10^4; ○, 9.2×10^3; •, 1.67×10^4; □, 2.33×10^4; ■, 4.34×10^4; ▩, 1.05×10^5; ▼, 2.05×10^5; ⊽, 3.96×10^5; ◡, 7.25×10^5; ◊, 1.11×10^6; ◆, 1.536×10^6; +, 1.959×10^6; ×, 2.35×10^6; ⌓, 2.79×10^6; ◓, 3.24×10^6.

in the measurements close to the wall, where the distance is comparable with the gauge size are also possible.)

As we have seen, in the φ, $\ln\eta$-plane the curves that represent the power laws for varying Reynolds numbers

$$\varphi = \left(\frac{1}{\sqrt{3}}\ln\mathrm{Re}+\frac{5}{2}\right)e^{(3\ln\eta)/(2\ln\mathrm{Re})} = F(\ln\eta,\mathrm{Re})\,, \qquad (10.52)$$

form a family of which the Reynolds number is the parameter. The

family possesses an envelope that satisfies both equation (10.52) and the equation $\partial_{\mathrm{Re}}F = 0$. The latter equation can easily be reduced to the form

$$\frac{3\ln\eta}{2\ln\mathrm{Re}} = \frac{\sqrt{3}}{10}\ln\eta\left[\left(1+\frac{20}{\sqrt{3}\ln\eta}\right)^{1/2}-1\right]. \qquad (10.53)$$

Eliminating $\ln\mathrm{Re}$ from (10.52) and (10.53) we obtain the equation of the envelope; this is represented in Figure 10.15. As is seen it is close to the straight line representing the universal logarithmic law with an empirically fitted constant $C_1 = 5.5$, even for rather moderate $\ln\eta$[†]. This seems to be natural because the envelope is the locus of the points where the derivative with respect to Reynolds number vanishes. It was, however, the first of the assumptions on which the derivation of the logarithmic law (10.45) was based.

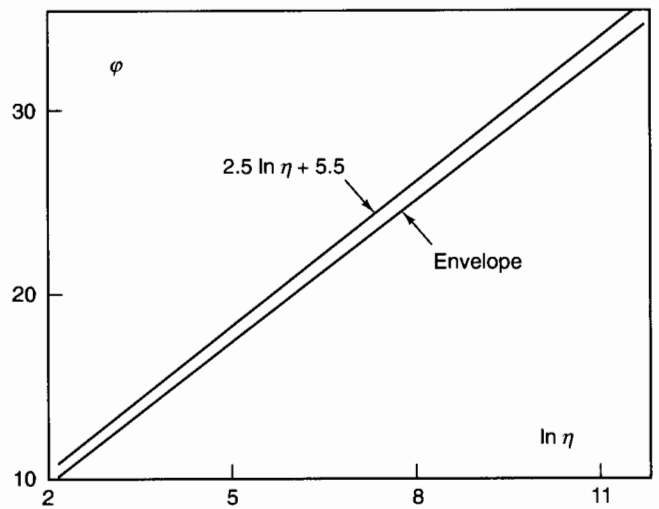

Figure 10.15. The envelope of the scaling law curves for fixed Re in the φ, $\ln\eta$-plane is very close to the generally accepted universal logarithmic law even at moderate $\ln\eta$.

Moreover, if we let $\ln\eta$ tend to infinity while remaining on one of the curves (10.52) at Re = const, the function $\Phi(\eta,\mathrm{Re})$ in the general similarity relation (10.43) obviously tends to infinity. However, if we let $\ln\eta$ tend to infinity while remaining on the envelope, i.e., we let $\ln\mathrm{Re}$ tend simultaneously to infinity, we will obtain a finite limit for $\Phi(\eta,\ln\mathrm{Re})$.

† The envelope is even closer to the straight line with the constant $C_1 = 5.1$, used for instance in the book by Monin and Yaglom (1971) (see Figure 10.11).

Indeed, for large $\ln \mathrm{Re}$ the relation (10.53) gives $(3\ln\eta)/(2\ln \mathrm{Re}) \to 1$, whence and from (10.52) we obtain

$$\varphi = \frac{\sqrt{3}e}{2}\ln\eta + \text{const}, \quad \Phi(\eta, \mathrm{Re}) \to \frac{\sqrt{3}e}{2}. \tag{10.54}$$

Therefore at large $\ln\eta$ all assumptions leading to the universal logarithmic law are fulfilled on the envelope and this envelope can be identified with this law. This allows us to obtain the value of the von Kármán constant:

$$\kappa = \frac{2}{\sqrt{3}e} \simeq 0.424. \tag{10.55}$$

Nikuradze (1932) himself, on the basis of processing his experimental data, arrived at the value $\kappa = 0.417$.

On the basis of the proposed scaling law (10.50) for the average velocity distribution a corresponding skin friction law can be proposed and compared with experimental data.

We define the skin friction dimensionless coefficient λ in the traditional way:

$$\lambda = \frac{\tau}{\rho\bar{u}^2/8} = 8\left(\frac{u_*}{\bar{u}}\right)^2. \tag{10.56}$$

According to (10.50) the following relation for the bulk average velocity $\bar{u}$ is obtained:

$$\begin{aligned}\bar{u} &= \frac{8}{d^2}\int_0^{d/2} u(z)\left(\frac{d}{2} - z\right)dz \\ &= u_*\frac{\sqrt{3}+5\alpha}{\alpha}\left(\frac{u_* d}{\nu}\right)^{\alpha}\frac{1}{2^\alpha(1+\alpha)(2+\alpha)}.\end{aligned} \tag{10.57}$$

In deriving (10.57) the fact was used that for developed turbulent flows in pipes we can neglect the contribution to the bulk flow rate of the viscous layer near the wall as well as the contribution of the region near the tube axis where the law (10.50) is not valid.

From (10.48),

$$\mathrm{Re} = \bar{u}d/\nu = e^{3/2\alpha} \tag{10.58}$$

whence and from (10.57) we obtain

$$\frac{u_* d}{\nu} = \left[e^{3/2\alpha}2^\alpha\frac{\alpha(1+\alpha)(2+\alpha)}{\sqrt{3}+5\alpha}\right]^{1/(1+\alpha)}, \tag{10.59}$$

and the final relation for the dimensionless skin friction coefficient λ corresponding to the scaling law (10.50) takes the form

$$\lambda = \frac{\tau}{\rho\bar{u}^2/8} = 8\left(\frac{u_*}{\bar{u}}\right)^2 = \frac{8}{\Psi^{2/(1+\alpha)}} \tag{10.60}$$

where

$$\Psi(\alpha) = \frac{e^{3/2}(\sqrt{3}+5\alpha)}{2^\alpha\alpha(1+\alpha)(2+\alpha)}, \quad \alpha = \frac{3}{2\ln \mathrm{Re}}. \tag{10.61}$$

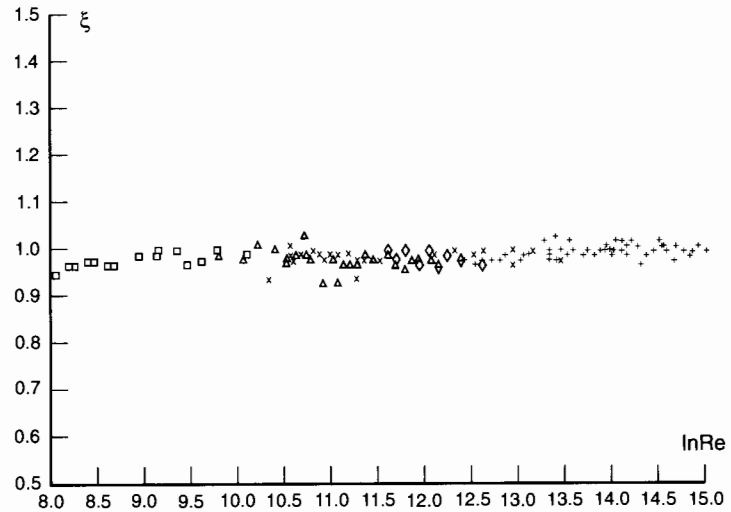

Figure 10.16. The experimental data for various pipes and various Reynolds numbers confirm the skin friction law (10.60), (10.61) which follows from scaling law (10.50) with rather good accuracy. The values of d are as follows: □, 1 cm; △, 2 cm, ◇, 3 cm; ×, 5 cm; +, 10 cm.

A comparison of values of λ predicted by (10.60) with experimental values (Nikuradze (1932), table 9) is presented in Figure 10.16. It was found to be less instructive to compare predictions (10.60), (10.61) with experimental data directly, since they coincide with very high accuracy. Therefore a different, more objective, form of comparison has been chosen: the quantity

$$\xi = \frac{\lambda_e}{\lambda} = \frac{\lambda_e}{8}\Psi^{2/(1+\alpha)}, \tag{10.62}$$

where λ_e is the experimentally determined value of the skin friction coefficient plotted as a function of $\ln \mathrm{Re}$. In table 9 of the paper, Nikuradze (1932) a total of 125 points is available, corresponding to various Reynolds numbers in a rather wide range from slightly supercritical ($\mathrm{Re} = 3.07 \times 10^3$) to very large ($\mathrm{Re} = 3.23 \times 10^6$). Ideally the quantity ξ would be equal to unity. As Figure 10.16 shows, nearly all deviations from this value lie within the experimental scatter range.

The coincidence of the experimental data concerning skin friction with predictions based on the scaling law (10.50) also contributes to the verification of this law.

10.2.2 The wall region of a turbulent shear flow – semi-empirical theory and Kolmogorov's similarity hypothesis

We now consider the wall region of the turbulent shear flow described in the preceding section in more a quantitative way, based on the semi-empirical theory proposed by Kolmogorov (1942). Kolmogorov's theory is based on closing the equations for the conservation of momentum and turbulent energy with the help of certain similarity hypotheses. Later we shall use this theory more than once; therefore it is appropriate to demonstrate here its basic ideas for a simple example, the wall region of a turbulent shear flow. Note that, independently, closely similar ideas were developed by Prandtl (1945).

We exclude from our consideration the region in close vicinity to the wall where the viscous stresses are comparable with the turbulent stresses due to momentum transfer by vortices. The equation for momentum balance for a shear flow can then be written in the form

$$-\rho\langle u'w'\rangle = \tau\,, \tag{10.63}$$

where u' and w', respectively, are the fluctuations in the velocity components longitudinal and transverse to the wall, ρ is the density of the fluid, and τ is the shear stress; in (10.63) we neglect the contribution of the viscous stresses in comparison with the turbulent Reynolds stresses. The equation for turbulent energy balance for a steady shear flow can be written in the form (Monin and Yaglom, 1971)

$$\langle u'w'\rangle\partial_z u + \partial_z\left\langle\left(\frac{p'}{\rho} + \frac{u'^2+v'^2+w'^2}{2}\right)w'\right\rangle + \epsilon = 0\,. \tag{10.64}$$

Here v' is the fluctuation in the transverse velocity component, p' the fluctuation in pressure, and ϵ the mean rate of dissipation of turbulent energy per unit mass of fluid. Equation (10.64) reflects the simple fact that the local balance of turbulent energy for a steady shear flow consists of the generation of turbulent energy by the mean motion (the first term), the diffusive influx of turbulent energy (the second term), and the dissipation of turbulent energy into heat (the third term). For the problem of interest the transfer of turbulent energy by diffusion is small and we can neglect it.

We introduce the coefficient k of momentum exchange by the relation

$$\langle u'w'\rangle = -k\partial_z u\,. \tag{10.65}$$

We stress that for a shear flow the relation (10.65) is simply a redesignation and does not involve any additional hypothesis.

As was said earlier, a developed turbulent flow contains a great number of vortices, creating irregular rapidly varying motion. The basic idea of Kolmogorov was that it is possible to assume as a first (perhaps, 'naive', as he used to say) approximation that the local structure of this set of vortices is statistically the same for all developed turbulent flows as far as dimensionless quantities are concerned. Therefore according to Kolmogorov's (1942) hypothesis, the momentum exchange coefficient and the rate of energy dissipation ϵ at a given point in the flow are determined only by the local values of two kinematic quantities of different dimensions, e.g. the mean turbulent energy per unit mass,

$$b = \tfrac{1}{2}\langle u'^2 + v'^2 + w'^2\rangle\,,$$

and the turbulence external length scale l. (Another possibility will be considered later). Dimensional analysis leads in the standard way to the relations

$$k = l\sqrt{b}\,, \quad \epsilon = \gamma^4 b^{3/2}/l\,, \tag{10.66}$$

where, by virtue of identification of the length scale to within a constant factor, the constant in the first relation can be taken to be equal to unity, and the constant γ is close to 0.5 by estimates from experimental data (see Monin and Yaglom, 1971).

Substituting (10.65) and (10.66) into (10.63) and (10.64), and neglecting in the latter equation the contribution of the diffusion of turbulent energy, we get a system of equations in the form

$$l\sqrt{b}\partial_z u = u_*^2, \quad l\sqrt{b}(\partial_z u)^2 - \frac{\gamma^4 b^{3/2}}{l} = 0\,, \tag{10.67}$$

where $u_* = (\tau/\rho)^{1/2}$ is the friction velocity.

This system is still not closed, since the turbulence length scale l is not yet defined. In accordance with subsection 10.2.1, in the wall region of a turbulent shear flow, where the friction velocity u_* is constant, the turbulence length scale l depends on the friction velocity u_*, the kinematic viscosity ν, the vertical coordinate z, and the external length scale Λ. Dimensional analysis gives

$$l = z\Phi_l(\mathrm{Re}_l, \mathrm{Re}_*)\,, \tag{10.68}$$

where, as before, $\mathrm{Re}_l = u_* z/\nu$ and $\mathrm{Re}_* = u_*\Lambda/\nu$ are the local and global Reynolds numbers. Under the assumption of complete similarity in both Reynolds numbers, at large Re_l and Re_* the function Φ_1 is identically equal to a constant that it is convenient to denote by $\kappa\gamma$, γ being the constant introduced earlier and κ a new constant (the von Kármán constant), so that

$$l = \kappa\gamma z\,. \tag{10.69}$$

Substituting (10.69) into (10.67), we get

$$u = \frac{u_*}{\kappa} \ln z + \text{const}, \quad b = \frac{u_*^2}{\gamma^2}, \tag{10.70}$$

i.e., the logarithmic law for the velocity distribution (10.45), obtained earlier from more general considerations. If we assume that for this flow similarity of the flow in the local Reynolds number is incomplete, then the relation for the turbulent length scale assumes the form

$$l = z\left(\frac{u_* z}{\nu}\right)^{-\alpha} \Phi_l(\mathrm{Re}_*), \tag{10.71}$$

and from this and (10.67) we find

$$\frac{z\partial_z u}{u_*} = \left(\frac{u_* z}{\nu}\right)^{\alpha} \Phi(\mathrm{Re}_*), \quad \Phi(\mathrm{Re}_*) = \frac{\gamma}{\Phi_l(\mathrm{Re}_*)}, \qquad \alpha = \alpha(\mathrm{Re}_*), \tag{10.72}$$

i.e. the scaling law (10.47), obtained earlier from more general considerations.

10.2.3 Unsteady phenomena in the viscous sublayer of a turbulent shear flow

In the last few decades fundamental investigations of turbulent shear flows in the immediate vicinity of a wall have been published. (See Kline, Reynolds, Schraub and Runstadler, 1967; Corino and Brodkey, 1969; Kim, Kline and Reynolds, 1971; Offen and Kline, 1975.) By a skilful combination of visualization methods (hydrogen bubbles and tracing pigments) and thermoanemometric methods it was shown in these papers that turbulent flow close to the wall has a complicated, essentially unsteady, and spatially inhomogeneous structure.

The question concerns the phenomena in a viscous sublayer where the global characteristics of the flow are governed by the shear stress τ, the density ρ, and the kinematic viscosity ν of the fluid, and also by some external length scale Λ, for example the momentum thickness of the boundary layer. Thus, the kinematic properties must be governed only by the friction velocity $u_* = (\tau/\rho)^{1/2}$, the external length scale Λ, and the kinematic viscosity ν. It turns out that, in the range of thickness of the order of some tens of the characteristic linear scale ν/u_* of the viscous sublayer, there arise with a statistically determined frequency local separations of the flow, as a result of which horseshoe-shaped vortices are generated, move deep into the flow, and in their own right stimulate the occurrence of new local separations. This generates a chequered pattern of longitudinal strips of the retarded flow. Interactions between the horseshoe vortices that arise, lead to the local loss of stability and

bursting. As is convincingly shown in the papers of Kline and his associates, basically it is just these bursts that determine the generation of turbulence close to a rigid boundary in a turbulent shear flow. An illustration of the character of the local flows that arise is given by the photograph in Figure 10.17, which shows the twisting by these flows of originally vertical lines of hydrogen bubbles.

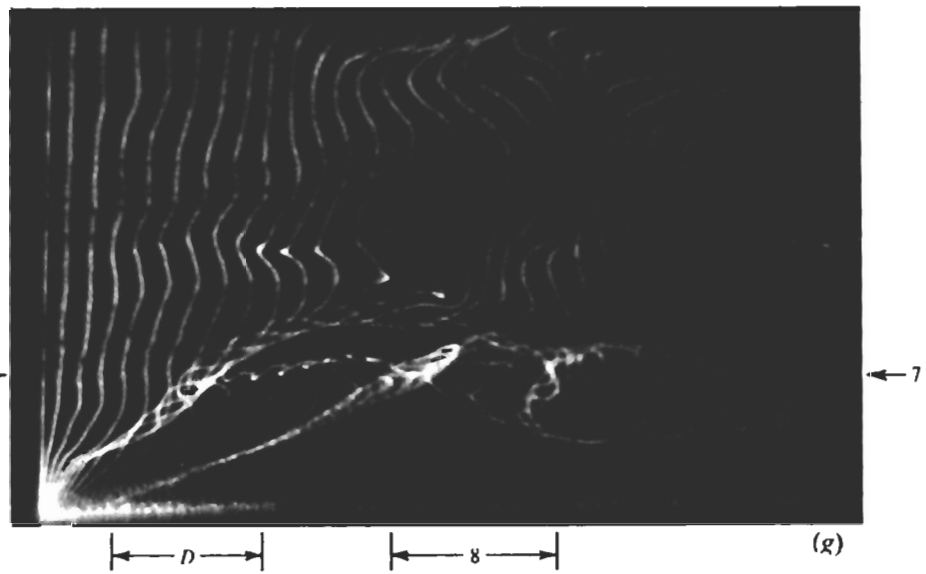

Figure 10.17. In the wall region of a turbulent shear flow there exists a complicated unsteady and spatially inhomogeneous flow. Shown in the photograph is the twisting by a vortex of initially vertical lines of hydrogen bubbles. From Kim, Kline and Reynolds (1971).

Despite the complicated character of the local flows in the viscous sublayer of a turbulent shear flow, some of their statistical characteristics are well described by scaling laws. We demonstrate this here for the mean time T_B between bursts, i.e., the mean period of the cyclic process occurring close to the wall. This quantity can depend, according to the above, on the friction velocity u_*, the kinematic viscosity ν, and the external length scale Λ, whence, applying dimensional analysis, we obtain

$$T_\mathrm{B} = \frac{\nu}{u_*^2} \Phi\left(\frac{u_* \Lambda}{\nu}\right). \tag{10.73}$$

The parameter $u_*\Lambda/\nu$ is very large, of order 100 or more; therefore it was natural to take, as a first assumption, one equivalent to the hypothesis of complete similarity in this parameter. This gives

$$T_\mathrm{B} = C\frac{\nu}{u_*^2}, \tag{10.74}$$

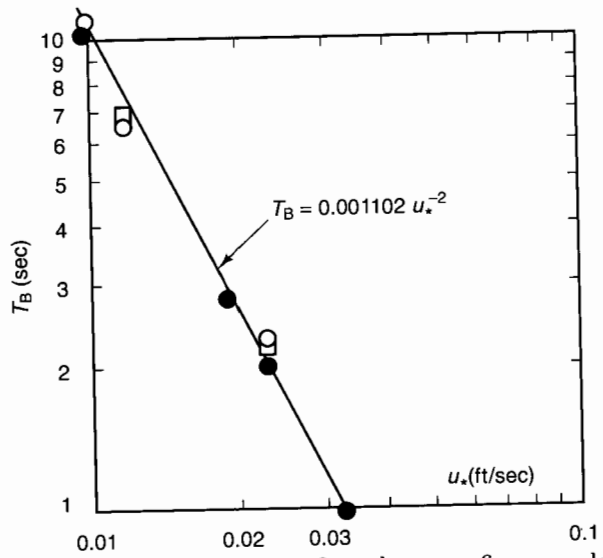

Figure 10.18. Experimental data at first glance confirm complete similarity of the dependence of the time T_B between bursts on the parameter $u_*\Lambda/\nu$, for large values of this parameter. From Kim, Kline and Reynolds (1971).

where C is a constant. The experimental data at first glance confirm the relation (10.74) (cf. Figure 10.18). However, an attempt to apply (10.74) to the experiments of B.J. Tu and W.W. Willmarth (see Rao, Narasimha and Badri Narayanan, 1971), in which significantly higher friction velocities were achieved, led to errors of more than an order of magnitude. Actually, as was shown by Rao, Narasimha and Badri Narayanan (1971), there is no complete similarity in the parameter $u_*\Lambda/\nu$. Consideration of more complete experimental data in the latter paper and that by Kim, Kline and Reynolds (1971) led to the relation

$$\Phi = 0.65\left(\frac{U\Lambda}{\nu}\right)^{0.73} \tag{10.75}$$

(see Figure 10.19). Here U is the free-stream velocity and Λ the momentum thickness of the boundary layer. As is well known the ratio u_*/U is close to a power-law function of the global Reynolds number in a restricted interval of this parameter. This relation therefore reveals what appears to be incomplete similarity with respect to the parameter $u_*\Lambda/\nu$.

10.2.4 Decay of a turbulent burst in a fluid at rest

1. The problem of the decay of instantaneously formed turbulent bursts

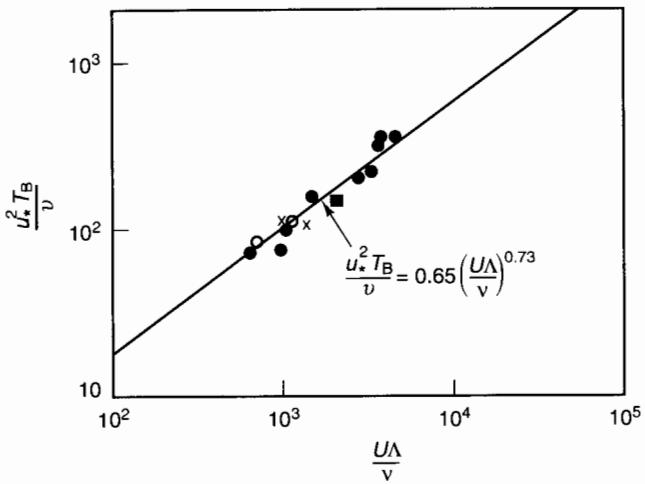

Figure 10.19. Experiments over a wider range of values of the parameter $U\Lambda/\nu$ show incomplete similarity in this parameter. From Kim, Kline and Reynolds (1971).

is of special interest for turbulence studies. Indeed, the formation of turbulent bursts by intersecting or self-intersecting vortices is (see the preceding subsection) one of the leading mechanisms of turbulence generation. From the theoretical viewpoint this problem deserves consideration as a fundamental local disturbance, like the heat source or the very intense explosion at the early stages of a nuclear blast considered in chapter 2. We will present here the solution for a symmetric initial form, based on several assumptions concerning the turbulence behaviour. Initially the burst has, generally speaking a non-symmetric form (Figure 10.20(a)). However, it then takes a more or less symmetric form and only thereafter begins to extend.

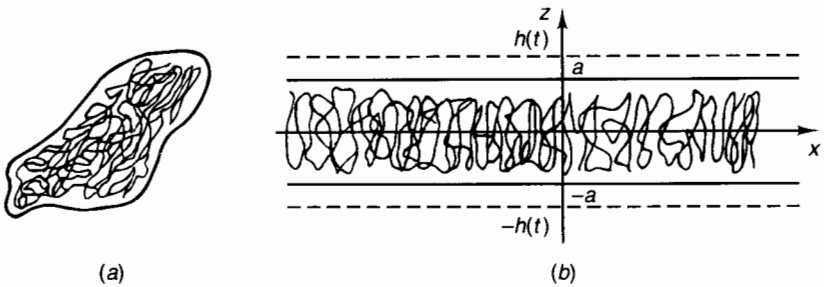

Figure 10.20. Two stages of a turbulent burst in a fluid at rest. (a) The burst initially has an arbitrary form; (b) the burst now has the form of a statistically horizontally uniform layer.

Thus, we shall consider the evolution (extension and decay) in a homogeneous quiescent fluid of a statistically horizontally-homogeneous turbulent burst (Figure 10.20(b)) enclosed initially in a layer between the horizontal planes $z = a$ and $z = -a$. Let the initial turbulent energy per unit area of the plane layer boundary be

$$Q = \int_{-a}^{a} b(z,0)dz \tag{10.76}$$

where $b(z,t)$ is, as before, the turbulent energy of unit mass of fluid.

The dimension of Q is clearly L^3T^{-2}. Evidently from two kinematic quantities Q and a a kinematic quantity of arbitrary dimension can be composed,; so, for instance, the initial conditions for the turbulent energy and the dissipation rate per unit mass can be presented in the form

$$b(z,0) = \frac{Q}{a}u_0(\zeta), \quad \epsilon(z,0) = \frac{Q^{3/2}}{a^{5/2}}v_0(\zeta)\,. \tag{10.77}$$

Here $\zeta = z/a$, $u_0(\zeta)$ and $v_0(\zeta)$ are dimensionless even functions, identically equal to zero at $|\zeta| \geq 1$.

Thus, all kinematic statistical properties of the motion for arbitrary time t at an arbitrary point z are determined by the parameters

$$Q, t, z, a\,. \tag{10.78}$$

The first two of these governing parameters have independent dimensions. Dimensional analysis gives, accordingly, the following relations for the turbulent energy of unit mass, $b(z,t)$, and the dissipation rate of turbulent energy per unit mass, $\epsilon(z,t)$:

$$b = \frac{Q^{2/3}}{t^{2/3}}B(\xi,\eta), \quad \epsilon = \frac{Q^{2/3}}{t^{5/3}}E(\xi,\eta) \tag{10.79}$$

where

$$\xi = \frac{z}{Q^{1/3}t^{2/3}}\,, \quad \eta = \frac{a}{Q^{1/3}t^{2/3}}\,. \tag{10.80}$$

Here $B(\xi,\eta)$, $E(\xi,\eta)$ are dimensionless functions of their dimensionless arguments. For a half-width $h(t)$ of the layer a relation is obtained from the same dimensional considerations,

$$h = Q^{1/3}t^{2/3}H(\eta)\,, \tag{10.81}$$

because, evidently h does not depend on z and does depend on three other arguments. Here $H(\eta)$ is a dimensionless function of its dimensionless argument. The basic interest is in considering the asymptotic solution at large times when the layer thickness is much larger than the initial one, $h(t) \gg a$, i.e., the asymptotics of the functions (10.79), (10.81) at $\eta \ll 1$.

2. The simplest assumption is that for $\eta \ll 1$ there is complete similarity in the parameter η. This means that finite limits different from zero exist of the functions $B(\xi,\eta)$, $E(\xi,\eta)$, and $H(\eta)$, as $\eta \to 0$,

$$B(\xi) = \lim B(\xi,\eta), \quad E(\xi) = \lim E(\xi,\eta), \quad \xi_0 = \lim H(\eta)\,, \tag{10.82}$$

so that the self-similar asymptotic solution takes the form

$$b = \frac{Q^{2/3}}{t^{2/3}}B(\xi), \quad \epsilon = \frac{Q^{2/3}}{t^{5/3}}E(\xi), \quad h = \xi_0 Q^{1/3}t^{2/3}\,. \tag{10.83}$$

This assumption is, however, incorrect. Indeed, the equation of turbulent energy balance for the case of a horizontally-homogeneous shearless flow assumes the form

$$\partial_t b + \partial_z q_b = -\epsilon \tag{10.84}$$

where q_b is the turbulent flux of turbulent energy. Let us integrate this equation within the limits $z = -h(t)$ to $z = h(t)$ taking into account that at the boundaries of the layer $z = \pm h(t)$ both turbulent energy and its flux vanish:

$$b(\pm h(t),t) = 0\,, \quad q_b(\pm h(t),t) = 0\,. \tag{10.85}$$

We obtain that the time derivative of the total turbulent energy per unit area of the layer is negative,

$$\frac{d}{dt}\int_{-h(t)}^{h(t)} b(z,t)dz = -\int_{-h(t)}^{h(t)} \epsilon(z,t)dz < 0 \tag{10.86}$$

because ϵ, the dissipation rate of turbulent energy, is a positive quantity within the turbulent layer. At the same time it follows from the asymptotic solution (10.83) that the turbulent energy per unit area

$$\int_{-h}^{h} b(z,t)dz = \frac{Q^{2/3}}{t^{2/3}}\int_{-h}^{h} B(\xi)dz = Q\int_{-\xi_0}^{\xi_0} B(\xi)d\xi = \text{const}\,Q \tag{10.87}$$

is time independent. The contradiction obtained proves that the assumption of complete similarity is incorrect.

3. We assume, therefore, incomplete similarity with respect to the parameter η, i.e., we assume that the functions $B(\xi,\eta), E(\xi,\eta)$ and $H(\eta)$ at $\eta \to 0$ have power-type asymptotics,

$$B = \eta^{\lambda_1}B_0\left(\frac{\xi}{\eta^{\nu_1}}\right), \quad E = \eta^{\lambda_2}E_0\left(\frac{\xi}{\eta^{\nu_1}}\right), \quad H = \text{const}\,\eta^{\nu_2}\,, \tag{10.88}$$

where λ_1, λ_2, ν_1, ν_2 are constants.

We can use the fact that the quantities b, ϵ and q should satisfy the turbulent energy balance equation (10.84) and therefore that this equation should be reduced to an ordinary differential equation involving the functions of one variable ξ/η^{ν_1}: $B_0\,(\xi/\eta^{\nu_1})$ and $E_0\,(\xi/\eta^{\nu_1})$. This allows

us to express three of the constants λ_1, λ_2, ν_1, ν_2 via one of them, say ν_1. The asymptotic solution is reduced to the form

$$b = At^{-2\mu}F(\zeta), \quad \epsilon = A^2t^{-2\mu-1}G(\zeta), \quad h = At^{1-\mu}. \tag{10.89}$$

Here

$$F(\zeta) = \text{const}_1\, B_0(\zeta), \quad G(\zeta) = \text{const}_2\, E_0(\zeta),$$
$$\zeta = \frac{z}{h} = \frac{z}{At^{(1-\mu)}}, \quad A = \text{const}\, Q^{(1-\mu)/2}a^{(3\mu-1)/2}, \quad \mu = \frac{1+2\nu_1}{3}. \tag{10.90}$$

We must emphasize two essential points: the parameter μ, which determines the layer extension and turbulent energy decay rate cannot be obtained from dimensional considerations, and both the initial bulk energy of the turbulent layer per unit area, Q, and the initial layer thickness a enter the constant A in some powers.

To determine the parameter μ an eigenvalue problem must be stated and solved.

First we shall use the (b, ϵ) semi-empirical turbulence model (the traditional notation is the k, ϵ model). This model, based on the idea of A.N. Kolmogorov (1942), was elaborated by D.B. Spalding, B.E. Launder and their associates (Launder, Morse, Rodi and Spalding, 1972; Launder and Spalding, 1974; Hanjalic and Launder, 1972). For a comprehensive review see Reynolds (1976). According to this model the dissipation rate ϵ is taken in addition to the specific turbulent energy as the second kinematic quantity necessary to determine all the kinematic properties of turbulent flow. In addition to the equation for turbulent energy balance (10.84) the equation for balance of the dissipation rate is used. This equation is obtained basically in the same way as the turbulent energy balance equation and, for the case under consideration of the horizontally-homogeneous layer and shearless flow, assumes the form (see, e.g., Reynolds, 1976)

$$\partial_t \epsilon + \partial_z q_\epsilon = -U. \tag{10.91}$$

Here q_ϵ is the turbulent flux of the dissipation rate and U is the rate of homogeneization of turbulent energy; they are the one-point moments of the velocity and the velocity-gradient fluctuations.

Let us introduce turbulent exchange coefficients, k_b for the turbulent energy and k_ϵ for the dissipation rate, according to the relations

$$k_b = -\frac{q_b}{\partial_z b}, \quad k_\epsilon = -\frac{q_\epsilon}{\partial_z \epsilon}. \tag{10.92}$$

We emphasize that for the case of a horizontally-homogeneous layer these relations do not contain any additional assumptions. According to the Kolmogorov similarity hypothesis, which is assumed to be applicable in the turbulent part of the flow, the turbulent vortex field in the

developed flow is statistically self-similar. Therefore all kinematic flow properties are determined, each to within a constant, by any two of them having different kinematic dimensions. We take as such the governing properties b and ϵ.

Dimensional analysis gives

$$k_b = \alpha\frac{b^2}{\epsilon}, \quad k_\epsilon = \beta\frac{b^2}{\epsilon}, \quad U = \gamma\frac{\epsilon^2}{b} \tag{10.93}$$

where the coefficients of α, β, γ, according to the assumed hypothesis, should be universal constants. Roughly speaking it is so, and these constants have been determined by comparison with experiment for some special cases (see, e.g., Reynolds, 1976).

Thus, equations (10.84) and (10.91) take the form

$$\partial_t b = \alpha\partial_z\left(\frac{b^2}{\epsilon}\partial_z b\right) - \epsilon \tag{10.94}$$

$$\partial_t \epsilon = \beta\partial_z\left(\frac{b^2}{\epsilon}\partial_z \epsilon\right) - \gamma\frac{\epsilon^2}{b} \tag{10.95}$$

and (10.94), (10.95) form a closed set of equations for the turbulent energy and turbulent energy dissipation rate.

4. After substitution of the solution in the form (10.89) into the system (10.94), (10.95), a set of ordinary differential equations is obtained for the functions $f = \beta F$ and $g = \beta G$:

$$\frac{\alpha}{\beta}\frac{d}{d\zeta}\left(\frac{f^2}{g}\frac{df}{d\zeta}\right) + (1-\mu)\zeta\frac{df}{d\zeta} + 2\mu f - g = 0 \tag{10.96}$$

$$\frac{d}{d\zeta}\left(\frac{f^2}{g}\frac{dg}{d\zeta}\right) + (1-\mu)\zeta\frac{dg}{d\zeta} + (1+2\mu)g - \gamma\frac{g^2}{f} = 0 \tag{10.97}$$

By symmetry, only one half of the layer, $0 \le z \le h(t)$, need be considered, with boundary conditions at $z = 0$ and $z = h(t)$. At the boundary $z = h(t)$ the turbulent energy b, the dissipation rate ϵ, and their fluxes q_b and q_ϵ must be continuous. However, outside the layer there is fluid at rest. Therefore at $z = h(t)$ the following conditions must be fulfilled.

$$b = 0, \quad \epsilon = 0, \quad q_b = 0, \quad q_\epsilon = 0. \tag{10.98}$$

From (10.98) and from (10.92) and (10.93) we find boundary conditions for the set (10.94), (10.95):

$$b = 0, \quad \epsilon = 0, \quad \frac{b^2}{\epsilon}\partial_z b = 0, \quad \frac{b^2}{\epsilon}\partial_z \epsilon = 0 \quad \text{at } z = h(t). \tag{10.99}$$

Using the self-similar representation of the solution (10.89) we obtain

a first group of boundary conditions for the system of ordinary equations (10.96), (10.97):

$$f = g = 0\,, \quad \frac{f^2}{g}\frac{df}{d\zeta} = 0\,, \quad \frac{f^2}{g}\frac{dg}{d\zeta} = 0 \quad \text{at } \zeta = 1\,. \tag{10.100}$$

Furthermore, owing to symmetry with respect to the middle plane of the layer, $z = 0$, the fluxes are equal to zero:

$$q_b = q_\epsilon = 0 \quad \text{at } z = 0\,. \tag{10.101}$$

From (10.101) and from (10.92) and (10.93) we obtain the second group of boundary conditions, this time at the boundary $\zeta = 0$, for the system (10.96), (10.97):

$$\frac{f^2}{g}\frac{df}{d\zeta} = 0\,, \quad \frac{f^2}{g}\frac{dg}{d\zeta} = 0 \quad \text{at } \zeta = 0\,. \tag{10.102}$$

We have obtained, therefore, a boundary-value problem (10.100), (10. 102) for the system of second-order ordinary differential equations (10.96), (10.97), which contains a parameter μ. We shall restrict ourselves further to the case $\alpha = \beta$: the recommended values of the parameters α and β give for the ratio α/β an interval between 0.7 and 1.2.

A more detailed investigation shows that there exists a class of solutions f, g, that are positive at $0 \le \zeta \le 1$, identically equal to zero at $\zeta \ge 1$, continuous, having continuous quantities:

$$\frac{f^2}{g}\frac{df}{d\zeta}\,, \quad \frac{f^2}{g}\frac{dg}{d\zeta} \tag{10.103}$$

(the fluxes must also be continuous).

In the vicinity of the point $\zeta = 1$ at $\zeta < 1$ the solution satisfying the conditions (10.100) is expanded in series:

$$f = c(1-\mu)(1-\zeta) + \dots\,, \quad g = c^2(1-\mu)(1-\zeta) + \dots\,. \tag{10.104}$$

Here the positive quantity c, along with μ, is a parameter of the problem. Each pair of values c, μ determines uniquely non-trivial solutions to the system (10.96), (10.97) satisfying the conditions (10.100). It is necessary to find the values of the parameters c, μ for which the solutions also satisfy the conditions (10.102). Thus, as it is customary for self-similar solutions of the second kind we have obtained a nonlinear eigenvalue problem for determining the time degrees in the self-similar variables.

This problem is easily solved analytically. Indeed, let us assume that $g = cf$ over the whole interval $0 \le \zeta \le 1$. Substituting this relation into (10.96), (10.97) we obtain for the function $f(\zeta)$ two second-order

ordinary differential equations that coincide if $c = 1/(\gamma - 1)$. For this value of c the equation for f takes the form

$$\frac{1}{c}\frac{d}{d\zeta}\left(f\frac{df}{d\zeta}\right) + (1-\mu)\zeta\frac{df}{d\zeta} + 2\mu f - cf = 0\,. \tag{10.105}$$

Integrating from $\zeta = 0$ to $\zeta = 1$ and using boundary conditions (10.100) and (10.102), we obtain

$$(1 - 3\mu + c)\int_0^1 f\,d\zeta = 0 \tag{10.106}$$

whence

$$\mu = \frac{1+c}{3} = \frac{\gamma}{3(\gamma-1)} \tag{10.107}$$

because the function f is positive and so is its integral in (10.106). For the values $c = 1/(\gamma-1)$ and $\mu = \gamma/3(\gamma-1)$ the equation (10.105) can be simply integrated:

$$\begin{gathered} f = D(1-\zeta^2), \quad g = D(1-\zeta^2)(\gamma-1)^{-1} \quad (0 \le \zeta \le 1)\,. \\ f = g \equiv 0 \quad (\zeta \ge 1) \end{gathered} \tag{10.108}$$

where $D = (2\gamma/3 - 1)/2(\gamma-1)^2$. Thus, the solution (10.89) assumes the final form

$$\begin{gathered} b = \frac{A^2}{\alpha t^{2\mu}} D\left(1 - \frac{z^2}{h^2}\right)\,, \quad \epsilon = \frac{A^2}{\alpha t^{2\mu+1}}\frac{D}{(\gamma-1)}\left(1 - \frac{z^2}{h^2}\right) \quad (0 \le z \le h(t)) \\ h(t) = At^{(2\gamma-3)/3(\gamma-1)}\,, \quad b = \epsilon = 0 \quad (z \ge h(t)) \\ A = \text{const}\, Q^{(2\gamma-3)/6(\gamma-1)} a^{1/2(\gamma-1)} \end{gathered} \tag{10.109}$$

In particular, for the recommended value $\gamma = 2$ the form of the solution is especially simple:

$$\begin{gathered} b = \frac{A^2}{\alpha t^{4/3}} D\left(1 - \frac{z^2}{h^2}\right)\,, \quad \epsilon = \frac{A^2}{\alpha t^{7/3}} D\left(1 - \frac{z^2}{h^2}\right) \quad (0 \le z \le h(t)) \\ h(t) = At^{1/3}\,, \quad A = \text{const}\, Q^{1/6} a^{1/2}\,. \end{gathered} \tag{10.110}$$

So, the solution is essentially different from (10.83), which was obtained from 'naive' dimensional considerations.

5. Another closing of the system can be obtained within the frames of a different turbulence model, the so-called b, l model based on the same similarity hypothesis but a different choice of second governing kinematic quantity: the external length scale l instead of ϵ.

According to the dimensional analysis the relations

$$k_b = l\sqrt{b}\,, \quad \epsilon = c_1 b^{3/2}/l \tag{10.111}$$

hold, where c_1 is a constant (the constant in the relation for k_b can be

assumed to be equal to unity by corresponding renormalization of the length scale). The equation for turbulent energy balance (10.84) takes the form

$$\partial_t b = \partial_z l\sqrt{b}\partial_z b - c_1\frac{b^{3/2}}{l}. \tag{10.112}$$

To close this equation the simplest assumption, $l = \alpha_1 h$, $\alpha_1 = \text{const}$ is made: we assume that the length scale is constant over the turbulent layer and is proportional to its thickness. So, we assume that the characteristic size of the vortices is a fixed fraction of the layer thickness and so we neglect the time of adjustment of the vortices to the layer thickness. The equation (10.112) then assumes a closed but non-local form:

$$\partial_t b = \frac{2}{3}\alpha_1 h(t)\partial_{zz}^2 b^{3/2} - \frac{c_1}{\alpha_1}\frac{b^{3/2}}{h(t)}. \tag{10.113}$$

The non-locality of (10.113) is related to the fact that the width $h(t)$ entering the right-hand side is a global functional of the solution $b(z,t)$.

The asymptotic solution to the equation (10.113) is represented, as before, in the form (10.89):

$$b = A^2 t^{-2\mu} f(\zeta), \quad \zeta = \frac{z}{h}, \quad h = At^{1-\mu}.$$

For determining the function f and the parameter μ the following relations are obtained from equation (10.113), the boundary conditions (10.85) and the symmetry conditions:

$$\begin{gathered}\frac{d}{d\zeta}\left(\alpha_1\sqrt{f}\frac{df}{d\zeta}\right) + (1-\mu)\zeta\frac{df}{d\zeta} + 2\mu f - \frac{c_1}{\alpha_1}f^{3/2} = 0;\\ \frac{df^{3/2}}{d\zeta} = 0 \quad \text{at } \zeta = 0; \quad f = 0, \ \frac{df^{3/2}}{d\zeta} = 0 \quad \text{at } \zeta = 1.\end{gathered} \tag{10.114}$$

These relations again form a nonlinear eigenvalue problem. Due to the group invariance property the eigenvalue μ depends only on the combination c_1/α_1^2. The eigenvalue problem is easily solved numerically; its solution is represented in Figure 10.21.

The solutions based on the two closure hypotheses, i.e., the b, l and b, ϵ models, are basically identical. The most essential differences are the sharper decrease of turbulent energy near the boundary and the vanishing of the length scale $l = c_1 b^{3/2}/\epsilon$ at the boundary in the b, ϵ model.

6. Batchelor and Linden (1992) noted that in the problem of turbulent burst evolution there exists an invariant of instructive form.

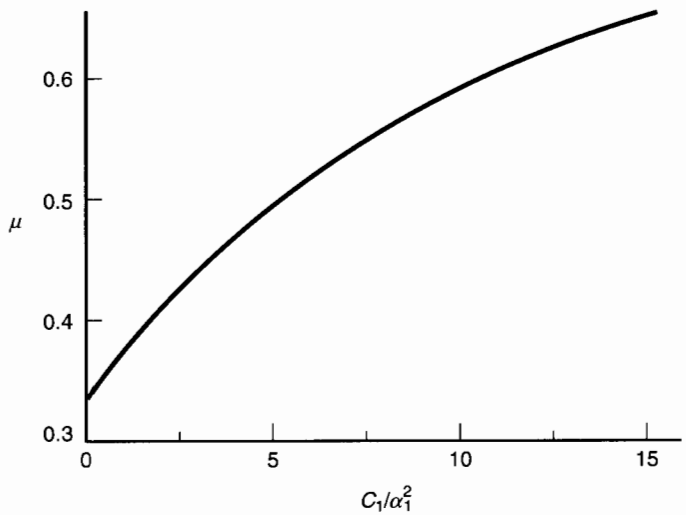

Figure 10.21. The eigenvalue μ in the b, l model versus the parameter c_1/α_1^2.

Consider the turbulent energy per unit area at time t:

$$Q(t) = \int_{-h}^{h} b(z,t)dz. \tag{10.115}$$

At the asymptotic stage of the motion, we have, according to the solution (10.89),

$$Q(t) = \text{const}\, A^3 t^{1-3\mu}, \quad h = At^{1-\mu}, \tag{10.116}$$

where the constant equals $\int_{-1}^{1} f(\zeta)d\zeta$. Therefore the quantity

$$Q(t)[h(t)]^{(3\mu-1)/(1-\mu)} = \text{const}\, A^{2/(1-\mu)} = \text{const}_1 Q a^{(3\mu-1)/(1-\mu)} \tag{10.117}$$

is preserved in time at the asymptotic stage of turbulent-burst evolution. At the initial, non-self-similar stage of turbulent-burst evolution the relations (10.116) and (10.117) do not hold, but it is instructuve that the value of the integral (10.117) is preserved if instead of the initial distribution of turbulent energy its distribution at an arbitrary moment of time is taken.

Let us consider the relevant constants. Numerical calculation of the eigenvalue in the second variant (the b, l model) shows that the value $\mu = 2/3$, obtained in the b, ϵ model for the recommended value $\gamma = 2$ corresponds to $c_1/\alpha_1^2 \simeq 17$. According to (10.111), in the b, l model $l = c_1 b^{3/2}/\epsilon$, $k_b = c_1 b^2/\epsilon$. Comparing with (10.93), we obtain $c_1 = \alpha$. Therefore $\alpha_1 = (\alpha/17)^{1/2}$. The recommended (Reynolds, 1976) range of

values of α gives an estimation of c_1 as 0.06–0.085 and of α, as 0.063–0.071.

7. Thus, we have presented here, within the framework of the basic models of semi-empirical turbulence theory, the solution to the problem of the evolution of a turbulent burst having the form of a plane layer. In the same way the solutions for cylindrical ($\mu = 3/4$) and spherical ($\mu = 4/5$) bursts can be obtained. The problem statement and the solutions presented here were given in papers by Barenblatt (1983) and by Barenblatt, Galerkina and Luneva (1987).

The statement and solutions to the problem of turbulent-burst evolution considered in this section have many non-standard properties deserving special attention, as follows.

An important point in the problem statement is that the ambient fluid is quiescent. Therefore the turbulent energy, the turbulent energy dissipation rate, and their fluxes are equal to zero at the boundary of the burst. Zero is also a number, and this means that no additional constants enter the problem statement except the constants appearing in the equations. The values of these constants are more or less established.

Equation (10.113) for the turbulent energy in the b, l-model is non-traditional also from the mathematical viewpoint. We emphasize again that it is non-local because on its right-hand side we have a global functional of the solution. Therefore the work of Kamin and Vázquez (1992) was very important. They proved the existence and uniqueness of the solution to the initial-value problem for this equation. An especially important result of this work is that a self-similar solution of the second kind presented in point (5) above is indeed the asymptotics to the solution of the initial-value problem at $t \to \infty$. The coefficient A is the integral of this solution: taking the solution at any time instead of the initial condition we obtain the same value of A as for the asymptotics. The problems of the existence and uniqueness of the solution of the initial-value problem for (10.113) were considered also by Grebenev (1992).

In the paper by Hastings and Peletier (1992) some rigorous estimates for self-similar solutions of (10.113) were obtained. Chen and Goldenfeld (1992) applied to the initial-value problem for the non-local equation (10.113) the renormalization group technique and obtained by the ϵ-expansion method a very accurate result for the eigenvalue.

The system (10.94), (10.95) of quasi-linear parabolic equations, describing the evolution of the burst within the framework of the b, ϵ model has also attracted the attention of mathematicians. Bertsch, dal Passo and Kersner (1994) proved the existence and uniqueness of the solution

to the initial-value problem for this system in the case $\alpha = \beta$. They also proved that the self-similar solution of the second kind (10.109) is the asymptotics of the solution to the initial-value problem at $t \to \infty$, A being the integral of the solution to the initial-value problem. Hulshof (1993) considered self-similar solutions for the system (10.94), (10.95) at $\alpha/\beta \neq 1$, and proved the existence of solutions with 'compact support', i.e., $h(t) < \infty$ for $\alpha/\beta < 2$. M. Bertsch suggested that for $\alpha/\beta > 2$ the asymptotics is self-similar, but the thickness of the burst $h(t)$ instantaneously becomes infinite as for the linear heat conduction equation. This hypothesis has found confirmation in the numerical computations of V.M. Prostokishin (1994).

11

Scaling in geophysical fluid dynamics

11.1 Scaling laws for the atmospheric surface layer

Geophysical fluid dynamics has become in the last few decades a broad subject (see Pedlosky, 1979) with many applications in earth sciences and in engineering practice. In all branches of geophysical fluid dynamics using similarity considerations, scaling laws and self-similar solutions play an important, often decisive role. We have chosen in this chapter for demonstration's sake some topics from geophysical fluid mechanics related mainly to geophysical turbulence.

The *surface layer* of the atmosphere is usually modelled (see, e.g., Monin and Yaglom, 1971) by a turbulent flow that is statistically horizontally-homogeneous and stationary, and is bounded below by a horizontal plane. The shear stress τ in the surface layer is also assumed to be constant. The essential difference from the flow in the wall region considered in section 10.2 consists in the presence in the surface layer of thermal stratification – temperature inhomogeneity over the height of the layer†. The stratification is stable if the temperature increases with height and unstable in the opposite case. Owing to the thermal inhomogeneity, a vertical displacement of fluid particles, produced by a vertical velocity fluctuation, is accompanied by work done against the force of gravity (or extracted, depending on whether the stratification

† We do not consider here such supplementary factors as moisture, dust etc.

is stable or not). This work is either taken from the turbulent energy or added to it, thus influencing the turbulence level, i.e. the transfer of heat, mass and momentum, and consequently also influencing the vertical distribution of the mean longitudinal velocity across the flow. The effectiveness of the influence of thermal stratification on the balance of turbulent energy is governed by the product of the coefficient of thermal expansion of the air and the acceleration of gravity, the so-called *buoyancy parameter*. The air in the atmospheric surface layer is usually considered to be a thermodynamically ideal gas, for which the coefficient of thermal expansion is equal to $1/T$, where T is the absolute temperature. The atmospheric surface layer is not thick, so the variation in mean pressure and the corresponding variation in the density can be neglected. In general, the variations of density and absolute temperature in the surface layer are considered to be small, and their influence on the dynamics of the flow is taken into account only through the buoyancy, which governs the contribution of thermal stratification to the turbulent energy balance. Thus the state of motion at some point of the flow in the atmospheric surface layer is governed by the following quantities: (1) the friction velocity $u_* = \sqrt{\tau/\rho_0}$; (2) the reference density ρ_0; (3) the dynamic temperature T_*, introduced by analogy with the friction velocity through the relation

$$T_* = -\frac{\langle w'T' \rangle}{u_*} \tag{11.1}$$

(where w' is the vertical velocity fluctuation, T' the temperature fluctuation, and the quantity $\langle w'T' \rangle$ coincides to within a constant factor with the vertical heat flux, which is also assumed constant over the surface layer), the dynamic temperature T_* being positive in the case of stable stratification ($\partial_x T > 0$) and negative for unstable stratification; (4) the buoyancy parameter $\beta = g/T_0$ (where g is the acceleration due to gravity and T_0 is the reference temperature, which does not appear separately anywhere, since a change in T_0 turns out to influence the flow dynamics only through the buoyancy parameter, i.e., in combination with the force of gravity); (5) the vertical coordinate z; (6) the molecular kinematic viscosity of air, ν; (7) the molecular thermal diffusivity of air, χ; and (8) the external geometric length scale Λ (e.g. the height of the atmospheric surface layer).

The standard procedures of dimensional analysis give

$$\Pi_u = \frac{z\partial_z u}{u_*} = \Phi_u\left(\frac{z}{L_0}, \frac{u_* z}{\nu}, \frac{u_*\Lambda}{\nu}, \mathrm{Pr}\right), \tag{11.2}$$

$$\Pi_T = \frac{z\partial_z T}{T_*} = \Phi_T\left(\frac{z}{L_0}, \frac{u_* z}{\nu}, \frac{u_*\Lambda}{\nu}, \mathrm{Pr}\right), \tag{11.3}$$

where $\mathrm{Pr} = \nu/\chi$ is the Prandtl number and L_0 is the thermal length scale†,

$$L_0 = u_*^2/\beta T_* . \tag{11.4}$$

The existing similarity theory for flows in the surface layer of the atmosphere, which owes its origin to the pioneering work of Prandtl (1932a) and the works of A.S. Monin and A.M. Obukhov (see Obukhov, 1946; Monin, 1950; Monin and Obukhov, 1953, 1954), is based on the assumption of complete similarity of the flow in both Reynolds numbers, the local one, $\mathrm{Re}_l = u_* z/\nu$, and the global one, $\mathrm{Re}_* = u_*\Lambda/\nu$. The plausibility of such an assumption and, consequently, of neglecting the dependence on Re_l and Re_* in (11.2) and (11.3) is usually argued on the basis of the very large values of both Reynolds numbers (for the local one, very large values outside a small region close to the surface itself whose height does not exceed a few millimeters). Here the assumption of the existence of finite limits of the functions Φ_u and Φ_T as $\mathrm{Re}_l \to \infty$ and $\mathrm{Re}_* \to \infty$ is accepted implicitly. If the functions Φ_u and Φ_T tend to finite limits as $\mathrm{Re}_l \to \infty$ and $\mathrm{Re}_* \to \infty$ in accordance with the assumption of complete similarity, then for sufficiently large Re_l and Re_* a universal similarity law, independent of the Reynolds numbers, must hold:

$$z\partial_z u/u_* = \Psi_u(z/L_0, \mathrm{Pr}), \tag{11.5}$$

$$z\partial_z T/T_* = \Psi_T(z/L_0, \mathrm{Pr}). \tag{11.6}$$

This is called in the literature the Monin–Obukhov similarity law. In the special case when thermal stratification of the flow disappears, we again arrive at the universal logarithmic law, considered in subsection 10.2.1.

The considerations presented in subsection 10.2.1 show that even in the case of a thermally neutral flow one detects a weak dependence of the universal function on both Reynolds numbers. This weak dependence allowed us to introduce the assumption of incomplete similarity of the flow in the local Reynolds number, which is apparently not contradicted by the experimental data on flows in smooth pipes, etc. It is natural to make a similar assumption for thermally stratified flows in the surface layer of the atmosphere (Barenblatt and Monin, 1976, 1979a).

† This definition of the thermal length scale follows Yaglom (1974) and is somewhat different from the conventional one.

11.2 Flows with strongly stable stratification

As discussed earlier, in spite of many years of continuous effort by many researchers, including top-level people in physics, mathematics, and mechanics, hydrodynamic turbulence remains a challenge for even the simplest case, a homogeneous incompressible fluid. Fluid lamination by density under the gravity field – *stratification* – additionally complicates the pattern of turbulent flows and leads to the appearance of substantially new effects.

Flow stratification introduces into our considerations a characteristic vertical length scale – the vertical length at which the density variation reaches a magnitude at which it will influence the flow dynamics. Stratification is considered to be strong if the characteristic vertical flow length scale is substantially larger than this scale. In this and the following sections scaling laws are considered for phenomena related to turbulent flows with strongly stable stratification. Some of these phenomena are of basic interest for geophysical fluid mechanics.

First, one of the simplest stratified flows is considered, turbulent flow in the wall region, where the strongly stable stratification is due to suspended small heavy particles. Examples of such flows are sediment transporting rivers, high-energy benthic bottom layers in the ocean, and dust storms. Considering flow stratification by suspended particles is attractive owing to the simple formulae at which we arrive, which allow one to explain a seemingly paradoxical phenomenon: under certain conditions the heavy particles can accelerate the flow!

In the case of stable stratification created by temperature and/or salinity an essentially new factor appears, internal waves. An instructive problem will be considered preliminarily: heat transfer in the oceanic *upper active layer* where the temperature (and salinity) distribution is subject to seasonal variations. As is known the density of sea water differs from the density of fresh water by three to four per cent, whereas its density fluctuations have the order of tenths of one per cent. Nevertheless these tiny density variations can influence the flow dynamics in an essential way. The temperature distribution over depth in the upper active ocean layer has the typical form represented schematically in Figure 11.1. The *upper homogeneous layer* where temperature and salinity†, and, consequently, density are nearly uniformly distributed, is

† For simplification's sake we will speak further only about temperature stratification.

the result of turbulent mixing. This mixing is carried out by the simultaneous actions of shear and of convection, which causes heavier fluid particles to sink. These particles thus come to the flow depth from the surface layer where the fluid is heavier, because this layer is cooled, and its salinity increased by evaporation from the oceanic surface and also by the breaking of surface waves. The depth of the homogeneous layer is time dependent: in moderate latitudes it grows in the fall-winter period and decreases in spring. The upper homogeneous layer is supported by a region where the temperature variation is sharp, the *upper thermocline*, which terminates at the depth where seasonal temperature variations vanish. This depth, i.e., the depth of the oceanic upper active layer, has an order of magnitude of about 200–250 m.

Analysis of the mean temperature distribution in the strongly stably stratified upper thermocline shows that an adequate model of this distribution is the Hertz travelling thermal wave, whereas the magnitude of the effective thermal diffusivity coefficient appears to be constant, to rather high accuracy. This coefficient is of order $10^{-1} - 1\text{cm}^2/\text{s}$, surprisingly, at first sight, being intermediate in value between the turbulent thermal diffusivity coefficient in the upper homogeneous layer, estimated as 10^3 cm^2/s, and the molecular thermal diffusivity coefficient, of order 10^{-3} cm^2/s. At the same time high-precision measurements show (this is discussed in detail in the monograph Fedorov (1976)) that the instantaneous temperature distribution over the depth is never smooth (as appeared to be the case earlier when these measurements were performed by highly inertial gauges), but has a rather step-wise character: intervals where the temperature is nearly constant alternate with intervals where there are large temperature, salinity, and, consequently, density gradients.

This is explained by a peculiar intermittence of the turbulence in flows with strongly stable stratification. The turbulence in such flows is not uniformly distributed everywhere, but is concentrated within patches. It is generated and then decays rather rapidly and is closely connected with internal waves. The interaction between internal waves and turbulence is illustrated by an instructive experiment performed by O.M. Phillips, which is described and analyzed below.

Internal waves also determine the very structure of turbulence in a strongly stable stratified flow. For various reasons the internal waves break, forming patches of mixed fluid that collapse through being squeezed at the level of their density. This collapsing of mixed fluid patches is also considered below. It is shown that at all its basic stages the collapse is characterized by various scaling laws. The most durable stage

of collapse is the final, viscous one, where the drag to the patch-extension driving force is due mainly to viscous force. It may occur that the patch extension at this stage is so slow that the patch can seem to the unprepared observer as being non-extending.

It is essential to note that the fluid inside the patch is uniform or close to being uniform, whereas outside the patch it is strongly and stably stratified. Therefore outside the patch the turbulence must spend part of its energy in working against the buoyancy force, whereas inside the patch it does not. Hence outside the patches the turbulence decays rapidly, and inside it is supported at a higher level. This very effect gives rise to the peculiar, intermittent, archipelago-like character of turbulence in a flow with strongly stable stratification.

The inhomogeneous and strongly anisotropic character of turbulence under strongly stable stratification was predicted by A.N. Kolmogorov in the late nineteen-forties. The existence of pancake-form turbulent patches (*blini*, from a similar Russian word) in the atmosphere and ocean under strong stratification conditions was established by Phillips (1967).

Turbulence in a shear flow, if it is sufficiently strong, can support sediment which would fall down in a non-turbulent or weakly turbulent flow. The capturing of falling sediment by turbulent patches can make the latter visible by contrast in an ambient fluid with weaker turbulence. It is plausible that this explains at least partially discoidal formations in the atmosphere, which have attracted rather wide attention, as well as 'turbidity clouds' in the ocean.

11.3 The regime of limiting saturation of a turbulent shear flow laden with sediment

We turn now to the consideration of a flow laden with small suspended particles. The volume and mass concentrations of particles are assumed to be very small (e.g. in rivers carrying a large amount of sediment, their volume and mass concentrations rarely exceed several ten-thousandths). Nevertheless, the dynamic action of the particles on the flow can turn out to be crucial, owing to the vast influence of the force of gravity. Furthermore, the particles are assumed to be much smaller than the internal turbulence scale; therefore the viscous relaxation time of the particles is negligible and one can assume that the horizontal components of the instantaneous velocities of the particles and the fluid coincide, and

that the vertical ones differ by a constant quantity a, the velocity of free fall of the particles in the unbounded fluid.

We consider again the wall region of the flow (for example, the surface layer of the atmosphere or the bottom layer of a channel). The momentum equation in this region remains just the same as for the pure fluid, since the influence of the particles on the density of the mixture is negligibly small.

The equation of conservation of mass for the load is obtained by setting equal to zero the total flux of particles through unit horizontal area. This flux is the sum of the flux of turbulent transport of particles, $\langle s'w' \rangle$, and the flux of settling particles, $-as$, so that

$$\langle s'w' \rangle - as = 0 . \tag{11.7}$$

Here s and s' are the mean volume concentration of particles and its fluctuation, respectively.

Finally, the steady equation of turbulent energy balance assumes, if one neglects the contribution of the diffusion of turbulent energy, the form

$$\langle u'w' \rangle \partial_z u + \epsilon + \sigma \langle s'w' \rangle g = 0 . \tag{11.8}$$

Here $\sigma = (\rho_p - \rho)/\rho$ is the relative excess of the density of particles ρ_p over the density of the fluid ρ and ϵ is the dissipation rate of turbulent energy. The last term expresses the rate at which turbulent energy is consumed in the suspending of particles by the flow; the other terms were explained in subsection 10.2.2. Despite the smallness of the concentration of particles in the flow, this term can have a significant value, since the force of gravity is very large.

Equation (11.8) can be put into the form

$$\langle u'w' \rangle \partial_z u (1 - \mathrm{Ko}) + \epsilon = 0 , \tag{11.9}$$

where the dimensionless parameter

$$\mathrm{Ko} = -\frac{\sigma g \langle s'w' \rangle}{\langle u'w' \rangle \partial_z u} , \tag{11.10}$$

called the Kolmogorov number, expresses the relative consumption of turbulent energy on the suspending of particles by the flow. This parameter gives a natural criterion for the dynamic activity of the load, i.e., the influence of the suspended particles on the dynamics of the flow. A similar parameter for stratification due to temperature and/or salinity (see below) is called the Richardson number. We introduce, in analogy with the coefficient of momentum exchange, the coefficient of load exchange, according to the relation

$$\langle s'w' \rangle = -k_s \partial_z s . \tag{11.11}$$

We now assume, in the spirit of the Kolmogorov similarity hypothesis of semi-empirical turbulence theory, that this coefficient too, like the coefficient of momentum exchange and the mean rate of dissipation, depends only on the local turbulent energy of a unit mass and on the length scale of the turbulence. By dimensional analysis we then obtain

$$k_s = \alpha_s l \sqrt{b} , \tag{11.12}$$

where α_s is a constant.

In the problem being considered of a laden flow, in contrast to the flow of a pure fluid an additional parameter has appeared, the Kolmogorov number Ko, so that for the external scale of turbulence we have according to dimensional analysis,

$$l = z\Psi(\mathrm{Re}_l, \mathrm{Re}_*, \mathrm{Ko}) .$$

Under the assumption of complete similarity in the local and global Reynolds numbers† the turbulent length scale can be represented through a universal function of the Kolmogorov number,

$$l = \kappa\gamma z \Phi_l(\mathrm{Ko}) , \tag{11.13}$$

where $\Phi_l(0)$ is obviously equal to one. The turbulence scale decreases under the influence of the load, so the function Φ_l must decrease when its argument increases. Thus, under the assumption made, the basic system of equations for the wall region of a laden turbulent shear flow assumes the form

$$\begin{gathered} l\sqrt{b}\partial_z u = u_*^2 , \quad \alpha_s l \sqrt{b} \partial_z s + as = 0 , \quad b = \frac{u_*^2}{\gamma^2}(1 - \mathrm{Ko})^{1/2} , \\ l = \kappa\gamma z \Phi_l(\mathrm{Ko}) , \quad \mathrm{Ko} = \frac{\sigma g a s}{u_*^2 \partial_z u} . \end{gathered} \tag{11.14}$$

The system of equations (11.14) has some characteristic properties. First of all, it contains only the gradient of the velocity $\partial_z u$, and not the velocity itself. Furthermore, for the case of an unrestricted supply of particles on the underlying surface, in view of the back influence of the particles on the dynamics of the flow we can anticipate the existence of flow regime in which the flow absorbs the maximum possible amount of the sediment load for given friction velocity and other parameters.

† As was shown in chapter 10, this assumption is apparently invalid for neutral flow. However, we neglect here further discussion of this matter, for two reasons. First, the quantitative difference is not essential here and does not play any significant role: we do not have at our disposal sufficiently precise experimental data to distinguish complete and incomplete similarity in sediment-laden flow. Second, what we need here is a qualitative explanation, and this one is more transparent for the case of complete similarity.

This regime, which we shall call the *regime of limiting saturation*, must be described by a singular solution of (11.14), which in turn must be determined by the parameters appearing in the differential equations themselves. Thus the determination of the regime of limiting saturation does not require the prescribing of any boundary condition for the sediment concentration.

An essential point is that the system (11.14) is invariant with respect to the transformation group

$$s = S/\alpha\,, \quad z = \alpha Z\,, \quad u = U + \beta \tag{11.15}$$

($\alpha > 0$ and β being the group parameters), so that substituting (11.15) into (11.14) we obtain the same system (11.14) but in the variables S, U, Z. Let the singular solution corresponding to the regime of limiting saturation determine the velocity gradient and load concentration by the relations

$$\partial_z u = f(z)\,, \quad s = g(z)\,. \tag{11.16}$$

But the singular solution is determined only by the system itself and therefore it also must be invariant with respect to the group (11.15), i.e., it can be expressed in the form

$$\partial_z U = f(Z)\,, \quad S = g(Z)\,,$$

where f and g are the same functions as in the relations (11.16). Expressing U ,S and Z in terms of u, s, z, and α, we get for the functions f and g the functional equations

$$f(z) = \alpha f(\alpha z)\,, \quad g(z) = \alpha g(\alpha z)\,. \tag{11.17}$$

The solution of these functional equations is found in an elementary way,

$$f = \frac{C_1}{z}\,, \quad g = \frac{C_2}{z}\,, \tag{11.18}$$

where C_1 and C_2 are constants subject to determination. Substituting into (11.15) the relations

$$\partial_z u = \frac{C_1}{z}\,, \quad s = \frac{C_2}{z}\,, \quad \mathrm{Ko} = \frac{\sigma g C_2}{C_1^2} \equiv \mathrm{const}\,, \tag{11.19}$$

we obtain

$$C_1 = \frac{u_*}{\kappa(1-\mathrm{Ko})^{1/4}\Phi_l(\mathrm{Ko})} = \frac{u_*}{\kappa\omega}\,, \quad \omega = \frac{a}{\alpha_s \kappa u_*}\,, \tag{11.20}$$

whence we find a finite equation for determining the Kolmogorov number Ko, which is constant in the regime of limiting saturation:

$$\omega = (1-\mathrm{Ko})^{1/4}\Phi_l(\mathrm{Ko})\,. \tag{11.21}$$

But Φ_l is a non-increasing function of its argument, $\Phi_l(0) = 1$, and Ko by its physical meaning lies between zero and unity. Hence it follows

that for $\omega > 1$ there exists no root of (11.21), and for $\omega < 1$ a unique root exists. Therefore a necessary condition for the existence of a regime of limiting saturation is

$$\omega = \frac{a}{\alpha_s \kappa u_*} < 1\,. \tag{11.22}$$

The physical meaning of the condition (11.22) is transparent. In fact, the value of the friction velocity u_* is proportional to the mean square velocity fluctuation. Thus if the fluctuation is large, so that during the time in which a fluid mass is lifted up by the turbulent fluctuation the heavy particles inside it have no time to fall (the velocity a of free fall being relatively small), the particles come into the main core of the flow and become suspended in it. In the opposite case, the particles are transported by the flow in the bottom layer, do not reach the main core of the flow, and do not influence the flow dynamics in the main part of the stream.

From the first equation of (11.19), taking into account (11.20), we get for $\omega < 1$

$$u = \frac{u_*}{\kappa\omega}\ln z + \mathrm{const}\,. \tag{11.23}$$

This means that for the flow in the regime of limiting saturation, which can be realized for $\omega < 1$, the velocity distribution remains logarithmic, just as in a pure fluid, but a reduction of the von Kármán constant has occurred: instead of κ it is now equal to $\kappa\omega$. Therefore *under the same external conditions (the same friction velocity) the flow accelerates under the action of particles in comparison with the flow of pure fluid.*

Since the capture of particles by the flow is realized by turbulent fluctuations, the turbulent energy must decrease. Actually, the turbulent energy per unit mass for the regime of limiting saturation is equal to

$$b = b_0(1-\mathrm{Ko})^{1/2}\,, \tag{11.24}$$

where $b_0 = u_*^2/\gamma^2$ is the turbulent energy for the flow of pure fluid with the same friction velocity. But the turbulent flow drag depends on the intensity of the fluctuations, so it turns out that the *suspended particles decrease the turbulent drag.* It is clear that this conclusion is valid only under the conditions indicated above of horizontal or nearly horizontal flow and of small volume and mass concentrations of particles, etc. Under such conditions a drag reduction in the flow and an apparent decrease in the von Kármán constant under the action of suspended particles have been observed by experimentalists (Vanoni, 1946; Einstein and Ning Chen, 1955).

The theory presented here of the transport of particles by a turbulent flow was developed by Kolmogorov (1954), and Barenblatt (1953, 1955);

the derivation of the equations for the regime of limiting saturation on the basis of group considerations was given by Barenblatt and Golitsyn (1974).

Dust storms in the Earth's atmosphere, as well as in the atmosphere of Mars, can be explained by the effect discussed above (Barenblatt and Golitsyn, 1974). It also explains the acceleration of flows in rivers carrying a relatively large amount of sediment, which had been repeatedly noticed by hydrologists. Apparently flow acceleration due to strongly stable stratification by particles, temperature, and salinity can explain (Barenblatt, Galerkina and Lebedev, 1992, 1993) the formation of high-energy benthic boundary layers in the ocean. The discovery of these layers (Nowell and Hollister (1985), see also the rest of the issue of *Marine Geology* in which this paper is published; Weatherly and Kelly (1982)) was one of the most important events in modern oceanology.

11.4 Upper thermocline in the ocean – the travelling thermal wave model

Stratification in the ocean is established due to the non-uniform distribution over depth of temperature and/or salinity. In contrast with stratification due to suspended particles, considered in the previous section, here we have the mixing of stratifying agent and fluid on the molecular level. Hence the turbulent exchange intensity and consequently the heat and mass exchange intensities are closely related to internal waves. We shall see this as we consider an instructive problem regarding the temperature distribution in the oceanic upper thermocline in moderate latitudes. For the fall-winter period the upper thermocline is most clearly manifested and its lowering occurs.

Heat and mass exchange on the oceanic surface, including the falling of heavy cold fluid particles formed from breaking waves, leads to the formation of a peculiar oceanic boundary layer where temperature (and salinity) are influenced by the water-air interface. This layer – the upper active layer of the ocean – consists of the upper homogeneous layer, where the temperature is nearly constant, and the upper thermocline supporting it where, on the contrary, temperature variation is sharp (Figure 11.1). The depth of the upper active layer in the open ocean is at least an order of magnitude less than the total oceanic depth. Therefore the upper thermocline can be considered as a semi-infinite region $h < z < \infty$ (z is the depth measured from the oceanic surface, h

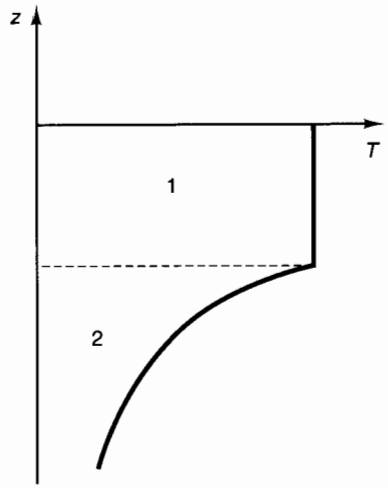

Figure 11.1. Schematic representation of the upper active layer of the ocean: (1) upper homogeneous layer; (2) upper thermocline.

is the depth of the upper homogeneous layer). The excess temperature – the difference between the current temperature and the mean annual temperature at a given point – therefore vanishes at infinity. If the natural observation data are averaged over a period of a month, the influence of short-time processes (daily variations, short-time random temperature anomalies, etc.) will disappear. The averaged parameters of the oceanic upper active layer, such as the speed of lowering of the upper homogeneous layer, $u = dh/dt$, and its excess temperature Θ_0 will be functions of some dimensionless 'slow' time T:

$$u = u(T), \quad \Theta_0 = \Theta_0(T)\,. \tag{11.25}$$

Let us neglect the influence of horizontal inhomogeneity, and let us assume furthermore that the motions governing the turbulence, and in consequence the heat and mass exchange mechanisms in the upper thermocline, are statistically steady, spatially homogeneous and small scale. Then, under these assumptions the heat conduction equation for the averaged excess temperature $\Theta(z,t)$ is obtained:

$$\partial_t \Theta = \kappa \partial^2_{zz} \Theta\,. \tag{11.26}$$

Here t is the ordinary dimensional time, and κ is the effective thermal diffusivity coefficient, which is constant according to our assumptions. Note, that in further considerations the variability of this coefficient, and, in particular, its dependence on temperature and/or temperature gradient could be taken into account without additional mathematical difficulty. Further analysis will show, however, that there is no need for this complication.

The excess temperature distribution satisfies the boundary conditions

$$\Theta(h,t) = \Theta_0(T)\,, \quad \Theta(\infty,t) = 0 \tag{11.27}$$

Let us introduce a moving coordinate $\xi = z - h$ reckoned from the thermocline's upper boundary, so that $\Theta = \Theta(\xi,t)$. Then equation (11.26) and the boundary conditions can be written in the form (cf. the analogous consideration in section 7.5)

$$\partial_t\Theta - u(T)\partial_\xi\Theta = \kappa\,\partial^2_{\xi\xi}\Theta \tag{11.28}$$

$$\Theta(0,t) = \Theta_0(T)\,, \quad \Theta(\infty,t) = 0\,. \tag{11.29}$$

The characteristic time scale in this problem $\tau = \kappa/u^2$, as will be seen, is of the order of days. The averaged excess temperature Θ is not influenced by short-time processes, so the characteristic time scale of t should be considered to be larger than τ. For large t/τ the solution to the problem (11.28), (11.29) asymptotically becomes steady, so that the time derivative in (11.28) disappears. The equation obtained can be integrated simply, and under boundary conditions (11.29) the solution achieves the form

$$\Theta = \Theta_0 \exp(-u\,\xi/\kappa)\,. \tag{11.30}$$

It is convenient to introduce a universal variable,- the relative excess temperature $\theta = (\Theta_0 - \Theta)/\Theta_0$. In terms of θ the solution (11.30) can be written in the form

$$\theta = 1 - \exp(-u\,\xi/\kappa)\,, \tag{11.31}$$

i.e., the relative excess temperature distribution appears to be self-similar. Self-similarity of the relative excess temperature distribution in the upper thermocline was found empirically by Kitaigorodsky and Miropolsky (1970), by processing natural data. Linden (1975) performed a successful attempt to process, on the basis of the self-similarity hypothesis, data obtained in his laboratory experiments concerning the salinity profile in the laboratory model of the upper thermocline. However, the self-similarity was not associated in these papers with a definite physical mechanism. In the preceding chapters we have seen repeatedly that self-similarity never occurs by chance, it always means that there exists a certain stabilization of the process. The settling down of the average temperature field to a steady travelling wave is another instructive example confirming this general rule. The model of a travelling wave for the upper thermocline was proposed and shown to agree with experimental data – both laboratory and natural data – in Barenblatt (1978b); independently and simultaneously an analogous model was proposed by Turner (1978). Note that the steady-state solution (11.30) for the heat

conduction equation with a moving heat source was found by the famous German physicist H. Hertz in the last century and since then has been used in many branches of mathematical physics. In particular, it plays a fundamental role in the theory of combustion, where it describes the temperature distribution ahead of the combustion region where the chemical reaction has not as yet started (see chapter 7). The travelling thermal wave model has also been much used in physical oceanology. Munk (1966) applied a similar model in a different physical situation; following his figurative expression, we might say that this model comes from oceanographic antiquity.

Integrating (11.31) we obtain

$$\frac{\kappa}{u} = \int_0^\infty (1-\theta)d\xi\,, \tag{11.32}$$

so that the relation (11.31) can be represented in universal form:

$$\ln\frac{1}{1-\theta} = \frac{\xi}{\int_0^\infty (1-\theta)d\xi} = \zeta\,. \tag{11.33}$$

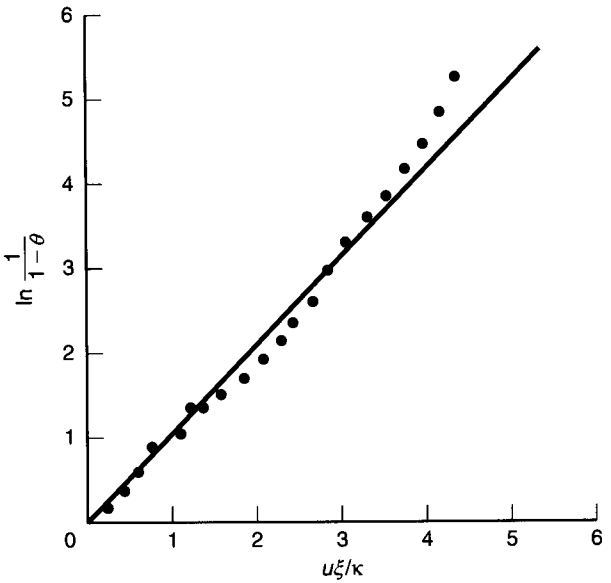

Figure 11.2. Results of the processing of natural data confirm the travelling wave model for the upper thermocline.

Therefore, if the proposed model is an adequate one then in the reduced coordinates

$$\ln \frac{1}{1-\theta}, \ \zeta$$

the experimental points should settle down along the bisectrix of the first quadrant. Efimov and Tsarenko (1980) processed numerous natural data using these coordinates and were able to confirm the travelling-wave model for the upper thermocline. In Figure 11.2 are presented Efimov's results of the processing of natural data by B.N. Filyushkin of the averaged October 1968–72 temperature profile at the 'Echo' weather station (34°0′ N and 48°0′ W). As is seen these data confirm the thermal travelling wave model for the upper thermocline and the constancy of the effective vertical temperature diffusivity coefficient†. The data presented allow one to give some instructive estimates. For natural measurements at the 'Echo' station the κ/u value, determined according to formula (11.32) is about 2×10^3 cm. The estimates for the averaged velocity of lowering of the thermoclines upper boundary give $u \sim 10^{-4} - 10^{-3}$ cm/s. Hence, using the previous estimate we find $\kappa \sim 10^{-1} - 1$ cm^2/s. It is important to note that this value is intermediate between the magnitude of the molecular thermal diffusivity coefficient of water, of order 10^{-3} cm^2/s, and the magnitude of the turbulent temperature diffusivity coefficient in the upper homogeneous layer, of order 10^3 cm^2/s. This estimate obtained for the effective vertical temperature diffusivity coefficient agrees with Munk's (1966) estimate for the value at an intermediate depth of the Pacific and corresponds to Stommel's (1958) global estimate. An analogous intermediate value is obtained for the data from laboratory experiments. This gives some basis for assuming (Phillips, 1977) that heat (and mass) exchange in the upper thermocline is governed by intermittent turbulence, related to the breaking of internal waves.

Internal waves are a phenomenon specific to fluid flows with stable stratification. When the stratification is 'discrete', i.e., if the fluid consists of several homogeneous layers and their densities decrease from bottom to top, the energy of the internal waves is mainly concentrated close to the interfaces between layers. In the case of continuous stable stratification the internal waves fill the whole space, if there exist in the fluid some sources of disturbance. Such sources always exist in the atmosphere and in the ocean (let us note even the tides, which provide in

† The systematic deviations in the upper part of this graph, corresponding to the lowest part of the thermocline, are apparently due to the processing procedure.

the ocean internal waves of huge amplitude and length), so that internal waves are a phenomenon occurring everywhere in the ocean and also in the atmosphere (see, e.g., Gossard and Hooke, 1975). The interaction between internal waves and turbulence is decisive for the whole pattern of turbulence in a stratified fluid.

11.5 Strong interaction of turbulence with internal waves. Deepening of the turbulent region

The strong nonlinear interaction of internal waves with turbulence leads to essentially new effects compared with those due to turbulence in neutral fluid flows. One such effect was demonstrated by Phillips (1976). The principal scheme of his remarkable experiment is as follows.

At the interface of two layers of liquids of different density internal waves are produced (Figure 11.3). After the establishing of steady waves turbulence was initiated by an oscillating grid at the upper boundary. Gradually the turbulent region propagated downwards from the upper boundary of the upper layer. Its lower boundary appears to be very sharp. The basic effect demonstrated was that when the turbulent front approached the interface of the two layers, the waves became smoothed out and disappeared practically instantaneously.

Note that in fact the tank in Phillips' experiment had the form of a circular cylinder, and turbulence was stirred up by a rotating disc bearing metallic ripples which covered the upper boundary of the upper layer, so that a rotating shear mean flow appeared. For theoretical consideration (Barenblatt, 1977) the problem statement was simplified: the fluid layers were assumed to be horizontally homogeneous, and turbulence was assumed to be stirred by an oscillating grid without shear. In fact, the simplified stirring scheme corresponds to a real experiment (Turner, 1968, 1973; Thompson and Turner, 1975).

Consider first the propagation of turbulence, stirred without the formation of shear flow, at the boundary $z = 0$ of an infinitely deep statistically horizontally-uniform layer of constant density. Since the flow is shearless, turbulence generation by a mean flow does not occur and the turbulent energy balance equation in the turbulent region can be written in the form

$$\partial_t b + \partial_z \left\langle \left(\frac{p'}{\rho} + \frac{u'^2 + u'^2 + w'^2}{2} \right) w' \right\rangle + \epsilon = 0 \qquad (11.34)$$

(the notation is the same as in subsection 10.2.2). We cannot neglect

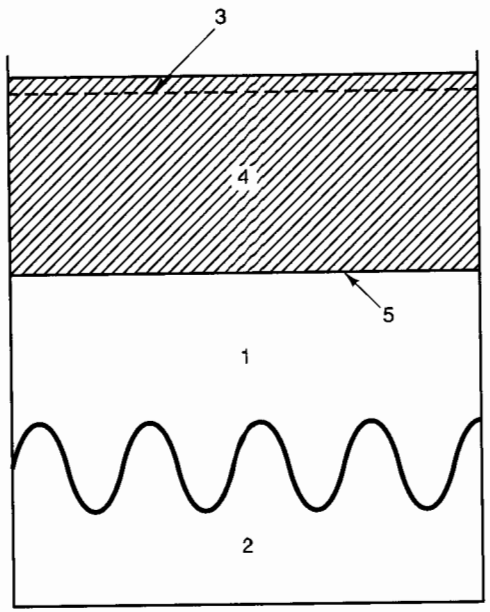

Figure 11.3. Principal scheme of Phillips' experiment: (1) light fluid layer; (2) heavy fluid layer; (3) oscillating grid producing turbulence; (4) turbulent region; (5) turbulent front.

the effect of turbulent energy diffusion here because this effect governs the 'entrainment' – the extension of the turbulent region.

The relation for the diffusion flux of turbulent energy can be written in the form

$$\left\langle \left(\frac{p'}{\rho} + \frac{u'^2 + u'^2 + w'^2}{2} \right) w' \right\rangle = -k_b \partial_z b \qquad (11.35)$$

where k_b is the turbulent energy exchange coefficient. We emphasize that the relation (11.35) simply introduces a new quantity k_b not related to any additional assumption.

Let us assume as before (subsection 10.2.2) the Kolmogorov similarity hypothesis. This gives (within the frame of the b, l model)

$$k_b = l\sqrt{b}\,, \quad \epsilon = \frac{c_1 b^{3/2}}{l} \qquad (11.36)$$

where c_1 is again a constant; according to subsection 10.2.4 the estimated range of its value is 0.06–0.085. Equation (11.34) then assumes the form

$$\partial_t b - l\sqrt{b}\partial_z b + c_1 \frac{b^{3/2}}{l} = 0\,. \qquad (11.37)$$

Equation (11.37) is relevant to the nonlinear heat conduction equations considered in chapter 2. Initial turbulence in the flow field is

absent, according to the experimental conditions, so the initial value of turbulent energy can be assumed equal to zero. The energy flux (per unit mass) q at the boundary is assumed to be constant (in fact, special organization of the experiment is required to maintain the energy flux at the boundary as time independent). Thus, the initial and boundary conditions appropriate to the problem under consideration take the form

$$b(z,0) = 0\,, \quad \left(l\sqrt{b}\partial_z b \right)_{z=0} = -q \qquad (11.38)$$

so that the turbulent energy depends on the quantities t, q, z whereas the turbulence length scale l, which we assume constant over the depth of turbulent region, depends on t and q. This assumption of a length scale that is constant over depth is related to an important idea of Townsend (1976) concerning the governing role of large vortices in turbulent exchange processes.

As in the problems of a strong thermal wave, considered in chapter 2, and of turbulent-burst evolution, considered in chapter 10, the solution is represented by a finite function, different from zero in a finite region $0 \le z \le h(t)$ only.

Dimensional analysis gives

$$b = q^{2/3} f\left(\frac{z}{h(t)} \right), \quad l = \alpha_1 h(t), \quad h(t) = \xi_0 q^{1/3} t\,. \qquad (11.39)$$

Here the constant α_1 can be considered as a known universal constant; the other constant ξ_0 is determined in the course of solution. The estimates performed in subsection 10.2.4 gave α_1 the range $\alpha_1 = 0.063 - 0.071$. Substituting (11.39) into (11.37) and (11.38) we obtain for the function f an ordinary differential equation

$$\frac{\alpha_1}{\xi_0}\frac{d}{d\xi}\left(\sqrt{f}\frac{df}{d\xi} \right) + \xi\frac{df}{d\xi} - \frac{c_1}{\alpha_1 \xi_0} f^{3/2} = 0\,, \quad \xi = \frac{z}{h(t)}\,, \qquad (11.40)$$

and boundary conditions

$$\left(\alpha_1 \sqrt{f}\frac{df}{d\xi} \right)_{\xi=0} = -1\,, \quad f(1) = 0\,, \quad \frac{df^{3/2}(1)}{d\xi} = 0\,. \qquad (11.41)$$

We recall that, like the solution to similar problems in chapters 2 and 10, the function f is different from zero for $0 \le \xi \le 1$, identically equal to zero for $\xi \ge 1$, and continuous, as is the derivative $df^{3/2}/d\xi$; the last two conditions (11.41) follow from these continuity conditions and the first condition (11.38). The constant ξ_0 is obtained as an eigenvalue of the problem (11.40), (11.41).

Therefore under the assumptions we have accepted the turbulent energy at a certain time instant t is different from zero in a region of finite

depth $h(t)$ growing linearly with time, so that the entrainment speed appears to be constant:

$$h = \xi_0 q^{1/3} t\,, \quad \frac{dh}{dt} = \xi_0 q^{1/3}\,. \tag{11.42}$$

The bulk turbulent energy in the turbulent region per unit boundary area grows linearly with time,

$$\int_0^h b dz = \sigma q t, \quad \sigma = \xi_0 \int_0^1 f(\xi) d\xi\,, \tag{11.43}$$

whereas the integral dissipation rate per unit area is time independent:

$$\int_0^h \epsilon dz = \tau q, \quad \tau = \frac{c_1}{\alpha_1} \int_0^1 f^{3/2} d\xi\,. \tag{11.44}$$

Integrating (11.40) from $\xi = 0$ to $\xi = 1$ and using the boundary conditions (11.41) we find an obvious relation between τ and σ: $\sigma = 1 - \tau$.

We note that the problem under consideration could be solved within the framework of the b, ϵ turbulence model. However, in the latter model the dissipation-rate flux must somehow be prescribed at the boundary, and up to now we have no physical argument adequate to determine this quantity. This point is in general a difficult aspect of using the b, ϵ model. The case of turbulent-burst evolution considered in subsection 10.2.4 was a lucky exception because this quantity turned out to be equal to zero due to symmetry.

We return to Phillips' experiment. The dynamics of the internal waves at the interface between the heavy and light fluids is described by simple potential theory and, as is known, the energy density of the waves rapidly (exponentially) decays with distance from the interface. Therefore, the pattern of steady waves at the interface is not influenced by turbulence until the turbulent front, propagating with finite velocity, reaches the vicinity of the interface. It is plausible to assume that turbulence creates a turbulent flux $\mathbf{j}$ of wave motion energy E_w directed opposite to its gradient (Benilov, 1973):

$$\mathbf{j} = -k_w \mathrm{grad}\, E_w\,. \tag{11.45}$$

Here k_w is the coefficient of wave energy exchange, which is introduced in the same way as the exchange coefficients of mass, temperature, momentum, etc. were introduced earlier. Therefore, applying here for qualitative reasoning the Kolmogorov similarity hypothesis we obtain the estimate

$$k_w \sim l\sqrt{b}\,. \tag{11.46}$$

Thus, until the turbulent front approaches the region of large wave energy gradient, i.e., the close vicinity of the interface, the coefficient k_w remains equal to zero because the turbulent energy is zero; also, when the turbulent front is far from the interface, the gradient of the wave energy in the turbulent region is exponentially small. Therefore the wave energy flux is small everywhere. However, when the turbulent front approaches the close vicinity of the interface the wave energy exchange coefficient there becomes different from zero, and, because close to the interface the gradient of wave energy is not small, the turbulent flux of wave energy increases sharply (Figure 11.4). Due to this flux the wave energy becomes more or less uniformly distributed over the whole upper layer. Thus, when the turbulent front arrives at the interface, the wave producer becomes ineffective: the wave energy due to turbulence becomes uniformly distributed over the whole upper part of the tank and not concentrated close to the interface as it was before the turbulent region approached the interface. This is the reason for the smoothing of the waves at the interface.

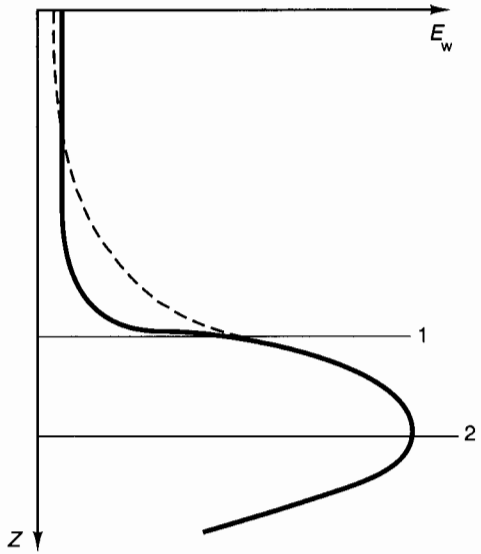

Figure 11.4. Wave energy redistribution over the whole volume of the turbulized fluid: (1) turbulent front; (2) interface.

It is clear that the special circumstances of the Phillips experiment are immaterial here: we have met, when analyzing this experiment, a phenomenon of a quite general nature. Indeed, we have seen how the turbulent region, extending in the ambient fluid, and sharply bounded by a front when the turbulence intensity in the ambient fluid is small, 'sucks' and redistributes the energy of waves approaching the region involved in wave motion. This leads to rapid smoothing of the waves. The phenomenon which we have just discussed is often observed when looking at the sea surface from the rear of a ship: the smooth mirror-like surface over the turbulent wake of the ship is in a sharp contrast with the ambient rippled surface. Also, those who practise water skiing observe a smooth track behind the speed-boat. This is due to the sucking of wave energy by the turbulent wake of the speed-boat. However, the skier feels also a frequent weak tremor due to turbulence.

Note that the remarkable fact of the presence of a sharp boundary between the turbulent and non-turbulent regions, which was basic in our previous considerations and has been obtained here from a mathematical model, has repeatedly been noted by experimentalists (see, especially, the paper by Kovasznay *et al.* (1970)†, and Turner's (1973) monograph where a review of earlier work can also be found).

11.6 The breaking of internal waves and extension of mixed-fluid patches in a stably stratified fluid

The interaction of internal waves and turbulence in a fluid having strongly stable stratification is not restricted to the redistribution of wave energy by turbulence considered in the previous section. In fact, turbulence in a stably stratified fluid has a peculiar, intermittent, spatial structure. Observations, in particular those in the upper layer of the ocean, show that it is concentrated in 'patches' of turbulence, pancake-form layers extending horizontally much further than their thickness (Fedorov, 1976). These pancake-form patches occur as sharply bounded and relatively long-lived formations. Even after the decay of turbulence, the fluid in the patches remains mixed (homogenized) for a rather long time. Therefore the origin and evolution of mixed-fluid patches in stably stratified fluids is of considerable interest, in particular in connection with the oceanic fine structure and microstructure.

† In this paper some proposals are also discussed concerning the mathematical modelling of the sharp boundary.

The initial formation of mixed-fluid patches is related to the destruction of internal waves which can be due to various reasons: simple breaking (Woods, 1968), shear or convective instability (Belyaev and Gesenzwei, 1978; Korotaev and Panteleev, 1977), resonance interaction, etc. After the destruction of internal waves patches of mixed fluid appear (Figure 11.5) and extend, being gradually squeezed by the ambient stratified fluid and intruding into it. It is clear that the intrusions will be squeezed at the vertical level $z = z_1$ where the density of the stratified fluid is equal to the mixed-fluid density. The mixing of fluid within the patch establishes an excess pressure there, which forms the driving force of intrusion: owing to this force the extension of the patch goes on.

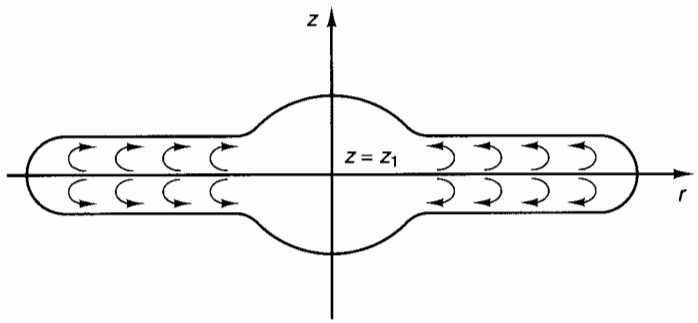

Figure 11.5. Mixed-fluid-patch intrusion into the ambient stratified fluid.

It is natural to distinguish three stages in the collapse-spreading of mixed fluid patches in a stably stratified fluid: (1) the initial stage, essentially a non-steady one, when the driving force of the intrusion substantially exceeds the drag forces; (2) an intermediate steady stage, when the driving force is in equilibrium with the form drag and the wave drag due to radiation of internal waves by spreading patches; and (3) a final, viscous stage, when internal waves are not radiated and the driving force is in equilibrium with the viscous drag. As we will see, each of these basic stages is governed by its own scaling laws. Between the basic stages there are some non-self-similar intermediate periods. After the viscous stage (3) the patch becomes mixed due to diffusion with the ambient fluid and disappears. Classification of these collapse stages of mixed-fluid patches goes back to the paper of Wu (1969). In this paper an important fact was observed: the volume of a patch remains constant from the early stages until the last observed extension period.

Let us consider these stages in sequence. In the first stage a particle in the mixed fluid will be falling, or being raised, to the plane of its density level $z = z_1$, with subsequent spreading along this plane. Therefore

the variation rate of the patch's planform area S at the first stage is proportional to the current patch area times the speed of fluid inflow to the plane $z = z_1$. Under conditions of free fall the speed of fluid inflow is proportional to the product of time and free fall acceleration. In turn the free fall acceleration is proportional to N^2, where N is a basic stratification parameter, the so-called Brunt–Väisäla frequency, defined by the relation†

$$N^2 = \frac{g}{\rho}\left|\frac{d\rho}{dz}\right| . \tag{11.47}$$

N is equal to the frequency of the linear internal wave that arises when the stably stratified fluid at rest is weakly disturbed‡. The patch's vertical size is not large, therefore the variation of N in the vertical direction can be neglected. Therefore for the first stage the following relation is obtained:

$$\partial_t S \sim SN^2 t . \tag{11.48}$$

Integrating, we obtain for small Nt

$$\frac{(S - S_0)}{S_0} \sim N^2 t^2 . \tag{11.49}$$

Here S_0 is the initial patch planform area. Thus, at the first stage the variation of the patch's characteristic length L is proportional to time squared:

$$\frac{L - L_0}{L_0} \sim N^2 t^2 , \quad \frac{dL}{dt} \sim L_0 N^2 t . \tag{11.50}$$

Indeed, for the case of a patch having the form of an elongated cylinder with horizontal axis, typical for a wake, S is proportional to L and the relation (11.50) is obtained from (11.49) directly. However, if the length sizes of the patch planform are about equal, for instance if the patch planform is circular, $S \sim L^2$. When $L - L_0 \ll L_0$, $S - S_0 \sim L^2 - L_0^2 \sim 2(L - L_0)L_0$, whence and from (11.49) the relation (11.50) is obtained again. Relations of the form (11.50) were obtained by Wu (1969) by processing the data of laboratory experiments with wakes. They were confirmed by the semi-quantitative theoretical analysis of Kao (1976), and by numerical calculations. They appear to be valid up to $t \sim 2.5/N$.

At the intermediate stage the intrusion-driving force is in equilibrium

† In the relation (11.47) and in what follows g is the acceleration due to gravity, and ρ is the potential density, i.e., the density obtained when the fluid pressure is reduced adiabatically to a certain standard value.

‡ A typical value of N is for the atmosphere is 10^{-2} s^{-1} and for the ocean is 10^{-3} s^{-1}.

with the form drag and the wave drag, so the governing parameters will be the basic stratification parameter N and the current mean patch thickness h. Dimensional analysis gives

$$\frac{dL}{dt} \sim Nh . \tag{11.51}$$

We now note that at this stage the patch extension rate is different for different planforms. In fact, as was said previously, the patch volume V is constant. Therefore for a wake-like patch having cross-sectional area S, $h \sim S/L$, and for a patch of circular planform $h \sim V/L^2$, and we obtain for these cases, correspondingly,

$$\frac{dL^2}{dt} \sim SN , \quad L \sim [SN(t - t_0)]^{1/2} , \tag{11.52}$$

$$\frac{dL^3}{dt} \sim VN , \quad L \sim [VN(t - t_0)]^{1/3} . \tag{11.53}$$

Here t_0 is the time of the origin of the second stage. Again, relations of the type (11.52) were obtained by Wu (1969) by processing laboratory experimental data, and confirmed by the semi-quantitative theoretical analysis of Kao (1976). They appear to be valid in the interval $3/N < t < 25/N$.

Let us consider the final, viscous stage of mixed-fluid patch collapse (Barenblatt, 1978a).

Under the assumptions made earlier in the section, the equation of mass conservation in the mixed fluid patch has the form

$$\partial_t h + \mathrm{div} h\mathbf{u} = 0 , \tag{11.54}$$

where $h(x, y, t)$ is the local patch thickness, x, y are the rectilinear coordinates in the $z = z_1$ plane, t is the time, and $\mathbf{u}$ is the mixed-fluid velocity, averaged over a given vertical line inside the patch. For the derivation of this equation it is enough to consider the mass balance in an elemental volume, or particle, of the patch, shown in Figure 11.6, and to take into account that no ambient fluid entrainment and no viscous erosion of the patch is occuring at this stage.

To determine the average velocity $\mathbf{u}$ consider the system of forces acting on the elemental particle (see Figure 11.6). It is bounded by the patch's upper and lower surfaces and by a cylindrical surface around an elemental area δS in the plane $z = z_1$. The intrusion-driving force for this particle is due to the gradient of the quantity ph, where p is the excess pressure over that of the ambient stratified fluid, averaged over the vertical within the patch:

$$\mathbf{F}_m = -(\mathrm{grad} ph)\delta S . \tag{11.55}$$

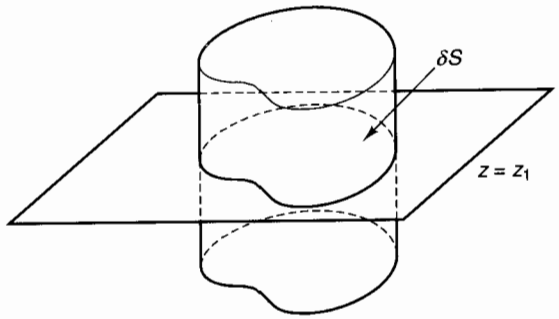

Figure 11.6. Elemental particle of a mixed-fluid patch.

Indeed, on each vertical line on the cylindrical boundary of the elemental particle a force $ph\mathbf{n}$ per unit contour length is acting here; $\mathbf{n}$ is a unit vector normal to the contour δC of the elemental area δS. The driving forces at the upper and lower patch boundaries are zero because the pressure there coincides with the pressure in the ambient stratified fluid. Applying Gauss's formula we obtain

$$\mathbf{F}_m = -\int_{\delta C} ph\,\mathbf{n}\,ds \simeq -(\mathrm{grad}ph)\delta S\,.$$

The drag force $\mathbf{F}_r$ acting on the particle can be calculated in the following way. At the stage under consideration the patch collapse is proceeding slowly, so that it is possible to neglect the accelerations within the patch and simplify the equations of motion. Integrating these simplified equations over the patch thickness we obtain that the drag force is proportional to the derivative over z of the actual fluid velocity at the upper or lower patch boundary. The velocity distribution can easily be found given boundary conditions at the upper and lower patch boundaries. Experiments and numerical calculations show that the fluid velocity at the upper and lower patch boundaries is much lower than the average velocity within the patch. This is due to the fact that above and below the patch the fluid motions are, during the collapse, in the reverse direction to the fluid motions inside the patch. Therefore, it can be assumed with adequate accuracy that the fluid velocity vanishes at the upper and lower patch boundaries. Integrating the simplified equations of motion under this condition it is possible to obtain the velocity distribution over the patch thickness, and, consequently, the relation for the drag force.

We will, however, derive this relation directly, using dimensional analysis. In fact, the drag force per unit planform area is governed by the local mean fluid velocity $\mathbf{u}$, the fluid's dynamic viscosity μ inside the

patch, and the local patch thickness h. Dimensional analysis gives us that this force is proportional to $\mu\mathbf{u}/h$. Therefore the viscous drag force $\mathbf{F}_r$ acting on the elemental particle of the patch is equal to

$$\mathbf{F}_r = c\frac{\mu\mathbf{u}}{h}\delta S \tag{11.56}$$

where c is a constant, which can be found by comparison with the well-known solution to the problem of viscous fluid motion between plane walls, according to which $\mathbf{F}_r = 12\mu\mathbf{u}\delta S/R$. Therefore we obtain that $c = 12$.

From the equality of the drag force (11.56) and the driving force (11.55) on the particle, we obtain

$$\mathbf{u} = -\frac{h}{c\mu}\,\mathrm{grad}ph\,. \tag{11.57}$$

Only the mean excess pressure in the mixed fluid remains to be determined. The density distribution in the stratified fluid near the $z = z_1$ plane, along which the patch is extending, can be considered as linear one owing to the small patch thickness. Evidently the extending patch is symmetric with respect to the plane $z = z_1$, so this divides the patch into two symmetric parts. Let us denote by p_1 and ρ_1 the pressure and density of the stratified fluid at the level $z = z_1$. Then, integrating the hydrostatic equation we obtain a relation for the pressure variation in the stratified fluid:

$$p = p_1 - \rho_1 g(z - z_1) + \rho_1\frac{N^2(z - z_1)^2}{2}\,. \tag{11.58}$$

Here, as before, N is the Brunt–Väisäla frequency, so $N^2 = ag$ and $a = |d\rho/dz|/\rho_1$. Furthermore, the pressure at a patch boundary coincides with the pressure of the ambient stratified fluid at the same height. Thus, the pressures at the upper point, $z = z_1 + h/2$, and the lower point, $z = z_1 - h/2$ on a vertical line within the patch are equal to

$$p_u = p_1 - \rho_1 g\frac{h}{2} + \rho_1\frac{N^2h^2}{8}\,,\quad p_l = p_1 + \rho_1 g\frac{h}{2} + \rho_1\frac{N^2h^2}{8}\,. \tag{11.59}$$

The pressure inside the patch is distributed hydrostatically because the fluid density in the patch is constant and equal to ρ_1:

$$p = p_1 - \rho_1 g(z - z_1) + \frac{\rho_1 N^2h^2}{8}\,. \tag{11.60}$$

The mean pressures averaged over a vertical line inside the patch and over a similar depth in the ambient fluid are correspondingly equal to

$$p_{ai} = p_1 + \rho_1\frac{N^2h^2}{8}\,,\quad p_{as} = p_1 + \rho_1\frac{N^2h^2}{24}\,. \tag{11.61}$$

The difference between these quantities gives the mean excess pressure over a given vertical line inside the patch:

$$p = p_{ai} - p_{as} = \frac{\rho N^2 h^2}{12}. \tag{11.62}$$

From relations (11.57) and (11.62) we obtain

$$\mathbf{u} = -\frac{\rho_1 N^2}{12c\mu} h \,\mathrm{grad} h^3 = -\frac{\rho_1 N^2}{4c\mu} h^3 \,\mathrm{grad} h. \tag{11.63}$$

After substituting this relation into the equation for mass conservation in the patch, we obtain for the patch thickness a nonlinear equation of heat conduction type:

$$\partial_t h = \kappa \Delta h^5, \quad \kappa = \frac{N^2}{20c\nu}, \tag{11.64}$$

where Δ is the two-dimensional Laplace operator and ν is the kinematic viscosity of the fluid inside the patch. In particular, for symmetric rectinlinear and axisymmetric one-dimensional motions, equation (11.64) assumes the respective forms

$$\partial_t h = \kappa \, \partial^2_{xx} h^5 \tag{11.65}$$

$$\partial_t h = \frac{\kappa}{r} \partial_r (r \partial_r h^5) \tag{11.66}$$

where x is a horizontal Cartesian coordinate and r is the horizontal polar radius. We met an analogous equation earlier, in chapter 2, when considering the initial stage of a nuclear explosion.

If the initial length sizes of the patch planform are about the same, it is natural to expect that the patch will become axisymmetric, presumably during the end of the second stage and the final viscous stage. The results of a numerical computation performed by E.I. Tikhomirova are presented in Figure 11.7: equation (11.64) was solved numerically† for a non-symmetric initial patch-thickness distribution $h(x, y, 0)$. As is seen, after even slight spreading the patch planform becomes indistinguishable from circular; therefore the patch collapse can be considered as axisymmetric and equation (11.66) can be used for its description. The equation for patch-volume conservation assumes the form

$$2\pi \int_0^\infty h(r,t) r dr = V = \mathrm{const}. \tag{11.67}$$

We are interested, first of all, in the intermediate-asymptotic stage of

† Numerical computation methods for the degenerate case – the vanishing of h at the boundary of the disturbed region – were used in this computation, developed by Samarsky and Sobol' (1963).

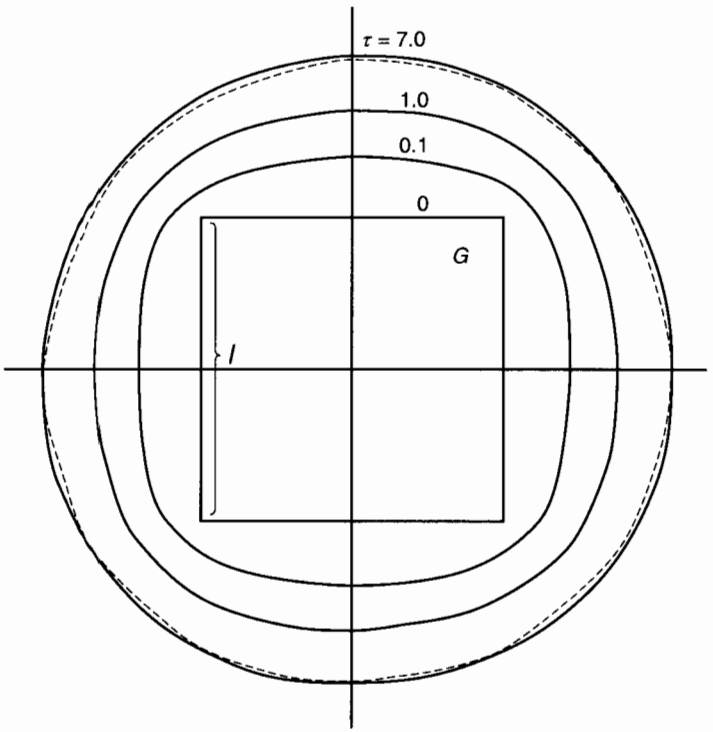

Figure 11.7. Numerical solution to equation (11.64) for a non-symmetric initial condition: $h(x, y, 0) = h_0$ for points x, y inside the square G; $h(x, y, 0) \equiv 0$ for points outside G; $\tau = \kappa h_0^4 t / l^2$. (The calculation was performed by E.I. Tikhomirova.)

patch extension when the patch planform diameter substantially exceeds its initial diameter. At this stage the random details of the initial patch-thickness distribution cease to be important. Therefore, as in Chapter 2, for an asymptotic description of the viscous stage of collapse we can assume an initial distribution in the form of a concentrated instantaneous source:

$$h(r, t_1) \equiv 0 \text{ at } r \neq 0, \quad 2\pi \int_0^\infty h(r, t_1) r dr = V \tag{11.68}$$

where t_1 is the moment taken as the beginning of the self-similar viscous stage.

The problem solution here is completely analogous to that for the instantaneous heat source problem in Chapter 2. The solution to equation (11.66) under the initial condition (11.68) depends on the quantities

$t - t_1$, κ, V and r. Dimensional analysis shows that the solution is self-similar and can be represented in the form

$$h = \left[\frac{V}{2\pi\kappa(t-t_1)}\right]^{1/5} f(\zeta)\,, \quad \zeta = \frac{r}{[V^4\kappa(t-t_1)/16\pi^4]^{1/10}}\,. \tag{11.69}$$

From (11.69) and (11.66) an ordinary differential equation follows for the function $f(\zeta)$:

$$\frac{d^2f^5}{d\zeta^2} + \frac{1}{\zeta}\frac{df^5}{d\zeta} + \frac{\zeta}{10}\frac{df}{d\zeta} + \frac{1}{5}f = 0\,. \tag{11.70}$$

This equation, when multiplied by ζ, is reduced to an equation in total derivatives. After integrating and using the conditions (11.67) and (11.68) we obtain a very simple relation for the function f:

$$f(\zeta) = \begin{cases} (\frac{10^{1/5}}{6})^{1/4}\left(1 - \frac{\zeta^2}{\zeta_0^2}\right)^{1/4} & \text{for } 0 \le \zeta \le \zeta_0\,, \\ 0 & \text{for } \zeta \ge \zeta_0 = \frac{10^{3/5}}{2} \approx 2\,. \end{cases} \tag{11.71}$$

Therefore the patch has at each moment a finite radius $r_0(t)$; this is the peculiar property of the nonlinear equation (11.64) that distinguishes the latter from the linear heat conduction equation (cf. chapter 2). The relation for the patch radius is

$$r_0(t) = 2\left[\frac{V^4\kappa(t-t_1)}{16\pi^4}\right]^{1/10} \simeq 0.55V^{4/10}\nu^{-1/10}\left[\frac{N^2}{(t-t_1)}\right]^{1/10} \tag{11.72}$$

which reveals that it grows with time very slowly. For the maximum patch thickness at time t we obtain the expression

$$h(0,t) = h_0(t) = \left(\frac{10^{1/5}}{6}\right)^{1/4}\left[\frac{V}{2\pi\kappa(t-t_1)}\right]^{1/5} \simeq 1.5\left[\frac{V\nu}{N^2(t-t_1)}\right]^{1/5}, \tag{11.73}$$

so that its decay in time also proceeds very slowly. It is of interest to consider the form of the patch's cross-section as represented in the reduced self-similar variables $r/r_0(t)$, $h/h_0(t)$ on Figure 11.8. The patch thickness is nearly constant and only at the very edge does it shrink abruptly, so that the patch has in fact a discoidal form.

Similarly, if the patch has a wake-like form, as do the patches of mixed fluid in the wakes of aircraft, often seen in the sky, equation (11.65) can be used, x being the horizontal coordinate along the wake's symmetry axis. The conservation condition for the volume of the mixed-fluid patch assumes the form

$$\int_{-\infty}^{\infty} h(x,t)dx = S = \int_{-\infty}^{\infty} h(x,0)dx = \text{const}\,; \tag{11.74}$$

here S is the patch's cross-sectional area. The initial conditions for

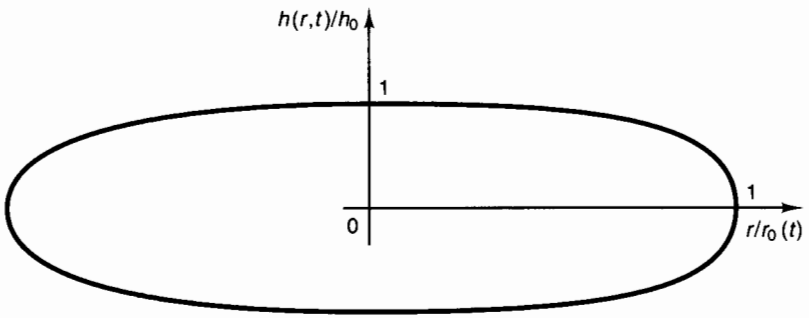

Figure 11.8. The form of a mixed-fluid patch at the viscous stage is nearly a discoidal.

an intermediate-asymptotic solution of instantaneous source type are represented in the form

$$h(x,t_1) \equiv 0 \text{ at } x \neq 0\,, \quad \int_{-\infty}^{\infty} h(x,t_1)dx = S\,, \tag{11.75}$$

and the solution, which may be obtained analogously to the previous one, is

$$h = \left[\frac{S^2}{4\kappa(t-t_1)}\right]^{1/6} f_1(\zeta)\,, \quad \zeta = \frac{x}{[S^4\kappa(t-t_1)/16]^{1/6}} \tag{11.76}$$

$$f_1(\zeta) = \begin{cases} A\left(1 - \frac{\zeta^2}{\zeta_0^2}\right)^{1/4} & \text{for } (0 \le \zeta \le \zeta_0) \\ 0 & \text{for } (\zeta \ge \zeta_0) \end{cases} \tag{11.77}$$

$$\zeta_0 = 15^{1/6}\left[\frac{2\Gamma(7/4)}{\Gamma(1/2)\Gamma(5/4)}\right]^{2/3} \approx 1.72\,, \quad A = \left(\frac{\zeta_0^2}{15}\right)^{1/4} \approx 0.67.$$

so that the relation for the edge of the patch $x = \pm\, x_0(t)$ is

$$x_0(t) = \zeta_0\left[S^4\kappa(t-t_1)/16\right]^{1/6}, \tag{11.78}$$

and maximum patch thickness decays with time as follows:

$$h(0,t) = h_0(t) = A\left[\frac{S^2}{4\kappa(t-t_1)}\right]^{1/6}. \tag{11.79}$$

Comparison of the intermediate asymptotics (11.72) and (11.78) with the intermediate asymptotics for the previous stage, (11.52), (11.53), leads to an important conclusion: after transition to the viscous stage, spreading of the patch slows down sharply, so that if observed at time intervals that are not too large, the patch can seem invarying. The scaling law of 1/6 (11.76) was obtained in a semi-quantitative way by

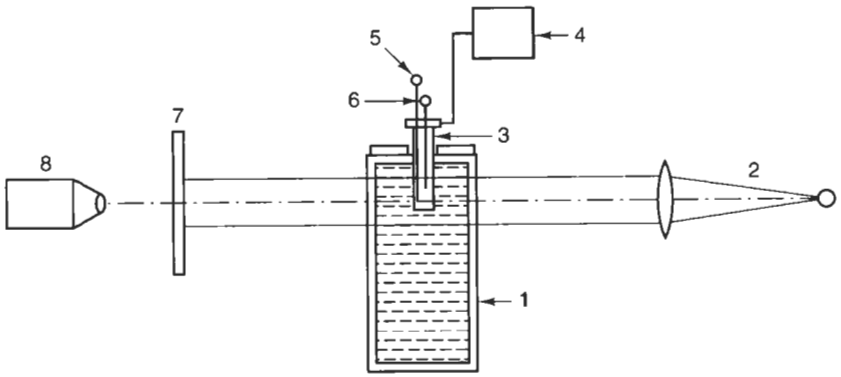

Figure 11.9. The scheme of the laboratory set-up for investigating the spreading of a mixed-fluid patch of circular planform (Zatsepin, Fedorov *et al.*, 1978). 1, the tank with stratified fluid; 2, shadowgraph; 3, glass tube; 4, DC electric motor; 5, mixer; 6, piston; 7, screen; 8, photographic or movie camera.

Maxworthy (1973) and, using the more detailed analysis presented here, by Barenblatt (1978a).

The relation (11.72) for the spreading of a patch of circular planform looks remarkably simple, so its experimental checking was important. This was performed in an elegant laboratory experiment by Zatsepin, Fedorov, *et al.* (1978). The following experimental scheme was used (Figure 11.9). Into an open Plexiglass tank filled by linearly density-stratified fluid a vertical hollow cylindrical tube was slowly introduced, under the fluid level. The fluid in the lower part of the tube, separated by a piston at rest, was then stirred by a special mixer. After allowing sufficient time for the fluid motion to decay the tube was slowly raised, releasing a patch of mixed fluid which started to spread into the ambient stratified fluid. The experimental set-up allowed the observation and recording of the two last stages of the patch's collapse. Photographs similar to those presented in Figure 11.10 demonstrate that, as expected, soon after the collapse starts, spreading of the patch slows sharply and the patch at this stage has the form of a disc with blunted edges, similar to that presented in Figure 11.8. The patch volume, kinematic fluid viscosity, fluid, and tube diameter were the same in all experiments. Therefore, if the relation (11.72) is valid then experimental points plotted in the coordinates

$$\log[2r_0(t)/D]\,,\ \log[N^2(t-t_1)] \tag{11.80}$$

should lie on a single straight line with slope 1/10. This is confirmed by the graph of Figure 11.11. The value $t_1 = 10$ s was obtained by the

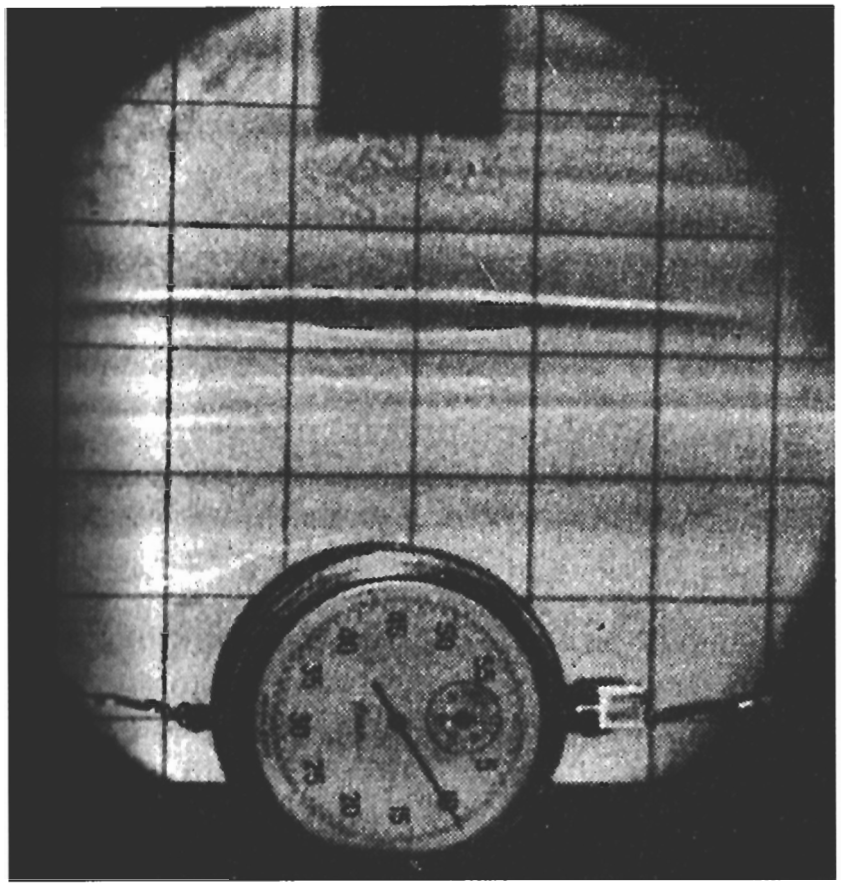

Figure 11.10. The shadow image of a spreading mixed-fluid patch (after Zatsepin, Fedorov *et al.*, 1978).

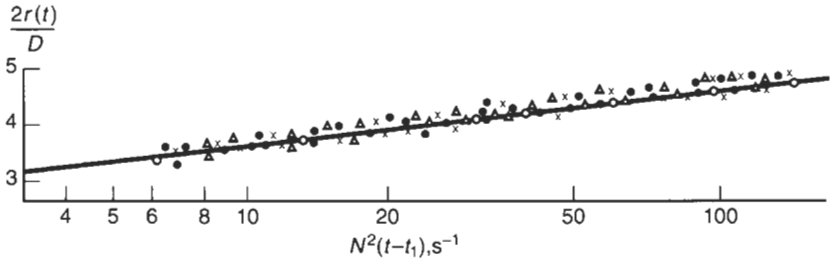

Figure 11.11. Results of experiment confirm the one-tenth law. •, $N = 0.63\ \mathrm{s}^{-1}$, ×, $N = 1.00\ \mathrm{s}^{-1}$, Δ, $N = 0.58\ \mathrm{s}^{-1}$ (after Zatsepin, Fedorov *et al.*, 1978).

same method of extrapolation as in Figure 10.7. Thus, the one-tenth law (11.72) received experimental confirmation by Zatsepin, Fedorov *et al.* (1978). It turned out also that the duration of the final viscous stage

is at least one order of magnitude longer than the duration of the two first stages; it reached in these experiments the value of about $300/N$.

It may be of interest for some applications to consider the case where the stratification is not continuous but stepwise: a two-layer fluid of density ρ_1 in the upper layer and density ρ_2 in the lower layer. Then for a viscous intrusion of intermediate density ρ_3 along the interface between the two fluid layers an equation similar to (11.64) is obtained but with a different exponent, 4 instead of 5 (Barenblatt, 1978a; Huppert, 1982):

$$\partial_t h = \kappa \Delta h^4, \quad \kappa = \frac{(\rho_2 - \rho_3)(\rho_3 - \rho_1)}{8c\mu(\rho_2 - \rho_1)} g. \tag{11.81}$$

In the special case $\rho_2 = \infty$ (viscous flow along the solid interface),

$$\kappa = \frac{(\rho_3 - \rho_1)g}{8c\mu}. \tag{11.82}$$

In the above-mentioned papers an axisymmetric solution of (11.81) was also presented, which corresponds to the spread of an initially concentrated viscous intrusion:

$$h = \left[\frac{V}{2\pi\kappa(t-t_1)}\right]^{1/4} f(\zeta), \quad \zeta = \frac{r}{[V^3\kappa(t-t_1)/8\pi^3]^{1/8}},$$
$$f(\zeta) = \begin{cases} (\frac{8^{1/4}}{5})^{1/3}\left(1 - \frac{\zeta^2}{\zeta_f^2}\right)^{1/3} & (0 \le \zeta \le \zeta_f), \\ 0 & (\zeta \ge \zeta_f = \frac{8^{3/4}}{\sqrt{3}}). \end{cases} \tag{11.83}$$

Thus the intrusion spreads along the interface of the layers according to

$$r_f(t) = 8^{3/4} 3^{-1/2} [V^3 \kappa (t - t_1)/8\pi^3]^{1/8}. \tag{11.84}$$

The solution (11.83) was compared with experiment in Huppert (1982); a good agreement was found.

In the paper Diez, Gratton and Gratton (1992) the same equation as (11.81) was derived and the axisymmetric focussing problem – an analogue of the Guderley very intense implosion problem in gas dynamics – was obtained. (For a rigorous investigation of the focussing problem for the general porous-medium equation see the paper by Aronson and Graveleau (1993).) The focussing problem for equation (11.81), like the Guderley problem in gas dynamics, has a self-similar intermediate asymptotics of the second kind. Comparison of this solution with a specially performed experiment, also reported in Diez, Gratton and Gratton (1992), leads to good agreement. It is an instructive example of the comparison of a self-similar solution of the second kind with an experiment that is physical, not numerical.

11.7 Several phenomena related to turbulence in a stably stratified fluid

Under strong stable stratification turbulence is suppressed owing to a large consumption of turbulent energy in work done against the buoyancy force. In fact, the equation for the turbulent energy balance in a stratified fluid has the form

$$\partial_t b = -\langle u'w'\rangle \partial_z u - \epsilon - \partial_z[\langle b'w'\rangle + \langle p'w'\rangle/\rho] - \overline{\rho' w'} g/\rho. \tag{11.85}$$

The last term is new in comparison with the same equation for a homogeneous fluid and determines the energy consumption rate for the work against the buoyancy force. Owing to the large value of the acceleration due to gravity, g, the contribution of this term is substantial in spite of the fact that the magnitude of the density fluctuations ρ' is small in comparison with the mean density ρ, and the contribution of ρ' to other terms in the equation is small and can be neglected. Therefore the turbulence cannot exist under natural conditions for long times in the whole fluid volume (Monin and Ozmidov, 1981). In fact, turbulence is concentrated in pancake-form layers, vertically uniform owing to turbulent mixing and separated by relatively thin layers (laminar sheets, see Woods, 1968), where a sharp variation in temperature, salinity, density, electroconductivity, and sound speed, as well as other thermodynamic properties, and sometimes also in flow velocity, is concentrated. This laminated vertical structure of flow fields, which is revealed by steps on vertical profiles of temperature, density, and other thermodynamic properties, is called, depending on the vertical scale, the *microstructure* or *fine structure* of flow fields. Numerous field experiments specially performed from research vessels by the method of continuous vertical sounding have revealed that this phenomenon exists practically everywhere in the world's oceans.

Smoothing the distributions of density or temperature over depth one obtains a curve that characterises large-scale stratification (a similar smooth curve is obtained when averaging data over time). The stability parameter of the shear flow for a stably stratified fluid is the Richardson number

$$\mathrm{Ri} = \frac{|d\rho/dz|\, g}{\rho(\partial_z u)^2} = \frac{N^2}{(\partial_z u)^2}. \tag{11.86}$$

Instability in a shear flow is commonly related to reaching a critical value $\mathrm{Ri}_{\mathrm{cr}} = 0.25$ in the Richardson number: this was a theoretical result of Miles (1961, 1963). In stable flows $\mathrm{Ri} > \mathrm{Ri}_{\mathrm{cr}}$. As a rule, large scale stratification is stable from the viewpoint of this criterion,

so Ri > 0.25. However, if the microstructure is taken into account, intervals with Ri < 0.25 are observed on the graph Ri(z), i.e., instability regions. Apparently, in some of these intervals turbulence generation at the moment of sounding was observed†. This generation of turbulence is related to internal waves: the Richardson number is obviously minimal at the crests and hollows of internal waves. Moreover, other such mechanisms of turbulence generation are plausible, such as the breaking of internal waves, their resonance interaction, etc. For mixed-fluid patches in the atmosphere and ocean that appear after the breaking of internal waves, the rapid generation of a continuous spectrum, i.e., the formation of developed turbulence, is characteristic even for short times after breaking (Belyaev, Losovatsky and Ozmidov, 1975; SethuRaman, 1980). This is understandable, because after fluid stirring following the breaking of internal waves the fluid in the stirred region becomes density homogeneous, so the energy consumption rate due to work against the buoyancy flow (the last term of equation (11.85)) vanishes there. Therefore in the patch of mixed fluid formed in a shear flow conditions arise for the generation and rather long-term existence of turbulence at higher levels than in the ambient stratified fluid. In fact, the turbulent energy inflow due to the work done by the Reynolds stresses against the velocity gradient (the first term on the right-hand side of equation (11.85)) is consumed in the patch of mixed fluid by viscous dissipation into heat only, which is a relatively small effect; the third term on the right-hand side of equation (11.85), which is related to turbulent energy transfer, vanishes after integration over the patch thickness, so it does not influence the mean value of the turbulent energy. Thus, mainly owing to internal waves, the turbulence in fluids with strongly stable stratification has a specifically intermittent, 'archipelago' character. Furthermore, the patches of mixed fluid collapse basically in the same way as described in the previous section, where the turbulence inside the patch was not accounted for explicitly. The difference consists only in the time variation in the turbulent viscosity. Note its effect should not be substantial. This is seen already from the fact that the fluid viscosity within the patch enters the patch extension law (11.72) to the degree 1/10, so its variation over three orders of magnitude changes the radius only by a factor of

† Loss of stability in a steady homogeneous shear flow considered in Miles' (1961) paper, does not mean the origin of turbulence. Therefore the reaching of the critical value $\mathrm{Ri}_{cr} = 0.25$ as the condition of turbulence generation should be considered with a certain care. Analysis of experiments in the ocean shows (Monin and Ozmidov, 1981) that the critical Richardson number related to the origin of turbulence is close to 0.1.

two. It is plausible therefore that the turbulent patches in a fluid with strong stratification also have the form of circular discs and expand very slowly at the final stage. It is also plausible that the microstructure and fine structure in the ocean are related to pancake-form patches of fluid having constant temperature and density. These patches are in fact patches of mixed fluid, of various length scales, which arise mainly due to the breaking of internal waves, and are at the longest, final, viscous, stage of their evolution. The above considerations also give us a plausible explanation (Barenblatt and Monin, 1979b) of discoidal formations in the atmosphere, which have repeatedly attracted attention in recent years ('flying saucers').

Indeed, under strong stable stratification in the atmosphere (SethuRaman, 1980) and in the ocean (Woods, 1968) internal wave breaking is going on and so patches of mixed air or fluid appear. The patches of mixed fluid collapse, reach a discoidal form, and under sufficiently strong shear become turbulized. In this respect the paper of SethuRaman (1980) is of special interest. SethuRaman observed and registered the breaking of internal waves, as well as the creation and long-term existence of localized turbulence patches, under conditions of strong temperature inversion (strongly stable stratification) and strong shear of wind velocity (Figure 11.12). It is essential to note that, as SethuRaman's observations showed, sharply localized turbulence arising as a result of internal wave breaking (Figure 11.12(c)) is not a burst at the very moment of wave breaking, which then rapidly decays (cf. Figure 11.12(a)). On the contrary, it develops rather slowly and is maintained for rather a long time (more than an hour). The creation and long-term maintenance of localized turbulence can be explained, according to what was said above, by the work done by the Reynolds stresses on the strong wind-velocity shear at small viscous dissipation, when turbulent-energy consumption by the work against the buoyancy force has disappeared. Indeed, after wave breaking and subsequent stirring the air density in the patch should be homogeneous or close to homogeneous.

Discoidal patches of stirred turbulized air in the atmosphere sometimes, although rather rarely, become visible. Such visibility can be explained in the following way.

Let us assume that for some reason a certain amount of suspended particles, e.g. an aerosol, appears in the atmosphere. Under ordinary conditions these particles fall more or less uniformly over the area (Figure 11.13). To support the particles in a suspended state it is necessary (see section 11.3) for the ratio of the velocity of free fall to the mean

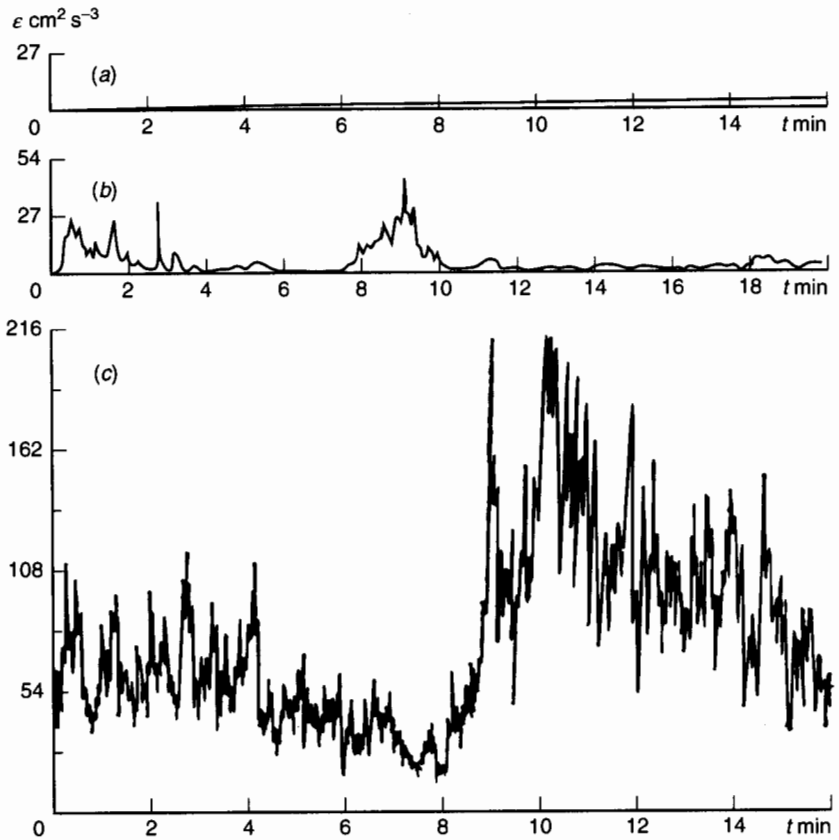

Figure 11.12. A turbulence-intensity measure – the dissipation rate ϵ – at different stages of internal wave breaking. (a) $z = 183$ m, no internal waves; (b) $z = 40$ m, the beginning of internal wave breaking, $z = 40$ m, (c) after internal wave breaking. (SethuRaman, 1980).

square velocity fluctuation to be less than a certain critical value. In the stratified air between the patches, the turbulence, according to what was said above, is low and cannot support the particles. In contrast, the turbulence in the patches can be sufficiently high to suspend the particles. The suspended particles increase the optical thickness of the patch and it becomes visible when the ambient air is illuminated by the Sun or Moon. Indeed, for the patch to be visible it is enough that its optical thickness τ is around one hundredth to one tenth. The necessary concentration of particles can be estimated by the relation $n = \tau/2\pi r^2 H$, where H is the effective patch thickness and r is the particle radius; we obtain for $H \sim 10^3$ cm and particles of size 3 μm (having a velocity of free fall

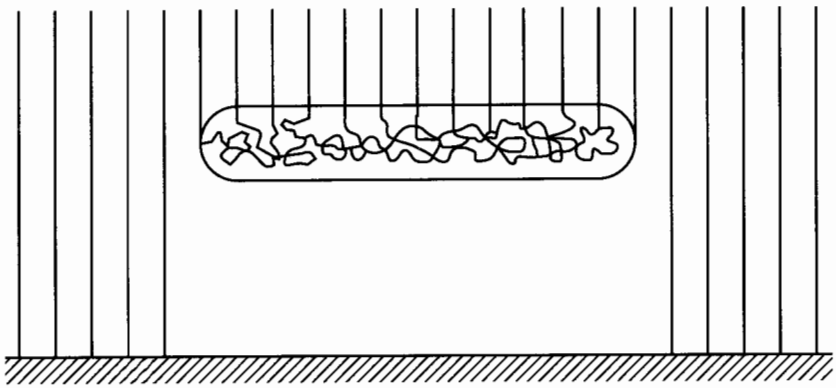

Figure 11.13. In a stratified fluid particles continue falling where the turbulence intensity is low, but are trapped by a discoidal patch where the turbulence is high.

of the order of several cm/s) a concentration n of order $10 - 10^2$ cm^{-3}. This value is quite realistic for dust clouds.

In the course of the extension of a patch its thickness is reduced, and the shear intensity necessary for supporting turbulence in the patch increases. When the available shear becomes insufficient to support turbulence, the patch drops the particles and becomes mixed with the ambient air.

An analogous explanation can be given of 'turbidity clouds' in the ocean.

References

Ablowitz, M.J. & Clarkson, P.A. (1991). *Solitons, Nonlinear Evolution Equations and Inverse Scattering.* Cambridge University Press.

Abramowitz, M. & Stegun, I.A., eds. (1970). *Handbook of Mathematical Functions.* Dover Publications, New York.

Adamsky, V.B. (1956). Integration of a system of autosimulating equations for the problem of a short-duration shock in a cold gas. *Soviet Phys. Acoustics* **2** (1), 1–7.

Aldushin, A.P., Zeldovich, Ya.B. & Khudyaev, S.I. (1979). *Flame propagation in a reacting gas mixture.* Preprint, Institute of Chemical Physics, Chernogolovka.

Alexandrov, S.E. & Goldstein, R.V. (1993a). On the separated flows in the theory of plasticity. *Izvestiya, Russian Ac. Sci. Mech. Solids* **4**, 144–149.

Alexandrov, S.E. & Goldstein, R.V. (1993b). The flow of plastic mass in a converging channel: the singularities of a solution. *Doklady, Russian Ac. Sci.* **332** (3), 314–316.

Amit, D. (1989). *Field Theory, the Renormalization Group and Critical Phenomena,* 2nd edition, World Scientific, Singapore etc.

Andrade, E.N. da C. (1910). On the viscous flow of metals and allied phenomena. *Proc. Roy. Soc.* **A84**, 1–12.

Anderson, D.M. & Davis, S.H. (1993). Two-fluid viscous flow in a corner. *J. Fluid Mech.* **257**, 1–31.

Andrianov, I.V. & Kholod, E.G. (1993). Intermediate asymptotics in nonlinear dynamics of shells. *Izvestiya, Russian Ac. Sci., Mech. Solids* **2**, 172–7.

Andrushchenko, V.A., Barenblatt, G.I. & Chudov, L.A. (1975). Self-similar propagation of strong blast waves in the presence of radiation or energy release at the wave front. In *Progress in the Mechanics of Deformable Media, collection of papers dedicated to the 100th anniversary of B.G. Galerkin,* Shapiro, G.S. (ed.), 35–44, (in Russian) Nauka, Moscow.

Angenent, S.B. & Aronson, D.G. (1993). The focusing problem for the radially symmetric porous medium equation. *Euro. J. Appl. Math.*, (to appear).

Aronson, D.G. & Graveleau, J. (1993). A self-similar solution to the focusing problem for the porous medium equation. *Euro. J. Appl. Math.* **4**, 65–81.

Aronson, D.G. & Vázquez, J.L. (1993). Anomalous exponents in nonlinear diffusion. IMA Preprint No. 1165, University of Minnesota.

Bailey, R.W. (1929). *Transactions of Tokyo Sect. Meeting of the World Power Conference,* Tokyo.

Baldin, A.M. & Didenko, L.A. (1990). Asymptotic properties of hadron matter in relative four-velocity space. *Fortschritte der Physik* **38** (4), 261–332.

Barenblatt, G.I. (1952). On some unsteady motions of fluids and gases in a porous medium, *Prikl. Mat. Mekh.* **16** (1), 67–78.

Barenblatt, G.I. (1953). On the motion of suspended particles in a turbulent flow, *Prikl. Mat. Mekh.* **17** (3), 261–274.

Barenblatt, G.I. (1954). On limiting self-similar motions in the theory of unsteady filtration of gas in a porous medium and the theory of the boundary layer, *Prikl. Mat. Mekh.* **18** (4), 409–414.

Barenblatt, G.I. (1955). On the motion of suspended particles in a turbulent flow, occupying a half-space or a plane open channel of finite depth, *Prikl. Mat. Mekh.* **19** (1), 61–88.

Barenblatt, G.I. (1956). On certain problems of the theory of elasticity, which arise in the theory of the hydraulic fracture of the oil stratum. *Appl. Math. Mech. (PMM)* **20** (4), 475–486.

Barenblatt, G.I. (1959a). On the equilibrium cracks formed in brittle fracture. *Appl. Math. Mech. (PMM)* **23**: (3), 434–44; (4), 706–21; (5), 893–900.

Barenblatt, G.I. (1959b). The problem of thermal self-ignition. In: Gelfand, I.M. *Some Problems of the Theory of Quasi-Linear Equations,*, Russian Mathematical Surveys Vol. **14** (2), 137–42.

Barenblatt, G.I. (1962). Mathematical theory of equilibrium cracks in brittle fracture. *Adv. Appl. Mech.* **7**, 55–129.

Barenblatt, G.I. (1964). On certain general concepts of the mathematical theory of brittle fracture. *Appl. Math. Mech. (PMM)* **28** (4), 630–43.

Barenblatt, G.I. (1977). Strong interaction of gravity waves and turbulence. *Izvestiya, USSR Ac. Sci., Atmos. Oceanic Phys.* **13** (8), 581–83.

Barenblatt, G.I. (1978a). Dynamics of turbulent spots and intrusions in a stably stratified fluid. *Izvestiya, USSR Ac. Sci., Atmos. Oceanic Phys.* **14** (2), 139–45.

Barenblatt, G.I. (1978b). Self-similarity of temperature and salinity distributions in the upper thermocline. *Izvestiya, USSR Acad. Sci., Atmos. Oceanic Phys.* **14** (11), 820–23.

Barenblatt, G.I. (1979). *Similarity, Self-similarity, and Intermediate Asymptotics* (1st Russian edition Gidrometeoizdat, Leningrad, 1978; 2nd Russian edition, Gidrometeoizdat, Leningrad, 1982). Plenum, New York, London.

Barenblatt, G.I. (1983). Self-similar turbulence propagation from an instantaneous plane source. In *Non-linear dynamics and turbulence,* Barenblatt, G.I., Iooss, G. & Joseph, D.D. (eds.), 48–60, Pitman, Boston.

Barenblatt, G.I. (1987). *Dimensional Analysis,* Gordon and Breach, New York, London.

Barenblatt, G.I. (1991). On the scaling laws (incomplete self-similarity with respect to Reynolds number) for the developed turbulent flows in tubes. *C.R. Acad. Sci. Paris,* **313**, Sér. II, 107–12.

Barenblatt, G.I. (1993a). Scaling laws for fully developed turbulent shear flows. Part 1. Basic hypotheses and analysis. *J. Fluid Mech.* **248**, 513–20.

Barenblatt, G.I. (1993b). Intermediate asymptotics, scaling laws and renormalization group in continuum mechanics. *Meccanica* **28**, 177–83.

Barenblatt, G.I. (1993c). Some general aspects of fracture mechanics. In *Modelling of Defects and Fracture Mechanics*, Herrmann, G. (ed.), pp. 29–50. Springer-Verlag, Vienna, New York.

Barenblatt, G.I. (1994). *Scaling Phenomena in Fluid Mechanics*. Cambridge University Press.

Barenblatt, G.I. & Botvina, L.R. (1981). Incomplete self-similarity of fatigue in the linear range of crack growth. *Fatigue of Engineering Materials and Structures* **3**, 193–212.

Barenblatt, G.I. & Botvina, L.R. (1982). A note concerning power-type constitutive equations of deformation and fracture of solids. *Int. J. Eng. Sci.,* **20** (2), 187–91.

Barenblatt, G.I. & Botvina, L.R. (1983). The self-similarity of fatigue fracture. The damage accumulation. *Izvestiya, USSR Ac. Sci., Mech. Solids* **44**, 161–5.

Barenblatt, G.I. & Botvina, L.R. (1986). Similarity methods in mechanics and physics of fracture. *Physical and Chemical Mechanics of Materials* (1), 57–62.

Barenblatt, G.I. & Botvina, L.R. (1993). Self-oscillatory modes of fatigue fracture and the formation of self-similar structures at the fracture surface. *Proc. Roy. Soc. London* **A442**, 489–94.

Barenblatt, G.I. & Christianovich, S.A. (1955). On the failure of the roof in mine-workings. *Izvestiya, USSR Ac. Sci., Techn. Sci.* **11**, 73–86.

Barenblatt, G.I., Entov, V.M. & Ryzhik, V.M. (1990). *Theory of Fluid Flows Through Natural Rocks.* Kluwer Academic Publishers, Dordrecht, Boston, London.

Barenblatt, G.I., Galerkina, N.L. & Lebedev, I.A. (1992). Mathematical model of lower quasi-homogeneous oceanic layer: general concepts and sealing-off model. *Izvestiya, Russian Ac. Sci., Atmos. Oceanic Phys.* **28** (1), 68–74.

Barenblatt, G.I., Galerkina, N.L. & Lebedev, I.A. (1993). Mathematical model of lower quasi-homogeneous oceanic layer: effects of temperature and salinity stratification and tidal oscillations. *Izvestiya, Russian Ac. Sci., Atmos. Oceanic Phys.* **29** (4), 537–42.

Barenblatt, G.I., Galerkina, N.L. & Luneva, M.V. (1987). Evolution of turbulent burst. *Inzhenerno-Fizichesky Zh. (Zh. Eng. Phys.)* **53**, 733–40.

Barenblatt, G.I. & Gavrilov, A.A. (1974). On the theory of self-similar degeneracy of homogeneous isotropic turbulence. *Sov. Phys. JETP* **38** (2), 399–402.

Barenblatt, G.I. & Goldenfeld, N.D. (1995). Does fully developed turbulence exist? Reynolds number independence versus asymptotic covariance. *Phys. Fluids* **7** (12), 3078–3082.

Barenblatt, G.I. & Golitsyn, G.S. (1974). Local structure of mature dust storms. *J. Atmos. Sci.* **31**, 1917–33.

Barenblatt, G.I., Guirguis, R.H., Kamel, M.M., Kuhl, A.L., Oppenheim, A.K. & Zeldovich, Ya.B. (1980). Self-similar explosion waves of variable energy at the front. *J. Fluid Mech.* **99** (4), 811–58.

Barenblatt, G.I. & Krylov, A.P. (1955). On elasto-plastic regime of filtration. *Izvestiya, USSR Ac. Sci., Tech. Sci.* **2**, 14–26.

Barenblatt, G.I. & Monin, A.S. (1976). *Similarity Laws for Stratified Turbulent Shear Flows. Report of the Fourth All-Union Congress on Theoretical and Applied Mechanics*, 41, Naukova Dumka. Kiev.

Barenblatt, G.I. & Monin, A.S. (1979a). Similarity laws for turbulent stratified shear flows. *Arch. Rat. Mech. Anal.* **70** (4), 307–17.

Barenblatt, G.I. & Monin, A.S. (1979b). On a plausible mechanism of the phenomenon of discoidal formations in the atmosphere. *Doklady, USSR Ac. Sci.,* **246** (4) 834–837.

Barenblatt, G.I. & Monin, A.S. (1983). Similarity principles for the biology of pelagic animals. *Proc. Natl. Acad. Sci. USA* **80** (6), 3540–42.

Barenblatt, G.I. & Prostokishin, V.M. (1993). Scaling laws for fully developed turbulent shear flows. Part 2. Processing of experimental data. *J. Fluid Mech.* **248**, 521–9.

Barenblatt, G.I. & Sivashinsky, G.I. (1969). Self-similar solutions of the second kind in nonlinear filtration. *Appl. Math. Mech. (PMM)* **33** (5), 836–45.

Barenblatt, G.I. & Sivashinsky, G.I. (1970). Self-similar solutions of the second kind in the problem of propagation of intense shock waves. *Appl. Math. Mech. (PMM)* **34** (4), 655–62.

Barenblatt, G.I. & Vishik, M.I. (1956). On the finite speed of propagation in the problems of unsteady filtration of fluid and gas in a porous medium. *Appl. Math. Mech. (PMM)* **20** (4), 411–17.

Barenblatt, G.I. & Zeldovich, Ya.B. (1957a). On the dipole-type solution in the problem of a polytropic gas flow in a porous medium. *Appl. Math. Mech. (PMM),* **21** (5), 718–20.

Barenblatt, G.I. & Zeldovich, Ya.B. (1957b). On the stability of flame propagation. *Appl. Math. Mech. (PMM)* **21** (6), 856–9.

Barenblatt, G.I. & Zeldovich, Ya.B. (1971). Intermediate asymptotics in mathematical physics. *Russian Math. Surveys* **26** (2), 45–61.

Barenblatt, G.I. & Zeldovich, Ya.B. (1972). Self-similar solutions as intermediate asymptotics. *Ann. Rev. Fluid Mech.* **4**, 285–312.

Batchelor, G.K. (1967). *An Introduction to Fluid Dynamics.* Cambridge University Press.

Batchelor, G.K. & Linden, P.F. (1992). Discussion at the Fluid Mechanics Seminar, DAMTP, University of Cambridge.

Bechert, K. (1941). Differentialgleichungen der Wellenausbreitung in Gasen. *Ann. Phys.* **39** (5), 357–72.

Belyaev, V.S. & Gesentzwei, A.N. (1978). Shear instabilities of internal waves in the ocean. *Izvestiya, USSR Ac. Sci., Atmos. Oceanic Phys.* **14** (6), 459–63.

Belyaev, V.S., Losovatsky, I.D. & Ozmidov, R.V. (1975). Relationships between small-scale turbulence parameters and local stratification conditions in the ocean. *Izvestiya, USSR Ac. Sci., Atmos. Oceanic Phys.* **11** (7), 448–52.

Benbow, J.J. (1960). Cone cracks in fused silica. *Proc. Phys. Soc.* **B75**, 697–99.

Benilov, A.Yu. (1973). Generation of ocean turbulence by surface waves. *Izvestiya, USSR Ac. Sci., Atmos. Oceanic Phys.* **9** (3), 160–4.

Beretta, E., Bertsch, M. & Dal Passo, R. (1995). Non-negative solutions of a fourth-order nonlinear degenerate parabolic equation. *Arch. Rat. Mech. Anal.* **129** (2), 175–200.

Bernis, F. & Friedman, A. (1990). Higher order nonlinear degenerate parabolic equations. *J. Diff. Equations* **83** (1), 179–206.

Bernis, F., Peletier, L.A. & Williams, S.M. (1992). Source type solutions of a fourth order nonlinear degenerate parabolic equation. *Nonlinear Anal., Theory, Meth. Applic.* **18** (3), 217–34.

Bertozzi, A.L., Brenner, M.P., Dupont, T.F. & Kadanoff, L.P. (1993). Singularities and similarities in Interface Flows. Preprint, Ryerson Laboratory, University of Chicago.

Bertozzi, A.L. & Pugh, M. (1995). The lubrication approximation for thin viscous films: regularity and long time behavour of weak solutions. *Comm. Pure Appl. Math.* (in press).

Bertsch, M., Dal Passo, R. & Kersner, R. (1994). The evolution of turbulent bursts: the $b - \epsilon$ model. *Euro. J. Appl. Math.* **5** (4), 537–557.

Birkhoff, G. (1960). *Hydrodynamics, a Study in Logic, Fact, and Similitude*, 2nd edition. Princeton University Press.

Bluman, G.W. & Cole, J.D. (1974). *Similarity Methods for Differential Equations*, Springer-Verlag, New York, Heidelberg, Berlin.

Boatto, S., Kadanoff, L.P. & Olla, P. (1993). Travelling wave solutions to thin film equations. Preprint, Ryerson Laboratory, University of Chicago.

Bogolyubov, N.N. & Shirkov, D.V. (1955). On the renormalization group in quantum electrodynamics. *Doklady, USSR Ac. Sci.*, **103** (2), 203–6.

Bogolubov, N.N. & Shirkov, D.V. (1959). *Introduction to the Theory of Quantized Fields.* Wiley Interscience, New York, London.

Bose, E. & Bose, M. (1911). Über die Turbulenzreibung verschiedener Flüssigkeiten. *Physikalische Zeitschrift* **12** (4), 126–35.

Bose, E. & Rauert, D. (1909). Experimentalbeitrag zur Kenntnis der turbulenten Flüssigkeitsreibung. *Physikalische Zeitschrift* **10** (12), 406–9.

Botvina, L.R. (1989). *The Kinetics of Fracture of Structural Materials.* Nauka, Moscow.

Brailovsky, I. & Sivashinsky, G.I. (1994). Oscillatory propagation of reaction waves sustained by external sources of energy (to appear).

Bricmont, J. & Kupiainen, A. (1992). Renormalization group and the Ginzburg-Landau equation. *Comm. Math. Phys.* **150**, 193–208.

Bridgman, P.W. (1931). *Dimensional Analysis.* Yale University Press, New Haven.

Brushlinsky, K.V. & Kazhdan, Ya.M. (1963). On auto-models in the solution of certain problems of gas dynamics. *Russian Math. Surveys* **18** (2), 1-22.

Budiansky, B. & Carrier, G.F. (1973). The pointless wedge. *SIAM J. Appl. Math.* **25** (3), 378–87.

Bui, H.D. (1977). *Mécanique de la Rupture Fragile.* Masson, Paris.

Cane, B.J. & Greenwood, G.W. (1975). The nucleation and growth of cavities in iron during deformation at elevated temperatures. *Metal Sci.* **9** (2), 55–60.

Carothers, S.D. (1912). Plane strain in a wedge. *Proc. Roy. Soc. Edinburgh* **23**, 292–306.

Carrier, G.F. & Pearson, C.E. (1976). *Partial Differential Equations, Theory and Technique.* Academic Press, New York, San Francisco, London.

Carslaw, H.W. & Jaeger, J.C. (1960). *Conduction of Heat in Solids*, 2nd edition. Clarendon, Oxford.

Castaing, B., Gagne, Y. & Hopfinger, E.J. (1990). Velocity probability density functions of high Reynolds number turbulence. *Physica D.* **46** 177–200.

Chen, L.-Y. & Goldenfeld, N. (1992). Renormalization-group theory for the propagation of a turbulent burst. *Phys. Rev.* **A45** (8), 5572–4.

Chen, L.-Y., Goldenfeld, N. & Oono, Y. (1991). Renormalization-group theory for the modified porous-medium equation. *Phys. Rev.* **A44** (10), 6544–50.

Chen, L.-Y., Goldenfeld, N. & Oono, Y. (1994). Renormalization group theory for global asymptotic analysis. *Phys. Rev. Lett.* (submitted).

Chernyi, G.G. (1961). *Introduction to Hypersonic Flow* (trans. R.F. Probstein). Academic Press, New York.

Cole, J.D. (1968). *Perturbation Methods in Applied Mathematics.* Blaisdell, Toronto, London.

Cole, J.D. & Wagner, B.A. (1995) On self-similar solutions of Barenblatt's non-linear filtration equation. *Euro. J. Appl. Math* (in press).

Collins, R.E. (1961). *Flow of Fluids through Porous Materials.* Reinhold, New York.

Corino, E.R. & Brodkey, R.S. (1969). A visual investigation of the wall region in turbulent flow. *J. Fluid Mech.* **37** (1), 1-30.

Daniell, P.J. (1930). The theory of flame motion. *Proc. Roy. Soc.* **A126**, 393–402.

Dempsey, J.P. (1981). The wedge subjected to tractions: a paradox resolved. *J. Elasticity* **11**, 1–10.

Diez, J.A., Gratton, R. & Gratton, J. (1992). Self-similar solution of the second kind for a convergent viscous gravity current. *Phys. Fluids* **A4** (6), 1148–55.

Drazin, P.G. & Johnson, R.S. (1989). *Solitons: An Introduction.* Cambridge University Press.

Dryden, H.L. (1943). A review of the statistical theory of turbulence. *Quart. J. Appl. Math.* **1**, 7–42.

Dundurs, J. & Markenscoff, X. (1989). The Sternberg-Koifer conclusion and other anomalies of the concentrated couple. *ASME J. Appl. Mech.* **56**, 240–5.

Dussan, V., E.B. & Davis, S.H. (1986). Stability in systems with moving contact lines. *J. Fluid Mech.* **173**, 115–30.

Dussan, V., E.B., Ramé E. & Garoff, S. (1991). On identifying the appropriate boundary conditions at a moving contact line: an experimental investigation. *J. Fluid Mech.* **230**, 97–116.

Efimov, S.S. & Tsarenko, V.M. (1980). Self-similarity of the temperature distribution in the upper thermocline. *Izvestiya, USSR Ac. Sci., Atmos. Oceanic Phys.* **16** (6), 429–33.

Eilenberger, G. (1981). *Solitons. Mathematical Methods for Physicists.* Springer-Verlag, Berlin, Heidelberg, New York.

Einstein, H.A. & Ning Chen (1955). *Effects of Heavy Sediment Concentration Near the Bed on the Velocity and Sediment Distribution.* University of California MRD Series Report No. 8.

Entov, V.M. (1994). Private communication.

Fedorov, K.N. (1976). *Fine Thermohaline Structure of Ocean Water.* Gidrometeoizdat, Leningrad.

Fisher, R.A. (1937). The wave of advance of advantageous genes. *Ann. Eugenics*, **7**, 355–69.

Fordy, A.P. (ed.) (1990). *Soliton Theory: A Survey of Results.* Manchester University Press, Manchester, New York.

Forsyth, P.J.E. (1976). Some observations and measurements on mixed fatigue tensile crack growth in aluminium alloys. *Scripta Metall.* **10**, 383–6.

Fourier, J. (1822). *Théorie analytique de la chaleur.* Firmin Didot, Paris.

Frankel, M., Roytburd, V. & Sivashinsky, G. (1994). A sequence of period doubling and chaotic pulsations in a free-boundary problem modelling thermal instabilities. *SIAM J. Appl. Math.* (to appear).

Gad-el-Hak, M. & Corrsin, S. (1974). Measurements of the nearly isotropic turbulence behind a uniform jet grid. *J. Fluid Mech.* **62** (1), 115–43.

Gardner, C.S.J., Greene, J.M., Kruskal, M.D. & Miura, R.M. (1967). A method for solving the Korteweg-de-Vries equation. *Phys. Rev. Lett.* **19**, 1095–97.

Gell-Mann, M. & Low, F.E. (1954). Quantum electrodynamics at small distances. *Phys. Rev.* **95**, 1300–12.

Germain, P. (1973). Méthodes asymptotiques en mécanique des fluids. In *Dynamics of Fluids*, R. Balian & J.L. Peube (eds.), 7–147. Gordon and Breach, London, etc.

Germain, P. (1986a). Mécanique, tome I. Ecole Polytechnique, Ellipses, Paris.

Germain, P. (1986b). Mécanique, tome II. Ecole Polytechnique, Ellipses, Paris.

Ginzburg, I.S., Entov, V.M. & Theodorovich, E.V. (1992). Renormalization group method for the problem of convective diffusion with irreversible sorption. *Appl. Math. Mech. (PMM)* **56** (1), 59–96.

Goldenfeld, N. (1989). The approach to equilibrium: scaling and the renormalization group. Invited lecture at the Conference on Non-linear Phenomena, Moscow, USSR Ac. Sci., 19–22 September.

Goldenfeld, N. (1992). *Lectures on Phase Transitions and the Renormalization Group.* Addison-Wesley.

Goldenfeld, N., Martin, O. & Oono, Y. (1989). Intermediate asymptotics and renormalization group theory. *J. Scient. Comput.* **4**, 355–72.

Goldenfeld, N., Martin, O. & Oono, Y. (1991). Asymptotics of partial differential equations and the renormalization group. In *Proc. NATO Advanced Research Workshop on Asymptotics Beyond all Orders, La Jolla*, S. Tanvera (ed.). Plenum Press.

Goldenfeld, N., Martin, O., Oono, Y. & Liu, F. (1990). Anomalous dimensions and the renormalization group in a non-linear diffusion process. *Phys. Rev. Lett.* **65** (12), 1361–64.

Goldenfeld, N. & Oono, Y. (1991). Renormalization group theory for two problems in linear continuum mechanics. *Physica A.* **177**, 213–19.

Goldstein, S. (1939). A note on the boundary layer equations. *Proc. Camb. Phil. Soc.* **35**, 338–40.

Goldstein, R.V. & Vainshelbaum, V.M. (1978). Material scale length as a measure of fracture toughness in fracture mechanics of plastic materials. *Int. J. Fracture,* **14** (2), 185–201.

Golitsyn, G.S. (1973). *Introduction to the Dynamics of Planetary Atmospheres.* Gidrometeoizdat, Leningrad.

Gossard, E.E. & Hooke, W.H. (1975). *Waves in the Atmosphere.* Elsevier, New York.

Grebenev, V.N. (1992). The dynamic system that arises in the problem of the evolution of a turbulent layer of a homogeneous fluid. *Comput. Math. and Math. Phys.* **32** (1), 103–13.

Griffith, A.A. (1920). The phenomenon of rupture and flow in solids. *Phil. Trans. Roy. Soc. London* **A221**, 163–98.

Guderley, K.G. (1942). Starke kugelige und zylindrische Verdichtungsstösse in der Nähe des Kugelmittelpunktes bzw. der Zylinderachse. *Luftfahrtforschung* **19** (9), 302–12.

Häfele, W. (1955). Zur analytischen Behandlung ebener, starker, instationärer Stosswellen. *Z. Naturforschung* **10a** (9/10), 693–7.

Hahn, H.G. (1976). *Bruchmechanik.* Teubner, Stuttgart.

Hain, K. & Hörner, S.V. (1954). Instationäre starke Stossfronten. *Z. Naturforschung* **9a** (12), 993–1004.

Hanjalic, K. & Launder, B.E. (1972). A Reynolds stress model of turbulence, and its application to thin shear flows. *J. Fluid Mech.* **52**, 609–38.

Harmon, L.D. (1973). Recognition of faces. *Scientific American* **229** (5), 70–82.

Hastings, S.P. & Peletier, L.A. (1992). On a self-similar solution for the decay of turbulent bursts. *Euro. J. Appl. Math.* **3**, 319–41.

Heiser, F.A. & Mortimer, W. (1972). Effects of thickness and orientation on fatigue crack growth rate in 4340 steel. *Met. Trans.* **3**, 2119–23.

Hill, R. (1992). Similarity analysis of creep indentation tests. *Proc. Roy. Soc. London* **A436**, 617–30.

Hill, R., Storåkers, B. & Zdunek, A.B. (1989). A theoretical study of the Brinell hardness test. *Proc. Roy. Soc. London* **A423**, 301–30.

Hinch, E.J. (1991). *Perturbation Methods.* Cambridge University Press.

Hinze, J.O. (1959). *Turbulence. An Introduction to its Mechanism and Theory.* McGraw-Hill, New York, Toronto, London.

Hinze, J.O. (1962). Turbulent pipe-flow, in *Mècanique de la turbulence*, 63–76. Edition du Centre Nat. Rech. Sci. Paris.

Hulshof, J. (1993). Self-similar solutions of the $k - \epsilon$ model for turbulence. Report No. W93-11, Mathematical Institute, University of Leiden.

Hulshof, J. & Vázquez, J.L. (1993). Self-similar solutions of the second kind for the modified porous medium equation. Report No. W93–04, Mathematical Institute, University of Leiden.

Huppert, H.E. (1982). The propagation of two-dimensional and axisymmetric viscous gravity currents over a rigid horizontal surface. *J. Fluid Mech.* **121**, 43–58.

Inglis, C.E. (1922). Some special cases of two-dimensional stress and strain. *Trans. Inst. Naval Arch.* **64**, 253–8.

Irwin, G.R. (1949). Fracture dynamics, in *Fracturing of Metals*, 147–66. ASM, Cleveland, OH.

Irwin, G.R. (1957). Analysis of stresses and strains near the end of a crack traversing a plate. *J. Appl. Mech.* **24**, 361–4.

Irwin, G.R. (1958). Fracture, in *Handbuch der Physik, Bd VI*, pp. 551-90. Springer, Berlin.

Irwin, G.R. (1960). Fracture mode transition for a crack traversing a plate. *Trans. ASME, Ser. D* **82**, 417–25.

Jeffrey, A. & Kakutani, T. (1972). Weak non-linear dispersive waves: a discussion centered around the Korteweg-de-Vries equation. *SIAM Review* **14** (4), 582–643.

Johnson, K.L. (1985). *Contact Mechanics*. Cambridge University Press.

Kadanoff, L.P. (1966). Scaling laws for Ising model near T_c. *Physics* **2** (6), 263–72.

Kadanoff, L.P., Götze, W., Hamblen, D., Hecht, R., Lewis, E.A.S., Paleiauskas, V.V.I., Rayl, M., Swift, J., Aspnes, D. & Kane, J. (1967). Static phenomena near critical points: theory and experiment. *Rev. Mod. Phys.* **39** (2), 395–431.

Kalashnikov, A.S. (1987). Some problems of qualitative theory of non-linear second-order parabolic equations. *Russian Math. Surveys* **42**, 169–222.

Kamenomostskaya, S.L. (Kamin) (1957). On a problem of the theory of filtration. *Doklady, USSR Ac. Sci.*, **116** (1), 18–20.

Kamin, S., Peletier, L.A. & Vázquez, J.-L. (1991). On the Barenblatt equation of elasto-plastic filtration. *Indiana Univ. Math. J.* **40** (4), 1333-62.

Kamin, S. & Vázquez, J.L. (1992). The propagation of turbulent bursts. *Euro. J. Appl. Math.* **3**, 263–72.

Kanel', Ya.I. (1962). On the stabilization of solutions of Cauchy problems met within the theory of combustion. *Matem. Sb.* **59** (101), 245–88.

Kao, T.W. (1976). Principal stage of wake collapse in a stratified fluid: two-dimensional theory. *Phys. Fluids* **19** (8), 1071–4.

Kapitza, S.P., (1966). A natural system of units in classical electrodynamics and electronics. *Sov. Phys. Uspekhi* **9**, 184.

Karpman, V.I. (1975). *Non-linear Waves in Dispersive Media*. Pergamon, Oxford.

Keller, L.V. & Friedmann, A.A. (1924). Differentialgleichungen für die turbulente Bewegung einer kompressiblen Flüssigkeit. In *Proc. First Int. Congress Appl. Mech.*, pp. 395–405. J. Waltman Jr, Delft.

Kerchman, V.I. (1971). On self-similar solutions of the second kind in the theory of unsteady filtration. *Appl. Math. Mech. (PMM)* **35** (1), 158–62.

Kestin, J. & Richardson, P.D. (1963). Heat transfer across turbulent incompressible boundary layers. *Int. J. Heat. Mass Transfer* **6** (2), 147–89.

Kevorkian, J. & Cole, J.D. (1980). *Perturbation Methods in Applied Mathematics*. Springer-Verlag, New York, Heidelberg, Berlin.

Kim, H.T., Kline, S.J. & Reynolds, W.C. (1971). The production of turbulence near a smooth wall in a turbulent boundary layer. *J. Fluid Mech.* **50** (1), 133–60.

Kistler, A.L. & Vrebalovich, T. (1966). Grid turbulence at large Reynolds numbers. *J. Fluid Mech.* **26** (1), 37–47.

Kitaigorodsky, S.A. & Miropolsky, Yu.Z. (1970). *Izvestiya, USSR Ac. Sci., Atmos. Oceanic Phys.* **6** (2), 97–102.

Kline, S.J., Reynolds, W.C., Schraub, F.A. & Runstadler, P.W. (1967). The structure of turbulent boundary layers. *J. Fluid Mech.* **30** (4), 741–74.

Kochin, N.E., Kibel', I.A. & Roze, N.V. (1964). *Theoretical Hydromechanics*, Vol. 1. Interscience, New York. Vol. 2 available from ASTIA as AD129210.

Kochina, I.N., Mikhailov, N.N. & Filinov, M.V. (1983). Groundwater mound damping. *Int. J. Eng. Sci.* **21** (4), 413–21.

Kolmogorov, A.N. (1941). The local structure of turbulence in incompressible fluids at very high Reynolds numbers. *Doklady, USSR Ac. Sci.* **30** (4), 299–303.

Kolmogorov, A.N. (1942). The equations of turbulent motion of incompressible fluids. *Izvestiya, USSR Ac. Sci., Phys.* **6** (1-2), 56–8.

Kolmogorov, A.N. (1954). On a new variant of the gravitational theory of motion of suspended sediment. *Vestn. MGU* **3**, 41–5.

Kolmogorov, A.N. (1962). A refinement of previous hypotheses concerning the local structure of turbulence in a viscous incompressible fluid at high Reynolds number. *J. Fluid Mech.* **13** (1), 82–5.

Kolmogorov, A.N., Petrovsky, I.G. & Piskunov, N.S. (1937). Investigation of the diffusion equation connected with an increasing amount of matter and its application to a biological problem. *Bull. MGU* **A1** (6), 1–26.

Korotaev, G.K. & Panteleev, N.A. (1977). Experimental investigations of hydrodynamic instability in the oceans. *Oceanology USSR* **17** (6), 914–53.

Kovasznay, L.S.G., Kilens, V. & Blackwelder, R.F. (1970). Large-scale motion in the intermittent region of a turbulent boundary layer. *J. Fluid Mech.* **41** (2), 283–325.

Kulikovsky, A.G. & Lyubimov, G.A. (1965). *Magnetohydrodynamics*. Addison-Wesley, Reading MA.

Lagerstrom, P.A. & Casten, R.J. (1972). Some basic concepts underlying singular perturbation techniques. *SIAM Review* **14** (1), 63–120.

Landau, L.D. & Lifshitz, E.M. (1986). *Theory of Elasticity*, 2nd edition. Pergamon Press, London.

Landau, L.D. & Lifshitz, E.M. (1987). *Fluid Mechanics*, 2nd edition. Pergamon Press, London.

Launder, B.E. & Spalding, D.B. (i972). *Mathematical Models of Turbulence*. Academic Press, London.

Launder, B.E., Morse, A.P., Rodi, W. & Spalding, D.B. (1972). Prediction of free shear flows – a comparison of six turbulence models. NASA Report SP 321.

Launder, B.E. & Spalding, D.B. (1974). The numerical computation of turbulent flows. *Comp. Math. Appl. Mech. Eng.* **3**, 269–89.

Lax, P.D. (1968). Integrals of nonlinear equations of evolution and solitary waves. *Comm. Pure Appl. Math.* **21** (5), 467–90.

Liebowitz, H. (ed.) (1968a). *Fracture. An Advanced Treatise, Vol. I.* Academic Press, New York, London.

Liebowitz, H. (ed). (1968b). *Fracture. An Advanced Treatise, Vol II.* Academic Press, New York, London.

Lighthill, J. (1978). *Waves in Fluids*. Cambridge University Press.

Linden, P.F. (1975). The deepening of a mixed layer in a stratified fluid. *J. Fluid Mech.* **71** (2), 385–405.

Ling, S.C. & Huang, T.T. (1970). Decay of weak turbulence. *Phys. Fluids* **13** (12), 2912–20.

Ling, S.C. & Wan, C.A. (1972). Decay of isotropic turbulence generated by a mechanically agitated grid. *Phys. Fluids* **15** (8), 1363–9.

Loitsiansky, L.G. (1939). Some basic laws of isotropic turbulent flow. *Proc. Central Aero-Hydrodynamic Institute, Moscow* **440**, 3–23. (In Russian.) Translated as Loitsiansky, L.G. (1945). Some basic laws of isotropic turbulent flow. NACA Technical Memo. No. 1079.

Ma, S.-K. (1976). *Modern Theory of Critical Phenomena*. Benjamin/Cummings, Reading MA.

Mandelbrot, B. (1975). *Les objects fractals: forme, hasard et dimension*. Flammarion, Paris.

Mandelbrot, B. (1977). *Fractals, Form, Chance and Dimension*. W.H. Freeman and Co., San Francisco.

Mandelbrot, B. (1982). *The Fractal Geometry of Nature.* W.H. Freeman and Co., San Francisco.

Maxworthy, T. (1973). Experimental and theoretical studies of horizontal jets in a stratified fluid. In *Proc. Int. Symposium on Stratified Flows, Novosibirsk*, 1972, 611–18. Am. Soc. Civ. Eng., New York.

McMahon, T.A. (1971). Rowing: a similarity analysis. *Science* **173**, 23 July 1971, 349–51.

Meyer, F. (1955). Zur Darstellung starker Stossfronten durch Homologie-Lösungen. *Z. Naturforschung* **10a** (9/10), 693–7.

Migdal, A.B. (1977). *Qualitative Methods in Quantum Theory.* W.A. Benjamin, Reading, MA.

Miles, J.W. (1961). On the stability of heterogeneous shear flow. *J. Fluid Mech.* **10** (4), 496–508.

Miles, J.W. (1963). On the stability of heterogeneous shear flow. *J. Fluid Mech.* **16** (2), 209–27.

Millionshchikov, M.D. (1939). Decay of homogeneous turbulence in a viscous incompressible fluid. *Doklady, USSR Ac. Sci.* **22** (5), 236–40.

Moffatt, H.K. (1964). Viscous and resistive eddies near a sharp corner. *J. Fluid Mech.* **18** (1), 1–18.

Moffatt, H.K. & Duffy, B.R. (1980). Local similarity solutions and their limitations. *J. Fluid Mech.* **96** (2), 299–313.

Monin, A.S. (1950). Turbulence in the atmospheric surface layer. *Coll. Sci. Inform. Hydromet. Science USSR, Moscow* (**1**), 13–27.

Monin, A.S. & Obukhov, A.M. (1953). Dimensionless characteristics of turbulence in the surface layer of the atmosphere. *Doklady, USSR Ac. Sci.* **93** (2), 223–6.

Monin, A.S. & Obukhov, A.M. (1954). Basic relationships for turbulent mixing in the surface layer of the atmosphere. *Proc. Inst. Theor. Geophys., USSR Ac. Sci.* **24** (151), 163–87.

Monin, A.S. & Ozmidov, R.V. (1981). *Oceanic Turbulence.* Gidrometeoizdat, Leningrad.

Monin, A.S. & Yaglom, A.M. (1971). *Statistical Fluid Mechanics. Mechanics of Turbulence*, Vol. 1. MIT Press, Cambridge, London.

Monin, A.S. & Yaglom,, A.M. (1975), *Statistical Fluid Mechanics. Mechanics of Turbulence*, Vol. 2. MIT Press, Cambridge, London.

Monin, A.S. & Yaglom, A.M. (1992). *Statistical Fluid Mechanics: Theory of Turbulence*, Vol. 1, 2nd Russian edition. Gidrometeoizdat, St Petersburg.

Munk, W. (1966). Abyssal recipes. *Deep Sea Research* **13**, 707–30.

Murray, J.D. (1977). *Lectures on Non-linear Differential Equation Models in Biology.* Clarendon Press, Oxford.

Muskhelishvili, N.I. (1963). *Some Basic Problems of the Mathematical Theory of Elasticity*, 2nd English edition. P. Noordhoff, Groningen.

Muskhelishvili, N.I. (1966). *Some Basic Problems of Mathematical Theory of Elasticity*, 5th Russian edition. Nauka, Moscow.

Nigmatulin, R.I. (1965). A plane strong explosion on a boundary of two ideal, calorically perfect gases. *Bulletin MGU, Ser. Matem. Mekh.* **1**, 83–7.

Nikuradse, J. (1932). Gesetzmässigkeiten der turbulenten Strömung in glatten Röhren. VDI Forschungscheft No. 356.

Nikolaeva, G.G. *et al.* (1975). Metabolism rate and size-weight characteristics of the *Rhithropanopeus harrisii tredantatus* crab from the Caspian Sea. *Oceanology USSR* **15**, 99–100.

Norton, F.H. (1929). *Creep of Steel at High Temperatures.* McGraw Hill, New York.

Novikov, S., Manakov, S.V., Pitaevsky, L.P. & Zakharov, V.E. (1984). *Theory of Solitions: The Inverse Scattering Method.* Consultants Bureau, New York, London.

Nowell, A.R.M. & Hollister, C.D. (1985). The objectives and rationale of HEBBLE. *Marine Geology* **66**, 1–12.

Obukhov, A.M. (1941). On the distribution of energy in the spectrum of a turbulent flow. *Doklady, USSR Ac. Sci.* **32** (1), 22–4.

Obukhov, A.M. (1946). Turbulence in thermally inhomogeneous atmosphere. *Proc. Inst. Theor. Geophys., USSR Ac. Sci.* **1**, 95–115.

Obukhov, A.M. (1962). Some specific features of atmospheric turbulence. *J. Fluid Mech.* **13** (1), 77–81.

Offen, G.R. & Kline, S.J. (1975). A proposed model of the bursting process in turbulent boundary layers. *J. Fluid Mech.* **70** (2), 209–28.

Oleinik, O.A. (1957). Discontinuous solutions of nonlinear differential equations. *Uspekhi Mat. Nauk* **12**, 3(75), 3–73.

Oleynik, O.A., Kalashnikov, A.S. & Chzhou Yui-lin (1958). The Cauchy problem and boundary problems for equations of the type of unsteady filtration. *Izvestiya, USSR Ac. Sci., Ser. Mat.* **22**, 667–704.

Oppenheim, A.K., Kuhl, A.C. & Kamel, M.M. (1972). On self-similar blast waves headed by the Chapman–Jouguet detonation. *J. Fluid Mech.* **55** (2), 257–70.

Oppenheim, A.K., Kuhl, A.L., Lundström, E.A. & Kamel, M.M. (1971). A systematic exposition of the conservation equations for blast waves. *J. Appl. Mech.* **38** (4), 783–94.

Oppenheim, A.K., Lundström, E.A., Kuhl, A.C. & Kamel, M.M. (1972). A parametric study of self-similar blast waves. *J. Fluid Mech.* **52** (4), 657–82.

Orowan, E. (1949). Fracture and strength of solids. *Rep. Progr. Phys. Soc. London* **12**, 185–232.

Ovsyannikov, L.V. (1978). *Group Analysis of Differential Equations.* Nauka, Moscow.

Panasyuk, V.V. (1968). *Limiting Equilibrium of Brittle Bodies with Cracks.* Naukova Dumka, Kiev.

Paquette, G.C., Chen, L.-Y., Goldenfeld, N. & Oono, Y. (1994). Structural stability and renormalization group for propagating fronts. *Phys. Rev. Lett.* **72**, 76–9.

Paquette, G.C. & Oono, Y. (1994). Structural stability and selection of propagation fronts in semilinear partial diffferential equations. *Phys. Rev. E* **49**, 2368–88.

Paris, P.C. & Erdogan, F. (1963). A critical analysis of crack propagation laws. *J. Basic Eng. Trans. ASME, Ser. D.* **85**, 528–34.

Parkhomenko, V.P., Popov, S.P. & Ryzhov, O.S. (1977a). On the influence of the initial velocity of particles on the unsteady axisymmetric gas motions. *Uchenye Zapiski (Research Notes) TSAGI,* **8** (3), 32–8.

Parkhomenko, V.P., Popov, S.P. & Ryzhov, O.S. (1977b). On the influence of the initial velocity of particles on the unsteady spherically symmetric gas motions. *Comput. Math. and Math. Phys.* **15** (5), 1325–9.

Parvin, M. & Williams, J.G. (1975). The effect of temperature on the fracture of polycarbonate. *J. Mater. Sci.* **10** (11), 1883–6.

Patashinsky, A.Z. & Pokrovsky, V.L. (1966). On the behaviour of ordering systems near the phase transition point. *J. Exp. Theor. Phys.* **50** (2), 439–47.

Pattle, R.E. (1959). Diffusion from an instantaneous point source with a concentration-dependent coefficient. *Quart. J. Mech. Appl. Math.* **12**, 407–9.

Pedlosky, J. (1979). *Geophysical Fluid Dynamics.* Springer-Verlag, New York, Heidelberg, Berlin.

Petrovsky, I.G. (1967). *Lectures on Partial Differential Equations.* Saunders, Philadelphia.

Phillips, O.M. (1967). The generation of clear-air turbulence by the degradation of internal waves. In *Atmospheric Turbulence and the Propagation of Radio Waves*, 130–8. Nauka, Moscow.

Phillips, O.M. (1976). Energy loss mechanisms from low-mode waves. Report on the Soviet-American Conference on Internal Waves, Novobirsk, December 1976.

Phillips, O.M. (1977). *The Dynamics of the Upper Ocean*, 2nd edition. Cambridge University Press, Princeton.

Polubarinova-Kochina, P.Ya. (1962). *Theory of Groundwater Movement.* Princeton University Press.

Prandtl, L. (1932a). Meteorologische Anwendungen der Strömungslehre. *Beiträge Phys. Atmos.* **19** (3), 188–202.

Prandtl, L. (1932b). Zur turbulenten Strömung in Röhren und längs Platten. *Ergebn. Aerodyn. Versuchsanstalt, Göttingen* **B4**, 18–29.

Prandtl, L. (1945). Ueber ein neues Formelsystem für die ausgebildete Turbulenz. *Nach. Ges. Wiss. Göttingen, Math.-Phys. Kl.*, 6–18.

Praskovsky, A. & Oncley, S. (1994). Measurement of Kolmogorov constant and intermittency exponent at very high Reynolds numbers. *Physics of Fluids* **6** (9), 2886–2889.

Prostokishin, V.M. (1994). Private communication.

Raizer, Yu.P. (1968). A high-frequency high-pressure gas flow discharge as a slow combustion process. *J. Appl. Mech. Tech. Phys.* **9** (3), 239–43.

Raizer, Yu.P. (1970). Physical foundations of the theory of cracks in brittle fracture. *Soviet Phys. Uspekhi* **100** (2), 329–47.

Raizer, Yu.P. (1977). *Laser-induced Discharge Phenomena.* Consultants Bureau, New York.

Rao, K.N., Narasimha, R. & Badri Narayanan, M.A. (1971). The bursting phenomenon in a turbulent boundary layer. *J. Fluid Mech.* **48** (2), 339–52.

Reynolds, O. (1895). On the dynamical theory of incompressible viscous fluids and the determination of the criterion. *Phil. Trans. Roy. Soc. London* **186**, 123–64.

Reynolds, W.C. (1976). Computation of turbulent flows. *An. Rev. Fluid Mech.* **8**, 183–208.

Richardson, L.F. (1922). *Weather Prediction by Numerical Process.* Cambridge University Press.

Richardson, L.F. (1961). The problem of contiguity: an appendix of statistics of deadly quarrels. *General Systems Year Book* **6**, 139–87.

Roesler, F. (1956). Brittle fracture near equilibrium. *Proc. Phys. Soc.* **B69**, 981–92.

Rosen, J.B. (1954). Theory of laminar flame stability, I, II. *J. Chem. Phys.* **22** (4), 733–48.

Samarsky, A.A. & Sobol', I.M. (1963). Examples of numerical computation of temperature waves. *Comput. Math. and Math. Phys.* **3** (4), 702–16.

Sapunkow, Ia.G. (1967). Convergent detonation waves under Chapman-Jouguet conditions in media with variable and constant initial densities. *Appl. Math. Mech. (PMM)* **31** (5), 945–8.

Schlichting, H. (1968). *Boundary Layer Theory*, 6th edition. McGraw-Hill, New York.

Sedov, L.I. (1944). Decay of isotropic turbulent motions of an incompressible fluid. *Doklady, USSR Ac. Sci.* **42** (3), 121–4.

Sedov, L.I. (1945). On some unsteady motions of compressible fluids. *Prikl. Mat. Mekh.* **9** (4), 293–311.

Sedov, L.I. (1946). Propagation of strong shock waves. *Prikl. Mat. Mekh.* **10**, 241–50, (Pergamon Translations, No. 1223).

Sedov, L.I. (1959). *Similarity and Dimensional Methods in Mechanics.* Academic Press, New York.

Sedov, L.I. (1971). *A Course in Continuum Mechanics.* Wolters-Noordhoff, Groningen.

SethuRaman, S. (1980). A case of persistent breaking of internal gravity waves in the atmospheric gravity waves in the atmospheric surface layer over the ocean. *Boundary-layer Meteorology* **19** (1), 67–80.

Shchelkachev, V.N. (1959). *Development of Oil-water Strata Under Elastic Drive.* Gostoptekhizdat, Moscow.

Shkadinsky, K.G., Khaikin, B.I. & Merzhanov, A.G. (1971). Propagation of a pulsating exothermic reaction front in the condensed phase. *Comb. Expl. Shock Waves* **7**, 15–22.

Shushkina, E.A., Kus'micheva, V.I. & Ostapenko, L.A. (1971). Energy equivalent of body mass, respiration, and calorific value of mysids from the Sea of Japan. *Oceanology USSR* **11** (6), 880–3.

Sobolev, S.L. (1954). On a new problem of mathematical physics. *Izvestiya, USSR Ac. Sci., ser. mat.* **18** (1), 3–50.

Sneddon, I.N. (1951). *Fourier Transforms.* McGraw-Hill, New York.

Staniukovich, K.P. (1960). *Unsteady Motion of Continuous Media.* Pergamon Press, New York.

Sternberg, E. & Koiter, W.T. (1958). The wedge under a concentrated couple: a paradox in the two-dimensional theory of elasticity. *J. Appl. Mech.* **25** (4), 575–81.

Stewart, R.W. (1951). Triple velocity correlations in isotropic turbulence. *Proc. Camb. Phil. Soc.* **47**, 146–57.

Stommel, H. (1958). The abyssal circulation. *Deep Sea Research* **5**, 80–2.

Storåkers, B. & Larsson, P.L. (1994). On Brinell and Boussinesq indentation of creeping solids. *J. Mech. Phys. Solids* (in press).

Stückelberg, E.C.G. & Peterman, A. (1953). La normalisation des constantes dans la théorie des quanta. *Helvetica Physica Acta* **XXVI**, 499–520.

Swift, J. (1992) *Gulliver's Travels.* Wordsworth Classics (see p. 124).

Tabor, D. (1951). *Hardness of Metals.* Clarendon Press, Oxford.

Taffanel, M. (1913). Sur la combustion des mélanges gazeux et les vitesses de réaction. *C. R. Ac. Sci. Paris* **157**, 714–7.

Taffanel, M. (1914). Sur la combustion des mélanges gazeux et les vitesses de réaction. *C. R. Ac. Sci. Paris* **158**, 42–5.

Taylor, G.I. (1910). The conditions necessary for discontinuous motion in gases. *Proc. Roy. Soc.* **A84**, 371–7.

Taylor, G.I. (1935). Statistical theory of turbulence, I-IV. *Proc. Roy. Soc.* **A151**, 421–78.

Taylor, G.I. (1941). The formation of a blast wave by a very intense explosion. Report RC-210, 27 June 1941, Civil Defence Research Committee.

Taylor, G.I. (1950a). The formation of a blast wave by a very intense explosion. I, Theoretical discussion. *Proc. Roy. Soc.* **A201**, 159–74.

Taylor, G.I. (1950b). The formation of a blast wave by a very intense explosion. II. The atomic explosion of 1945. *Proc. Roy. Soc.* **A201**, 175–86.

Taylor, G.I. (1963). *Scientific Papers*, G.K. Batchelor (ed.), Vol. 3, *Aerodynamics and the Mechanics of Projectiles and Explosions.* Cambridge University Press.

Thompson, S.M. & Turner, J.S. (1975). Mixing across an interface due to turbulence generated by an oscillating grid. *J. Fluid Mech.* **67** (2), 349–68.

Ting, T.C.T. (1984). The wedge subjected to tractions: a paradox reexamined. *J. Elasticity* **14**, 235–47.

Townsend, A.A. (1976). *Structure of Turbulent Shear Flow*, 2nd edition. Cambridge University Press.

Turner, J.S. (1968). The influence of molecular diffusivity on turbulent entrainment across a density interface. *J. Fluid Mech.* **33** (4), 639–6.

Turner, J.S. (1973). *Buoyancy Effects in Fluids.* Cambridge University Press.

Turner, J.S. (1978). The temperature profile below the surface mixed layer. *Ocean Modelling* **11**, 6–8.

Van den Booghaart, A. (1966). Crazing and characterisation of brittle fracture in polymers. In *Proc. Conf. Phys. Basis of Yield and Fracture*, Oxford University Press.

Van Dyke, M. (1975). *Perturbation Methods in Fluid Mechanics*, 2nd edition. Parabolic Press, Stanford.

Van Dyke, M. (1982). *An Album of Fluid Motions.* Parabolic Press, Stanford.

Vanoni, V. (1946). Transportation of suspended sediment by water. *Trans. Am. Soc. Civil Eng.* **111**, 67–133.

Vavakin, A.S. & Salganik, R.L. (1975). On experimental determination of rate dependence of fracture toughness. *Izvestiya, USSR Ac. Sci., Mech. Solids* **5**, 127–33.

Vlasov, I.O., Derzhavina, A.I. & Ryzhov, O.S. (1974). On an explosion on the boundary of two media. *Comput. Math. and Math. Phys.* **14** (6), 1544–52.

von Kármán, Th. (1911). Über die Turbulenzreibung verschiedener Flüssigkeiten. *Phys. Zeit.* **12** (8), 1071–4.

von Kármán, Th. (1930). Mechanische Ähnlichkeit und Turbulenz. *Nachrichten Ges. Wiss. Göttingen, Math-Phys. Kl.*, 58–76.

von Kármán, Th. (1957). *Aerodynamics.* Cornell University Press, Ithaca.

von Kármán, Th. & Howarth, L. (1938). On the statistical theory of isotropic turbulence. *Proc. Roy. Soc. London* **A164** (917), 192–215.

von Koch, H. (1904). Sur une courbe continue sans tangente obtenue par une construction géometrique élémentaire. *Arkiv Mat. Astron. Fys.* **2**, 681–704.

von Neumann, J. (1941). The point source solution. National Defence Research Committee, Div. B, Report AM-9, June 30, 1941.

von Neumann, J. (1963). The point source solution, in *Collected Works*, Vol. VI, 219–37. Pergamon Press, Oxford, New York, London, Paris.

von Weizsäcker, C.F. (1954). Genäherte Darstellung starker instationärer Stosswellen durch Homologie-Lösungen. *Z. Naturforschung* **9a**, 269–75.

Weatherly, G.L. & Kelly, E.A. (1982). 'Too cold' bottom layer at the bottom of Scotia Rise. *J. Marine Res.* **40**, 985–1012.

Whitham, G.B. (1974). *Linear and Nonlinear Waves.* Wiley, New York.

Williams, M.L. (1952). Stress singularities resulting from various boundary conditions in angular corners of plates in extension. *J. Appl. Mech.* **19** (4), 526–8.

Wilson, K. (1971). Renormalization group and critical phenomena, I, II. *Phys. Rev.* **B4** (9), 3174–83, 3184–205.

Woods, J.D. (1968). Wave-induced shear instability in the summer thermocline. *J. Fluid Mech.* **32** (4), 792–800.

Wu, J. (1969). Mixed region collapse with internal wave generation in a density stratified medium. *J. Fluid Mech.* **35** (3), 531–44.

Yaglom, A.M. (1974). Data on the characteristics of turbulence in the surface layer of the atmosphere. *Izvestiya, USSR Ac. Sci., Atmos. Oceanic Phys.* **10** (6), 566–86.

Zatsepin, A.G., Fedorov, K.N., Voropayev, S.I. & Pavlov, A.M. (1978). Experimental study of the spreading of a mixed region in a stratified fluid. *Izvestiya, USSR Ac. Sci., Atmos. Oceanic Phys.* **14** (2), 170–3.

Zeldovich, Ya.B. (1942). On the distribution of pressure and velocity in products of detonation blasts, in particular for spherically propagating detonation waves. *Zhurn. Eksper. Teor. Fiz.* **12** (9), 389–406.

Zeldovich, Ya.B. (1948). On the theory of flame propagation. *Zhurn. Fiz. Khimii* **22** (1), 27–48.

Zeldovich, Ya.B. (1956). The motion of a gas under the action of a short term pressure shock. *Akust. Zh.* **2** (1), 28–38, (*Sov. Phys. Acoustics* **2**, 25–35).

Zeldovich, Ya.B. (1978). The flame propagation in a mixture reacting at the initial temperature. Preprint, Institute of Chemical Physics, Chernogolovka.

Zeldovich, Ya.B. (1992). *Selected Works. Volume 1, Chemical Physics and Hydrodynamics.* Princeton University Press, Princeton.

Zeldovich, Ya.B. & Barenblatt, G.I. (1958). The asymptotic properties of self-modeling solutions of the nonstationary gas filtration equations. *Soviet Phys. Doklady* **3** (1), 44–7.

Zeldovich, Ya.B., Barenblatt, G.I., Librovich, V.B. & Makhviladze, G.M. (1985). *The Mathematical Theory of Combustion and Explosions.* Consultants Bureau, New York, London.

Zeldovich, Ya.B. & Frank-Kamenetsky, D.A. (1938a). Theory of uniform propagation of flames. *Doklady, USSR Ac. Sci.* **19** (2), 693–7.

Zeldovich, Ya.B. & Frank-Kamenetsky, D.A. (1938b). Theory of uniform propagation of flames. *Zhurn. Fiz. Khimii* **12** (1), 100–5.

Zeldovich, Ya.B. & Kompaneets, A.S. (1950). On the theory of propagation of heat with thermal conductivity depending on temperature. In *Collection of Papers Dedicated to the 70th Birthday of A.F. Ioffe*, 61–71. Izd. Akad. Nauk USSR, Moscow.

Zeldovich, Ya.B. & Kompaneets, A.S. (1960). *Theory of Detonation.* Academic Press, New York.

Zeldovich, Ya.B. & Raizer, Yu.P. (1966). *Physics of Shock Waves and High Temperature Hydrodynamic Phenomena*, Vol. I. Academic Press, New York, London.

Zeldovich, Ya.B. & Raizer, Yu.P. (1967). *Physics of Shock Waves and High Temperature Hydrodynamic Phenomena*, Vol. II, Academic Press, New York, London.

Zheltov, Yu.P. & Christianovich, S.A. (1955). On the hydraulic fracture of the oil stratum. *Izvestiya, USSR Ac. Sci. Techn. Sci.* **5**, 3–41.

Zhukov, A.I. & Kazhdan, Ia.M. (1956). Motion of a gas due to the effect of a brief impulse. *Soviet Phys. Acoustics* **2** (4), 375–381.

Index

Airy stress function 221
anomalous dimensions xiv, 175, 358
asymptotic conservation laws 200
atomic explosion 47, 48, 76, 90

blast waves 80, 87
boundary layer on a flat plate 163
Boussinesq approximation 59
breathing rate of animals 342
Britain, length of the West coast of 335
Brunt–Väisäla frequency 318, 321
buoyancy parameter 59, 297
Burgers equation 183

chaos 364
class of systems of units 30, 31, 32, 34
classification of self-similar solutions 25
classification of similarity rules 146
cohesion modulus 238, 239, 241
collapsing of mixed fluid patches 300
complete similarity 24, 25, 147, 150, 153, 154, 158, 159, 166, 173, 175, 177, 260, 265, 270, 272, 283, 284, 287, 298, 303, 341, 349, 350, 355
cone crack 241, 243
convection 59
covariance principle xii, 23, 149, 162
critical phenomena 365

Darcy's law 105, 346
decay of homogeneous isotropic turbulence 256, 259, 265
dimension 3, 28, 32
dimension function 32, 34, 35, 37, 38, 39, 40
dimensional analysis xii, 1, 2, 7, 9, 10, 11, 14, 17, 18, 19, 20, 22, 23, 28, 39, 43, 46, 48, 49, 50, 51, 53, 60, 63, 64, 69, 76, 78, 83, 91, 95, 103, 107, 111, 126, 142, 145, 146, 148, 149, 151, 153, 155, 155, 157, 158, 161, 162, 164, 165, 166, 167, 169, 170, 221, 226, 227, 228, 229, 230, 241, 260, 265, 266, 272, 281, 286, 289, 291, 297, 303, 313, 319, 320, 339, 341, 343, 348, 350, 352
dimensionless stiffness 231, 233
drag force 5, 6, 8, 9
ductile failure 244
dust storms 306

eigenvalue problem 102, 103, 252
eigenvalues, spectrum of 27, 203
elastic wedge,equilibrium of an 220
explosion at a plane interface 141
extension of mixed-fluid patches 316

fatigue 244